Techno-economic and Life Cycle Assessments of Oil Sands Products and Liquefied Natural Gas Supply Chains from Canada to Asia-Pacific and Europe

by

Krishna Sapkota

A thesis submitted in partial fulfillment of the requirements for the degree of

Master of Science

Department of Mechanical Engineering

University of Alberta

Abstract

The diversification of Canadian oil sands and natural gas markets is imperative for their long-term economic growth. In order to ensure a competitive spot in the natural gas and oil global market, it is considerably important for Canada to supply its natural gas and oil at a competitive price with lower greenhouse gas (GHG) emissions. Earlier studies on techno-economic and life cycle assessment modeling of the supply chain costs and environmental risks associated in the delivery of Canadian liquefied natural gas (LNG) and oil sands products mostly focus on exports to the U.S. This study addresses key gaps by conducting techno-economic and life cycle assessments (LCA) of the Canadian oil sands and LNG supply chains to Asia-Pacific and Western Europe, respectively.

This study conducts a comparative cost analysis of potential pathways for Canadian oil sands products (synthetic crude oil and diluted bitumen) and the LNG supply chain to seaport destinations in the Asia-Pacific and Western Europe, respectively, and develops comprehensive life cycle assessment (LCA) models to understand the GHG emissions associated with the respective supply chain. The total supply chain costs and life cycle GHG emissions of Canadian oil sands and the LNG supply chain from the production site to the Asia-Pacific (China, Japan, and India) and Europe, respectively, through the development of data-intensive techno-economic and life cycle analysis models. For Canadian oil sands, four pathways (two for synthetic crude oil (SCO) and two for dilbit) were considered for production (SAGD), transportation (SAGD-upgrader-port in Vancouver), upgrading, and shipping, and Canadian LNG includes two supply chain routes, one from the west coast and the other via the east coast of Canada, from recovery, processing, transmission, liquefaction, and shipping. The results show that the supply chain costs (C$) per barrel of bitumen to China, Japan, and India ranged from 61–87, 60–86, and 62–90. The cost for LNG exports to Europe is in the range of $11.40–$16.50/GJ, respectively, depending on the pathway. Overall supply chain costs of dilbit and

SCO are influenced most by production and upgrading costs. From the sensitivity analysis, it is observed that production and upgrading costs are mostly influenced by capital cost, while pipeline lifetime and capacity highly impact transportation (pipeline) and shipping costs, respectively.

It is found that life cycle (LC) well-to-wheel (WTW) GHG emissions for gasoline, diesel and jet fuel are from 102.5–132.8, 96.08–128.5, and 91.9–124.6 g-CO2eq/MJ, respectively. The total well-to-port (WTP) GHG emissions (including emissions from recovery, processing, transportation, liquefaction, shipping, and re-gasification at the destination port) from the Canadian production site to Europe are 22.9–42.1 g-CO_2eq/MJ, depending on the resources and pathway followed. It is also observed that the LC WTW GHG emissions from Canadian oil sands products are higher than from Saudi Arabian crude with 94.6, 91.7, and 83.3 g-CO_2eq/MJ for gasoline, diesel and jet fuel, respectively. This difference is largely because of the inclusion of an upgrader unit in the Canadian oil sands energy conversion chain, which significantly increases overall LC emissions. Irrespective of the pathway, the overall emissions can be reduced if the extraction technology is improved such that products require partial or no upgrading before being refined. The costs and GHG emissions values reported in the literature on the delivery of natural gas from countries like Russia, Algeria, Norway, and Qatar were lower than the Canadian LNG supply chain. Therefore, finding alternative sources of natural gas in Eastern Canada might provide the lowest cost and least GHG-intensive alternative to Canadian LNG.

Preface

This thesis is original work by Krishna Sapkota under the supervision of Dr. Amit Kumar. Chapter 2 of this thesis has been submitted as Sapkota K., Oni O. A., Kumar A., "Techno-economic assessment of the extraction, transportation, upgrading, and shipping of Canadian oil sands products to the Asia-Pacific region" to *Applied Energy*. Chapter 3 has been submitted as Sapkota K., Oni O. A., Kumar A., "A well-to-wheel life cycle assessment (LCA) of greenhouse gas emissions from Canadian oil sands supply chain for transportation fuels in China" to *International Journal of Life Cycle Assessment*. Chapter 4 has been submitted as Sapkota K., Oni O. A., Kumar A., "Techno-economic and life cycle assessment of the natural gas supply chain from production sites in Canada to north and southwest Europe" to *Natural Gas Science and Engineering by Elsevier*. I was responsible for the concept formulation, data analysis, model improvement, and manuscript composition. Dr. O. A. Oni contributed by reviewing the papers and providing useful inputs. Dr. A. Kumar was the supervisory author and was involved with the concept formation, results analysis, and manuscript composition.

Acknowledgments

Firstly, to my supervisor, Prof. Amit Kumar, thank you for providing endless guidance and support throughout my academic year. Your mentorship, encouragement, and advice have always inspired me and provided me enough space to think, allowed my personal and professional growth, and undoubtedly enriched my intellectual ability. It has been a privilege being part of your team. Your energy levels and commanding presence have made a lasting impression on me as a student and I feel lucky to have had the opportunity to work with you. This thesis would not have been possible without your consistent support.

I would like to thank the Sino-Canadian Energy and Environment Research and Education Initiative (SCENEREI), Tsinghua University (China), the NSERC/Cenovus/Alberta Innovates Associate Industrial Research Chair in Energy and Environmental Systems Engineering, and the Cenovus Energy Endowed Chair in Environmental Engineering for their financial support for this project. My warmest thanks go to representatives from Alberta Innovates (AI), Cenovus Energy Inc., and Suncor Energy Inc. for their inputs in various forms.

It is my great pleasure to thank Dr. Abayomi Olufemi Oni for reviewing all of my research papers and my thesis and providing me valuable suggestions. I really appreciate him for being accessible and willing to help whenever I needed. I thank my examining committee for critical judgments of my thesis and providing thoughtful and detailed comments. I thank Astrid Blodgett and Dr. Mahdi Vaezi for editorial assistance for all the papers.

My most appreciation to Dr. Andre McDonald for your heat conduction course and the knowledge and ideas you shared. To Richard Groulx and Gail Dowler, many thanks for your support and being accessible whenever needed.

I wholeheartedly thank to the organization that I had the privilege of being part of it. To the Nepal Scholars' Association University of Alberta, particularly Keshab Sharma and Khagendra Belbase, I am highly indebted for the invaluable supports and friendly environments endowed on me. To the University of Alberta Energy Club team, special appreciation and thanks for their active involvements and supports to make every event successful and enriching my experiences to help grow my leadership skills. To Umar Shafique, Aaron Liu, Ermin Chow, Edson Nogueira Junior, Thomas Roberts, and Huachao Li Fernando, thanks to all of you for bringing the interactive ideas and supports, whenever needed, to make the events more effective and outreaching to a larger audience, more importantly grooming my professional skills.

I acknowledge the support from my colleagues in the Sustainable Energy Research Lab for providing advice, moral support, good memories, and making a convivial place to work. In particular, I would like to thank Madhumita Patel for her friendship, suggestions, and creative interactions.

Very special thanks to my friends Luiz Fernando and Andres Camacho who always believed in me and encouraged me. It was a great pleasure for me to share rooms, drinks, dinner, and organize parties together. It was one of the best memories of my life.

I am eternally grateful to my mom for all the wisdom she has given me. I express my deepest gratitude to my family and relatives for their unconditional love, support, and encouragement and making it possible for me to get my MSc degree.

Above all, I would like to thank God for providing me good health, power to believe in my passion, and making me able to use my intellect to complete this thesis.

Table of Contents

List of Tables

List of Figures

Acronyms

ADU	Atmospheric distillation unit
API	American Petroleum Institute
AR	Atmospheric residue
bbl	Barrel
bcfd	Billion cubic feet per day
C	Canadian
CAPP	Canadian Association of Petroleum Producers
CD	Conventional diesel
CERI	Canadian Energy Research Institute
CG	Conventional gasoline
CNG	Compressed natural gas
CNOOC	China National Offshore Oil Company
CNPC	China National Petroleum Company
CPF	Central processing facility
cSt	Centistoke
DCFA	Discounted cash flow analysis
DCU	Delayed coking upgrader
DH	Diesel hydrotreater
EIA	U.S. Energy Information Administration
ESP	Electric submersible pump
EU	European Union
GDP	Gross domestic product
GH	Gas hydrotreater
GHG	Greenhouse gas
GHOST	GreenHouse gas emissions of current Oil Sands Technologies

GREET	Greenhouse gases, Regulated Emissions, and Energy Use in Transportation model
HCU	Hydroconversion upgrader
HFO	Heavy fuel oil
HRSG	Heat recovery steam generator
HVGO	Heavy vacuum gas oil
IGF	Induced gas flotation
iSOR	Instantaneous steam-oil ratio
kbd	Thousands barrel per day
Kg/d	Kilogram per day
km	Kilometer
kPa	Kilopascal
kWh	Kilowatt hour
LC	Life cycle
LCA	Life cycle assessment
LNG	Liquefied natural gas
LPG	Liquefied natural gas
LVGO	Light vacuum gas oil
MC$	Million Canadian dollar
MDO	Marine diesel oil
MMBtu	Million metric British thermal unit
mmscfd	Million metric standard cubic feet per day
MTPA	Millions tons per annum
MW	Megawatt
NEB	National Energy Board
NG	Natural gas

NH	Naphtha hydro treating
O&M	Operating and maintenance
ORF	Oil removal filter
PADD	Petroleum Administration for Defense District
PRELIM	Petroleum Refinery Life-cycle Inventory Model
SAGD	Steam Assisted Gravity Drainage
SCO	Synthetic crude oil
SFC	Specific fuel consumption
SMR	Steam methane reforming
SYPC	Shaanxi Yanchang Petroleum Company
tcf	Trillion cubic feet
VDU	Vacuum distillation unit
VR	Vacuum residue
WCS	Western Canadian Select
WTP	Well to Port
yr.	Year

Nomenclature

C_t	Total annual cost, \$/year
C_{tf}	Total fuel cost, \$/year
C_{OM}	Total Operating and Maintenance cost, \$/year
OI	Operating income of the unit, \$/year
R_t	Total revenue, \$/year

NI	Net income of the unit, $/year
C_c	Capital cost of unit, million dollar
i	Discount rate, %
k	Considered year
ID	Internal diameter, m
ΔP	Differential pressure, bar
P_E	Towing power
P_B	Brake power
η_H	Hull efficiency
η_o	Open water propeller efficiency
η_R	Relative rotative efficiency
η_s	Shaft efficiency

SCO and dilbit carrier specifications

V_c	Cargo volume
Δ	Displacement of the SCO/dilbit carrier, tonnes
L_{OA}	Overall length, meters
L_{PP}	Length between perpendiculars, meters
L_{wl}	Length on waterline, meters
L_D	Light displacement, tonnes
B	Breadth, meters
D_{design}	Design draught, meters
V	Sailing speed, m/s
T	Depth, meters

A	Air draft, meters
l_{cb}	Longitudinal center of buoyancy, meters
dwt	Dead weight tonnage, tonnes
Coefficients	
C_b	Block coefficient
C_m	Midship section coefficient
C_w	Water plane coefficient
C_p	Prismatic coefficient based on length on waterline
Engine fuel consumption	
SFO_m	Main engine specific fuel consumption, g/kWh
SFO_{aux}	Auxiliary engine specific fuel consumption, g/kWh

Chapter 1
Introduction

1.1 Background

1.1.1 Canadian Oil Sands

The limited ability of conventional crude to meet the growing demand for fuel has led to the need to diversify towards unconventional fossil resources such as oil sands. Canada's oil sands are the third largest oil reserves in the world, after those in Venezuela and Saudi Arabia [1]. Most of Canada's reserves (166 billion barrels) are in the province of Alberta [1]. These oil reserves, along with Canada's substantial oil production, have led to significant overseas interest, particularly from Asian countries [2], including the heavy financing of Canada's oil sands sector by Chinese companies [3] (see Appendix A, Table S2). In addition to investments from China, there has been significant involvement from Korean and Thai oil and gas companies [3]. All of this indicates considerable interest by Asia-Pacific countries in Canada's oil sands sector.

Emerging markets from the Asia-Pacific region, particularly China, Japan, and India, offer huge opportunities for Canadian oil sands supplies. Industries from both Canada (Athabasca oil sands Corporation, Nexen, etc.) and China (Petro China, Sinopec, China National Offshore Oil Company [CNOOC], etc.) are cooperating with joint venture investments in the Canadian oil sands sector to advance market opportunities for both countries [3]. Although it is of Canada's interest to gain access to emerging overseas markets, there is very limited strategic framework to bring these markets together. Therefore, it is necessary for the Canadian government, industry, and policy makers to develop a proper strategic framework for a trade market relationship, particularly in the oil sector.

Although Canada has vast oil reserves (166 billion barrels) in the province of Alberta [1], the delivery of oil sands products to Asia Pacific could be challenging. The challenges that could include infrastructure development, reliable supply of products, environmental concerns, and oil tanker traffic issues in the port of Vancouver, a western port city in Canada, arising from strategic policy constraints. To overcome these challenges, government, industry, and policy makers in both Asia Pacific and Canada need science-based credible information on cost of transportation of products to Asia Pacific and the associated environmental impacts with the transportation of Canadian oil sands product to Asia Pacific. The focus of this research is on supply chain cost and environmental impact side in the delivery of Canadian oil sands products in the form of synthetic crude oil (SCO) and dilbit (bitumen mixed with diluent to lower its viscosity) to Asia-Pacific region.

There is a high demand and limited supply of oil in the Asia-Pacific region. In order to meet demand, refinery capacities in the Asia-Pacific are increasing [4], which in turn provides opportunities to expand the future market of Canadian oil sands products. Eastern Asia, particularly China, India, and Japan, have the largest number of refineries [4]. The International Energy Agency (IEA)'s World Energy Outlook projects that these countries will consume 20.6 million barrel per day of oil by 2020 [5]. This figure suggests that the Pacific Basin is a valuable prospective market for Canada. Apart from product demand, the attractiveness of heavy crude oil to refiners in the Pacific Basin is driven by other factors such as refinery configuration, shipping consideration, and refining capacity [4]. The fast-growing economy of China alone is a substantial market for Canada. China imported on average nearly 6.2 million bbl/day of crude oil in 2014, an increase of 9% from 5.6 million bbl/day in 2013 [6]. Most of the crude oil is imported from the Middle East and Africa [7]. There are 56 large refineries in China (see Appendix A) [8]. China's installed crude refining capacity reached nearly 14.2 million bbl/d in 2015, about 680,000 bbl/d higher than in 2013 [7]. These refineries have been grouped based on their complexity and configuration and are shown in Table 1.

Table 1: Refinery capacity and configuration of China [8]

Crude Source	**Group A** **Deep Conversion Coking, cracking and hydro cracking**	**Group B** **Deep conversion coking and catalytic cracking**	**Group C** **Complex coking and hydro cracking**	**Group D** **Complex Catalytic cracking and or hydro cracking**	**Group E** **Other and miscellaneous independent**
Total crude oil produced (kbd)	2660	730	1724	1930	907

Crude Source	Group A Deep Conversion Coking, cracking and hydro cracking	Group B Deep conversion coking and catalytic cracking	Group C Complex coking and hydro cracking	Group D Complex Catalytic cracking and or hydro cracking	Group E Other and miscellaneous independent
Average API	32.5	31.5	32.2	33.2	32.7
Average wt.% of sulfur	0.88	0.80	0.66	0.57	0.47

The API ranges shown in Table 1 are within synthetic crude oil (SCO) ranges obtained after upgrading Canadian oil sands products; thus these products can be supplied to China in the form of SCO. Figure 1 shows that since 2009, refinery use in China has been between 82 and 86%. However, according to EIA 2015 [7], use is falling below these rates, which indicates that there are potential markets for Canadian oil sands products in China.

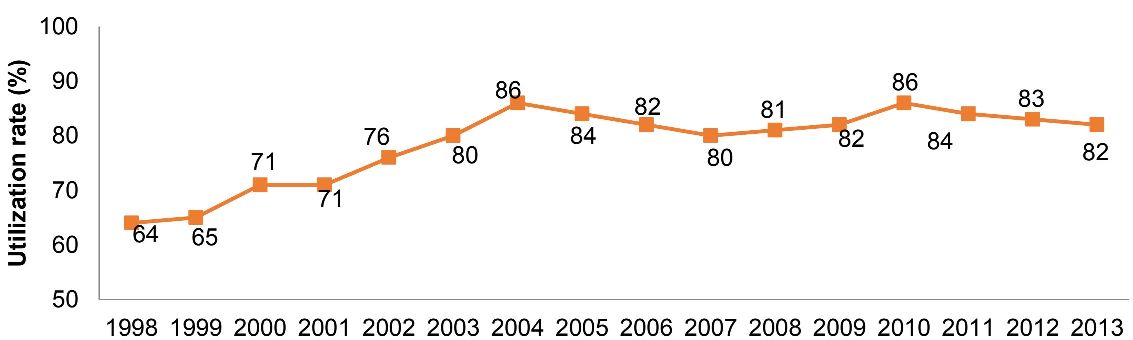

Figure 1: Utilization rates of refineries in China [9].

The refineries capacity in India reached 3.7 million bbl/d in 2010, with utilization rate more than 100% [8]. However, based on the information provided in the report [8], about the categories of refineries capability of handling the crude of API value ranged from 32.0-35.5, it is possible to supply Canadian oil sands products in the form of SCO in future with the possibility of expansion of their refineries capacity. While for Japan, the refineries capacity reached 3.8 million bbl/d in 2016 [10], however the expansion of these refineries in future is uncertain. Based on the information provided by Stratas Advisors [11], it might be possible that the refineries in Japan can handle the Canadian SCO.

China is the world's largest carbon dioxide emitter [12]. The transport sector in China is one of the fastest-growing GHG emission sources [13]. The CO_2 emissions from the sector increased from 79.67 Mt in 1985 to 887.34 Mt in 2009, with annual increase of 10.56% [14]. China faces the challenge of reducing the amount of GHG emissions produced annually. The Chinese government committed to reducing the CO_2 emissions per unit gross domestic product (GDP) by 40-45% by 2020 compared to the 2005 level [15]. However, due to the substantial increase in passenger transport with the rise in the economy, urbanization, and energy demand, GHG emissions are expected to increase. Therefore, in order to mitigate these emissions, Chinese government, industry and policy makers first need to understand the environmental impact of the life cycle (LC) emission of imported crude (Saudi Arabian crudes) as well as those that can occupy the future Chinese oil market (Canadian oil sands products).

Meanwhile, the oil import-to-demand ratio in the U.S., Canada's largest export market for energy products, particularly the U.S. PADD II market (where 60% of oil sands products are consumed [16]), is dropping. Due to a surge in crude oil production, particularly from the oil shale boom in the U.S. shale plays, U.S. oil imports have decreased overall [17]. To curtail the risk of Canada's dependence on a single market, diversification is necessary. However, due to limited publically available information on refineries in the Asia-Pacific, the demand for oil sands products to that region is uncertain. Thus there is a need for a study that includes both Asia-Pacific refinery configuration and supply chain costs of oil sands products to the Asia-Pacific.

According to CAPP, as of 2014, oil sands production was 2.2 million bbl/day, of which 1.2 million bbl/day were recovered from in situ and 0.9 million bbl/day from surface mining**.** Oil sands production is projected to increase to 3.1 million bbl/day by 2020 [5]. However, Canada's oil refinery capacity is expected to remain fairly constant at around 600,000 bbl/day to 2020 [18]. The surplus oil sands products need a route to the potential market in the Asia-Pacific. Canadian oil sands projects will benefit geographically as routes to the Pacific Basin do not have choke points like the Panama Canal, the Strait of Hormuz, and the Strait of Malacca. Furthermore, Canada's stable political system can help Asian countries build long-term oil sands export contracts for a reliable supply of oil sands products. Asia-Pacific countries thus can help Canada both in its search for a new potential market and market diversification. This suggests that the trade relationship between Asia and Canada is potentially complementary, particularly in the oil sector. To take full advantage of this relationship and ensure a competitive place in the global oil market, both regions require a detailed techno-economic and comprehensive well-to-wheel (WTW) life cycle assessment (LCA) to understand the environmental impacts and evaluate the delivered costs of this supply chain.

1.1.2 Demand and Supply of LNG in Europe

Over the past decade, the imperative of emerging strategies on energy security through liquefied natural gas (LNG) import has occupied an unprecedented spot in the foreign policy agenda of the European Union. However, the growth of gas imports and the natural gas market diversification in Europe will be influenced by global natural gas market trends. In recent years, the demand structure of natural gas in Europe shows variability; the natural gas consumption reached approximately 400 billion cubic meters (bcm) in 2015 [19], with the net import of liquefied natural gas (LNG) increasing by 15.8% to 37.6 million tonnes after five years of continuous decline between 2009 and 2014 [20]. This increase can be due to the convergence of Asian LNG spot prices and European LNG prices in 2015 [21] and the decline of domestic natural gas production in Europe. According to the European Commission, the European Union (EU) imported a significant portion of natural gas from Russia, approximately 40% of its imports in 2015 [19]. This strong dependency dominated by a single supplier can increase the risk of a reliable supply of natural gas, as evidenced by the geopolitical tension between the Ukrainian government and Gazprom [22]. Norway is considered a secure supply source of gas to Europe; almost 37% of the EU's import in 2015 were from that country [19]; however the natural gas supply from reserves like Sleipner and Gullfaks South are now declining due to depletion [23]. Soderbergh et al. [24] showed the limited potential for increased export of Norwegian natural gas to Europe in future with gas production projected to decline by 2030. The North Africa region, particularly Algeria, is facing many challenges in unlocking tapped gas resources due to military and political problems and lack of investment [25]. Therefore, exploring potential suppliers of LNG, particularly in Canada, through the development of new infrastructures has resulted in unprecedented interest from the European government and industrial leaders.

Natural gas is a vital source of energy in Europe and is expected to remain as clean and key source of energy supply in future. The Netherlands, Spain, German, Italy, the United Kingdom, and France account for three-quarters of European gas consumption, imported either by pipeline or LNG carriers to import terminals [26]. The regasification capacity of Europe's 23 major LNG import terminals was 201 bcm/yr in 2014, which could supply 41% of Europe's natural gas demand if fully used [27]. However, the use rate of LNG import terminals in 2014 was only 19% [27]. This provides a huge opportunity for Canadian LNG, which can supply 81% of the total capacity of the regasification facility, equivalent to 163 bcm. Apart from this, the European Union is highly interested in considering LNG an important source of their energy security, as evidenced by the adoption of the Energy Security Strategy in 2014 and Energy Union projects with high priority given to identifying and building new supply routes [19] as well as the 20 large-scale LNG import terminals currently planned, mostly in Europe [20]. All of these create a new opportunity for Canada to explore further the natural gas supply chain market. In order to understand the full potential of Canadian LNG in European markets, it is necessary to evaluate the delivered costs and life cycle GHG emissions risks of the Canadian natural gas supply chain to Western Europe.

1.1.3 Canadian Liquefied Natural Gas (LNG)

According to the National Energy Board, the Western Canada Sedimentary Basin (WCSB)[1] has tremendous natural gas potential with 855 trillion cubic feet (tcf) of remaining gas reserves in 2014, from which 14.7 billion cubic feet per day (bcf/d) were produced; production is projected to increase to 17.9 bcf/d by 2040 [28]. With advanced technology in fracturing and well drilling, natural gas production continuously exceeds domestic consumption and is expected to continue to do so in future. Canada's surplus natural gas production needs to find potential customers through the best possible route to Western Europe, in order to trade competitively. For European countries, Canada's stable political system is attractive, especially when the expected reliable supply of natural gas from Russia, Algeria, etc., is at risk because of geopolitical tension. The long-term natural gas export market can build consistent energy security that provides both a reliable supply of natural gas to Europe and a new market opportunity for Canada. Meanwhile, the U.S., Canada's only natural gas export market, has increased the supply risk and left Canada with no option but to explore a potential alternative gas market. The rapid development of the shale gas boom in the U.S. has lowered demand for Canadian natural gas [29]. Thus, exploring the potential market of Canadian LNG to Europe deserves significant research attention. In this work, the delivered costs and environmental impacts of the Canadian LNG supply chain through all the possible routes to European countries were evaluated.

[1] The WCSB includes parts of B.C., Alberta, Saskatchewan, and Manitoba

1.2 Literature review and research gap

Few studies include a techno-economic assessment (TEA) of the supply chain of the production, transportation, upgrading, and shipping of Canadian oil sands products. A few authors have focused on some of these processes individually by considering their energy consumption, emissions, and cost. A model, FUNNEL-GHG-OS (FUNdamental ENgineering PrinciplEs-based ModeL for Estimation of GreenHouse Gases in the Oil Sands), developed by Nimana et al. [30, 31], was used to estimate the energy consumption and GHG emissions in SAGD technology and upgraders. Some data on the economic feasibility of the SAGD plant can be found in the literature [32, 33]. Other studies [34, 35] investigated energy costs of Canadian oil sands operations. The findings of Giacchetta et al. [36] were based on an economic and environmental analysis of a SAGD facility. Tarnoczi [18] developed a life cycle assessment (LCA) model to compare the energy inputs and GHG emissions of pipeline and rail transportation for oil sands products. Two studies [37, 38] incorporated estimates of fuel consumption and associated emissions from shipping crude oil by tanker. None of these studies evaluate the supply chain costs of Canadian oil sands pathways to Asia-Pacific. The NEB (2006) estimated the supply costs for SAGD and the upgrader at the plant gate to be C$18-22 per barrel bitumen and C$39 per barrel SCO, respectively [39]. However, that study did not detail costs relating to technical parameters, variability in cogeneration systems, or upgraders. Earlier studies by Natural Resources Canada [40] and the Argonne National Laboratory [41] did not consider supply chain costs for each pathway. As of now, there are very few studies that focus on overall supply chain costs of oil sands products from production, transportation, upgrading, and shipping to the Asia-Pacific region.

Similarly, few published studies assess the life cycle (LC) GHG emissions associated with the transportation of Canadian oil sand products for use as transportation fuel in China. Most studies focus on LC emissions from conventional and non-conventional crudes imported from Canada to the U.S. A few studies modeled all the possible pathways of Canadian oil sands products [40-42]. An LCA model developed by Keesom et al. [43] compared LC GHG emissions of oil sands and other conventional crudes processed in the U.S. Yan and Crookes [44] assessed energy use and GHG emissions for different types of fossil fuel in China to identify the better choice in terms of their advantages in life cycle fossil use and GHG intensity. Nimana et al. [42] explored all the possible routes of Canadian oil sands supply chains from bitumen extraction to end use in vehicles by conducting a comprehensive LCA of transportation fuels derived from Canada's oil sands, but that study only considered transportation fuel use in the

U.S. Tarnoczi [18] conducted a life cycle assessment to evaluate LC energy inputs and the intensity of GHG emissions from pipeline and rail transportation of Canadian oil sands products. In a work by Verma et al. [45], the transportation costs of oil sands products via rail and pipeline were compared for different market distance and capacity by developing the techno-economic models. Nimana et al. [46] evaluated the energy use and greenhouse gas emissions of three scenarios of transporting SCO, dilbit and without return scenarios using bottom-up approach. Two LCA models, i.e., GREET (the Greenhouse gases, Regulated Emissions, and Energy Use in Transportation Model) [41] and GHGenius [40], were used to quantify WTW GHG emissions for transportation fuels derived from crude oil. None of these studies addresses the WTW GHG emissions from Canadian oil sands products for use as transportation fuel in Asia-Pacific countries. Other studies [47, 48] used the GHOST (GreenHouse gas emissions of current Oil Sands Technologies) model to calculate the upstream emissions from oil sands (rather than WTW LC emissions) with confidential data from industry. Charpentier et al. [49] reviewed thirteen LCA studies associated with oil sands operations to quantify the GHG emission intensities of fuel production pathways. Abella et al.'s [50] findings from PRELIM (Petroleum Refinery Life-cycle Inventory Model) were based on energy consumption and GHG emissions from the refining of crude slates. However, the life cycle GHG emission intensity of the Canadian oil sands supply chain in the delivery of oil sands products to China is still unknown.

There are no studies in the published literature focused on techno-economic and life cycle assessment modeling with the explicit consideration of supply chain costs and environment risk in the delivery of Canadian LNG to Western Europe. Previous research on techno-economic analyses of LNG supply chains is quite widespread and mostly focused on individual assessments of the processes involved in the supply chain such as gas processing (dehydration, gas sweetening, and natural gas liquid recovery in an LNG plant), shipping, and gas production. Some efforts have been made to conduct an economic analysis of natural gas processing with different technologies [51, 52], and other authors [53, 54] investigated the shipping cost of LNG, albeit with limited approaches of fundamental engineering principles. Javanmardi et al. [55] studied the cost of liquefying natural gas and transporting it from the South-Pars gas field in Iran to the potential natural gas market worldwide. Raj et al. [56-58] conducted the detailed techno-economic analysis of liquefied natural gas production facilities in Western Canada and evaluated the supply chain costs and life cycle GHG emissions in the delivery of Canadian LNG to Asia. Other research studies are focused in a life cycle analysis of extraction and processing shale gas using data from the shale gas reserves in the U.S. [59-62].

Although there is great interest from Canada and Europe in exploring the potential natural gas market, the minimum supply chain costs and the life cycle GHG emissions of the Canadian LNG supply chain in the delivery of LNG to Western Europe are still unknown. This research was conducted to address such gaps through the development of techno-economic and life cycle assessment models.

1.3 Research motivation

This work is motivated by the need to diversify the Canadian oil and gas export market in order to reduce the economic challenges Canada faces through its sole dependency on the U.S. market. Canadian oil and gas can be supplied to the market through different routes in different forms. It is important for Canada to have science-based credible information on cost and LC GHG emissions make informed decisions. The following points can further summarize the motivating factors and areas of research:

- In order to diversify the Canadian oil sands and natural gas markets from the single continental market to emerging overseas markets, it is necessary to benchmark the pathway that has the lowest supply chain costs.
- Canadian oil sands and LNG go to market in different forms through different flexible pathways that vary in supply chain costs. So, in order to determine the competitive price, it is necessary to quantify and compare the total supply chain cost of all potential pathways.
- It is important to compare life cycle (LC) GHG emissions from Canadian oil sands products and LNG supply chains for transportation fuels and electricity use in the Asia-Pacific region, particularly China and Western Europe, to understand the environmental risk associated in their delivery to the respective markets.
- With several possible supply chain pathways for Canadian oil sands and LNG, it is important that industry, policymakers, governmental and non-governmental organizations understand the implications and least GHG-intensiveness of these pathways using a life cycle analysis approach.
- To stress the areas where production, transportation, and upgrading costs could be decreased, it is necessary to understand the sensitivity of technical parameters on the production, transportation, upgrading, and shipping costs of Canadian oil sands products.
- To highlight the most GHG-intensive stage in total WTW GHG emissions and observe the possible areas of improvement in that stage, it is necessary to evaluate the

emissions of each unit operation and conduct a sensitivity analysis of technical parameter on GHG emissions.

To address these areas and help formulate a strategic policy on exporting oil sands products and natural gas, detailed data-intensive techno-economic and comprehensive life cycle assessment (LCA) models were developed.

1.4 Research objectives

The overall objectives of this study are to develop detailed data-intensive techno-economic and life cycle models for the delivery of Canadian oil sands products and LNG to Asia-Pacific and Western Europe, respectively. The specific objectives are to:

- Develop a detailed data-intensive techno-economic model to evaluate the production, transportation, upgrading, and shipping costs of Canadian oil sand products.
- Conduct a comparative cost analysis of potential pathways for Canadian oil sands products (SCO and dilbit) and LNG to seaport destinations in the Asia-Pacific and Western Europe, respectively.
- Quantify the comparative energy inputs and GHG emissions from Canadian oil sands products for transportation fuels in China.
- Develop a life cycle assessment (LCA) model in order to conduct a comprehensive well-to-port (WTP) life cycle analysis on the delivery of Canadian LNG to north and southwest Europe.
- Apply the developed LCA model to compare the LC GHG emissions among various possible pathways of oil sands products and LNG supply chains.
- Identify the pathway with the highest and lowest GHG emissions in the production of transportation fuels and electricity in China and Western Europe from Canadian oil sands products and LNG, respectively.
- Conduct sensitivity and uncertainty analyses for GHG emissions and supply chain costs with their corresponding technical parameters.

This research can help government, industry, and policy makers to better understand the GHG footprints and costs of Canadian oil sands and LNG supply chains.

1.5 Organization of the thesis

The thesis has five chapters, three appendices, a table of contents, a list of figures, a nomenclature, a list of acronyms, and references. This thesis is a combination of papers. Each chapter is intended to be read independently and is written in research paper format.

Chapter 2, A techno-economic assessment of the extraction, transportation, upgrading, and shipping of Canadian oil sands products to the Asia-Pacific region: This chapter describes the development of the data-intensive techno-economic model and evaluation of the production, transportation, upgrading, and shipping costs of Canadian oil sands products. The model is applied to conduct a comparative cost analysis of potential pathways for Canadian oil sands products (SCO and dilbit) to seaport destinations in the Asia-Pacific region. Appendix A contains additional details related to chapter 2 such as a resistance model of shipping, the shipping costs of different size tankers, refinery capacity in China, a sensitivity analysis, an SAGD flow model, and investment in the Canadian oil sand sector from the Asia-Pacific region.

Chapter 3, A well-to-wheel life cycle assessment (LCA) of greenhouse gas emissions from Canadian oil sands supply chain for transportation fuels China: This chapter seeks to quantify the comparative energy inputs and GHG emissions from Canadian oil sands products for their use as transportation fuels in China. The LCA model was used to evaluate the GHG emissions' intensity of eight routes that may serve Canada's oil sands markets in future. The WTW results were compared with the calculated WTW emissions values of Saudi Arabian crude for transportation fuel use in China.

Chapter 4, Techno-economic and life cycle assessment of the natural gas supply chain from Canada to north and southwest Europe: This chapter seeks to quantify the delivered costs and environmental risks associated with the delivery of Canadian LNG to north and southwest Europe. This study compared the delivered costs and environmental impacts of two supply chain routes to north and southwest Europe. The delivery costs and the LC GHG emissions of Canadian LNG are compared with those from the main exporting countries like Norway, Russia, and Algeria to European countries.

Chapter 5, Conclusions and Recommendations: This chapter concludes the findings and observations from chapters 2, 3, and 4. It also identifies possible areas of improvement in the current model and provides recommendations for future work.

Chapter 2[1]

A techno-economic assessment of the extraction, transportation, upgrading, and shipping of Canadian oil sands products to the Asia-Pacific region

2.1 Introduction

The oil shale boom in the U.S., along with technological advancements in drilling and fracturing, has increased oil production tremendously and decreased U.S. oil imports overall [17]. Currently, the Canadian oil sands market is highly dependent on a single customer. To reduce the economic risks in single market dependency, Canada needs to diversify its oil sands markets. However, the lack of data in the public domain about the complexity of the refineries in Asia-Pacific, particularly China, makes it difficult to predict the demand for suitable oil sands products there. Thus, there is a significant need for a data-based technical study that includes refinery configurations in Asia-Pacific as well as an economic study that focuses on overall supply chain costs of oil sands products to regions such as Asia-Pacific. There are few studies in the public domain on the feasibility of Canadian oil sands projects to supply products to China, Japan, and India. In order to understand the feasibility of the oil sands supply chain projects, first the minimum delivered cost for oil sands products supply chains needs to be investigated. In 2006 the NEB estimated the supply costs for SAGD and an upgrader at the plant gate to be C$18-$22 per barrel bitumen and C$39 per barrel SCO, respectively [39]. However, that study did not detail the costs relating to technical parameters, the impact of cogeneration systems, or upgrading configurations. Most studies focus on LC emissions from conventional and non-conventional crudes imported to the U.S., and some modeled all the possible Canadian oil sands products LC pathways. Few investigated energy costs of Canadian oil sands operations [34, 35]. None of these studies evaluate the supply chain costs of Canadian oil sands pathways.

This chapter details the economic assessment of each stage in the operations and evaluates the total supply chain cost in the delivery of dilbit and synthetic crude oil (SCO) to China, Japan, and India. The model was used to evaluate the supply chain costs of pathways (shown in Fig. 2) that may serve future Canadian oil sands markets.

---

[1] This version of chapter has been submitted to Applied Energy for publication: Sapkota K., Oni O. *A., Kumar A. Techno-economic assessment of the extraction, transportation, upgrading, and shipping of Canadian oil sands products to the Asia-Pacific region. Applied Energy, 2017 (in review)*

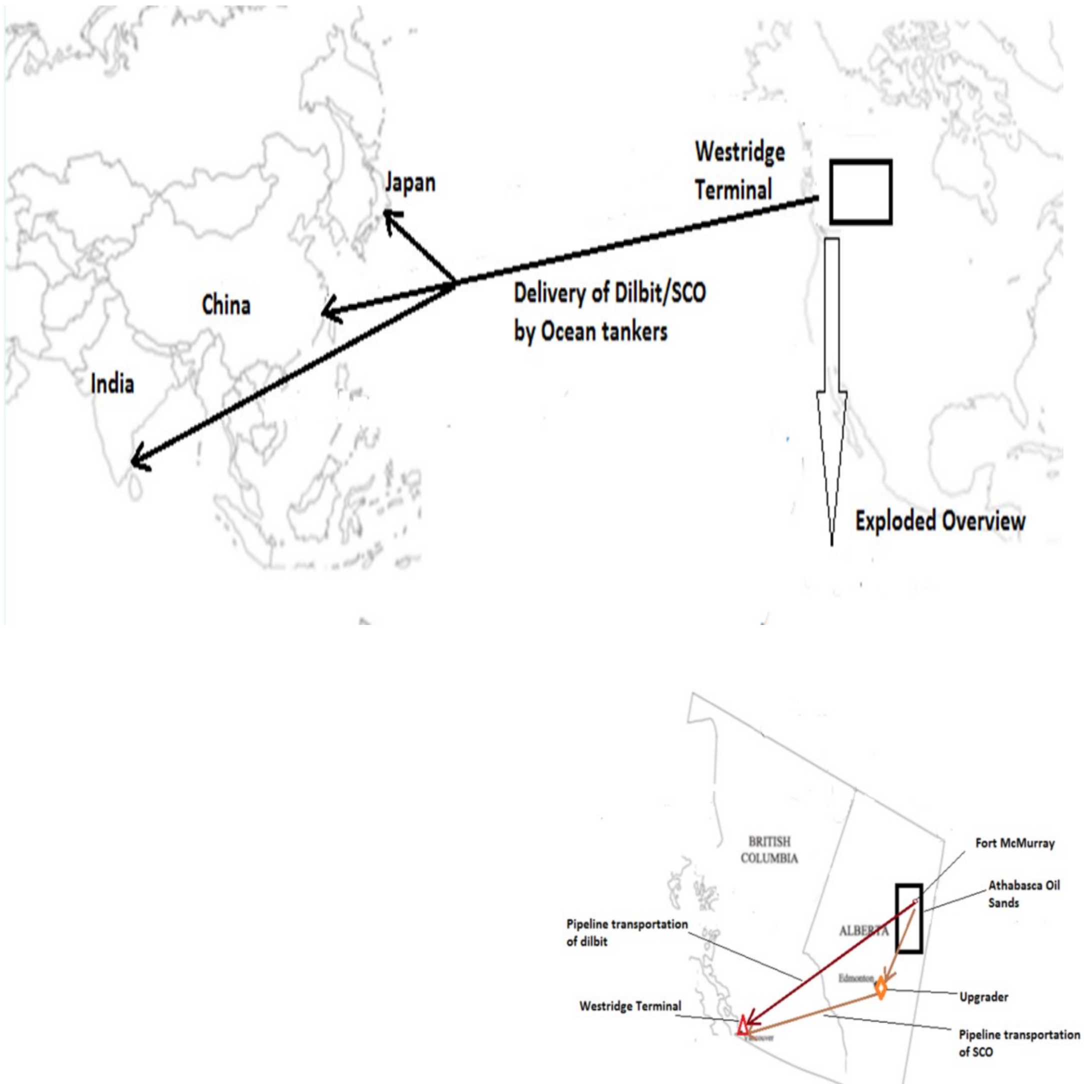

Figure 2: Overview map of the Canadian oil sands supply chain route from Canada to Asia-Pacific.

Although various technologies are used for the production of bitumen, this study focused on SAGD, which is the most widely used. Pathways were constructed using both delayed coking units (DCU) and hydroconversion units (HCU) to produce SCO. This section also describes the assumptions and methodology used to develop the model. The model quantifies the production, pipeline transportation, upgrading, and shipping costs in order to evaluate the total supply chain cost. The model further explores the impact of cogeneration and variability in diluent return conditions on the supply chain cost. In addition, uncertainty and sensitivity analyses were conducted for each unit operation.

2.2 System boundary and methodology

2.2.1 System boundary

Figure 3 shows the system boundaries used for the cost evaluation of Canadian oil sands products' supply chains. The boundaries include the production, upgrading, transportation, and shipping of SCO and dilbit to the Asia-Pacific region. Although various technologies are used to produce bitumen, this study focuses on SAGD, the most widely used technology [36]. The viscosity of the bitumen extracted from SAGD is high. For this reason, it is mixed with a diluent such as natural gas condensate or naphtha. The bitumen-to-diluent mixture is called dilbit and bitumen-to-diluent mixture is in a ratio of 70:30. This mixture enhances transportation by maintaining an appropriate viscosity and API value. In system boundary 1 (Fig. 3a), dilbit is transported from the extraction site to the upgrader via pipeline (500 km), then SCO is transported by pipeline (1147 km) to the Westridge terminal, and from there the SCO is transported to the destination port by oil tanker. In system boundary 2 (Fig. 3b), dilbit is transported by pipeline (1647 km) from the extraction site to the Westridge terminal, transported by oil tanker to the port, and upgraded in the destination country. In both systems, the tanker sails to the destination port fully loaded, discharges cargo, and sails back to the Westridge terminal in ballast. Shipping fuel cost is calculated based on an optimized speed as well as a short-term chartering contract in which the charterer pays fuel consumption costs, port and passage fees, and hiring cost on per-day basis to the ship owner. Seven scenarios were developed based on the fuel used in the main and auxiliary engines as well as on propulsion system in order to determine the most economical shipping pathway.

Variability in the cogeneration system and the diluent return condition is considered in both system boundaries. The pathways are set based on the two most common upgrader configurations, a delayed coking unit (DCU) and a hydro-conversion unit (HCU) [30, 63, 64]. SCO produced from an upgrader is transported to a sea port through Trans Mountain Pipeline. This is the only 300 kbd pipeline system in Canada that can transport both crude oil and refined products 1147 km to the Westridge sea port terminal [65]. System boundary 1 represents the existing pathway up to the Westridge terminal port. However, there is a possibility that an upgrader and more complex refineries will be added in the Asia-Pacific region, particularly China, in future. For this reason, system boundary 2, in which supplied dilbit is upgraded in China, is presented. With these system boundaries, four pathways were developed that are likely to be used by industry.

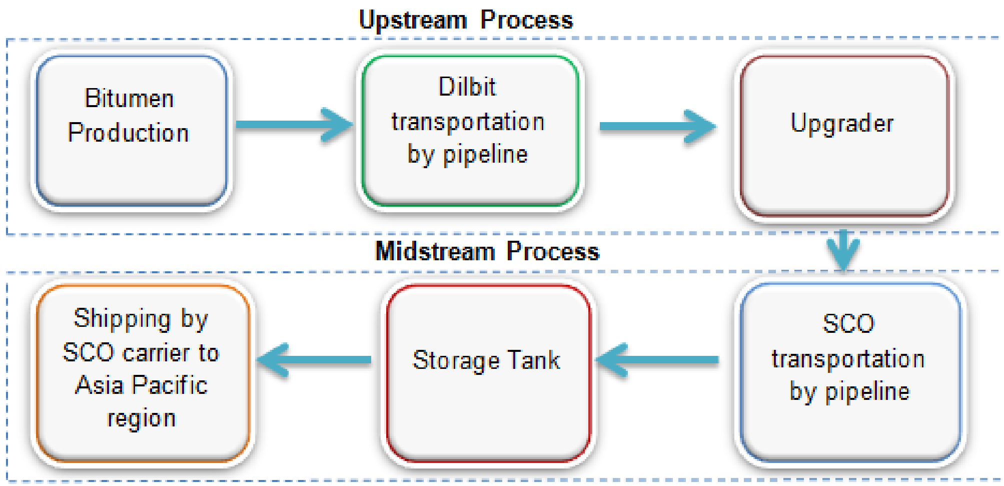

(A) System boundary 1

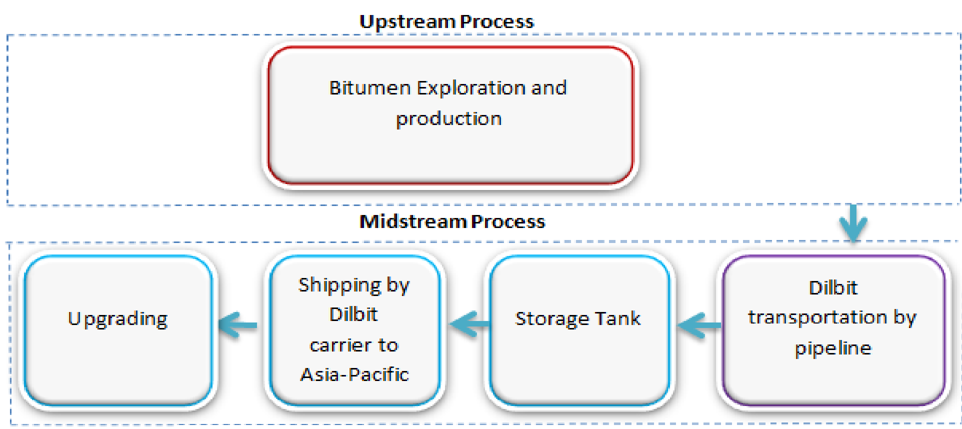

(B) System boundary 2

Figure 3: The Canadian oil sands supply chain: (A) System boundary 1 includes extraction by SAGD, dilbit transportation by pipeline (500 km), upgrading, SCO pipeline transportation (1647 km) to the Westridge terminal, and shipping to China. (B) System boundary 2 includes extraction by SAGD, dilbit transportation by pipeline (1647 km), shipping dilbit to China, and upgrading.

2.2.2 Cost estimate

A data-intensive techno-economic model was developed to estimate the production, transportation, upgrading, and shipping costs of Canadian oil sands products. All the unit processes were identified and the required equipment was characterized. Energy inputs to each unit operation were evaluated to find the energy cost of each unit. The capital costs of the

SAGD and upgrader for their designed capacity (single phase)[2] were estimated using the capacity factoring method. Data were collected from the literature and a scale factor was developed. In order to estimate the cost, discounted cash flow analysis (DCFA) was used for SAGD and upgrader operations. To estimate transportation costs, operation costs including capital, operating and maintenance, labor, and variable costs were added. All the costs were estimated in CAD$ for the year 2014. Eq. 11-14 in Appendix A were used to develop the DCFA model for the SAGD and upgrader unit.

The shipping costs of SCO and dilbit were calculated as shown in Figure 3. Most of the design data (overall length, draft, breadth, etc.) were obtained from the Clarkson data sheets [66]. Based on these design parameters, total calm water resistance was calculated using Holtrop and Mennen's approximate power prediction approach [67] and statistical power prediction method [68]. Air resistance and total calm water resistance was added to obtain the required towing power at a given vessel speed. The propeller efficiency is added to towing power to obtain the braking power. In this study, an engine margin of 10% and a sea margin (waves, winds, steering effects, etc.) of 15% was assumed, as given in the ITTC – Recommended Procedures and Guidelines [69]. All these margins were combined, along with propeller efficiency and towing power, to obtain the installed power of the engine. A suitable engine was selected based on the installed engine power values. This approach helps develop the main engine power required for the vessel. Using the time of travel and specific fuel consumption data for the selected engine, total fuel consumption of the main engine was calculated.

Auxiliary engine fuel consumption was calculated based on the power required at sea, for manoeuvring, and while dwelling. However, vessels do not use the total installed power of the auxiliary engine. Depending on factors like weather, loads of 13%, 45%, and 67% were considered when the vessel is at sea, manoeuvring, and dwelling, respectively [70]. Dwelling energy consumption includes primarily the power demand of lights, HVAC system (heating/ventilation/air conditioning), communications, and other power needs in the vessel at sea as well as in port. There is very little chance of precipitation forming in SCO, so no heating is required; however, Canadian dilbit contains a high percentage of asphaltenes and its viscosity is about 200 cSt [71], and so it needs to be heated to avoid precipitation in the tanker and to reduce viscosity while discharging. This study assumes that dilbit temperature is maintained at 30˚C in the tanker and 50˚C while discharging [72]. The other major costs are the vessel hiring

[2] The capital cost of operations significantly depends on whether it is a grass-root operation or the expansion of an existing system. A single phase project was chosen in this study in order to analyze the production and upgrading costs.

cost and port and passage fees. The hiring rate depends on the vessel size and is charged on a per day basis. The port and passage fees are estimated based on tanker gross register tons, particularly for the China and Vancouver ports (base case).

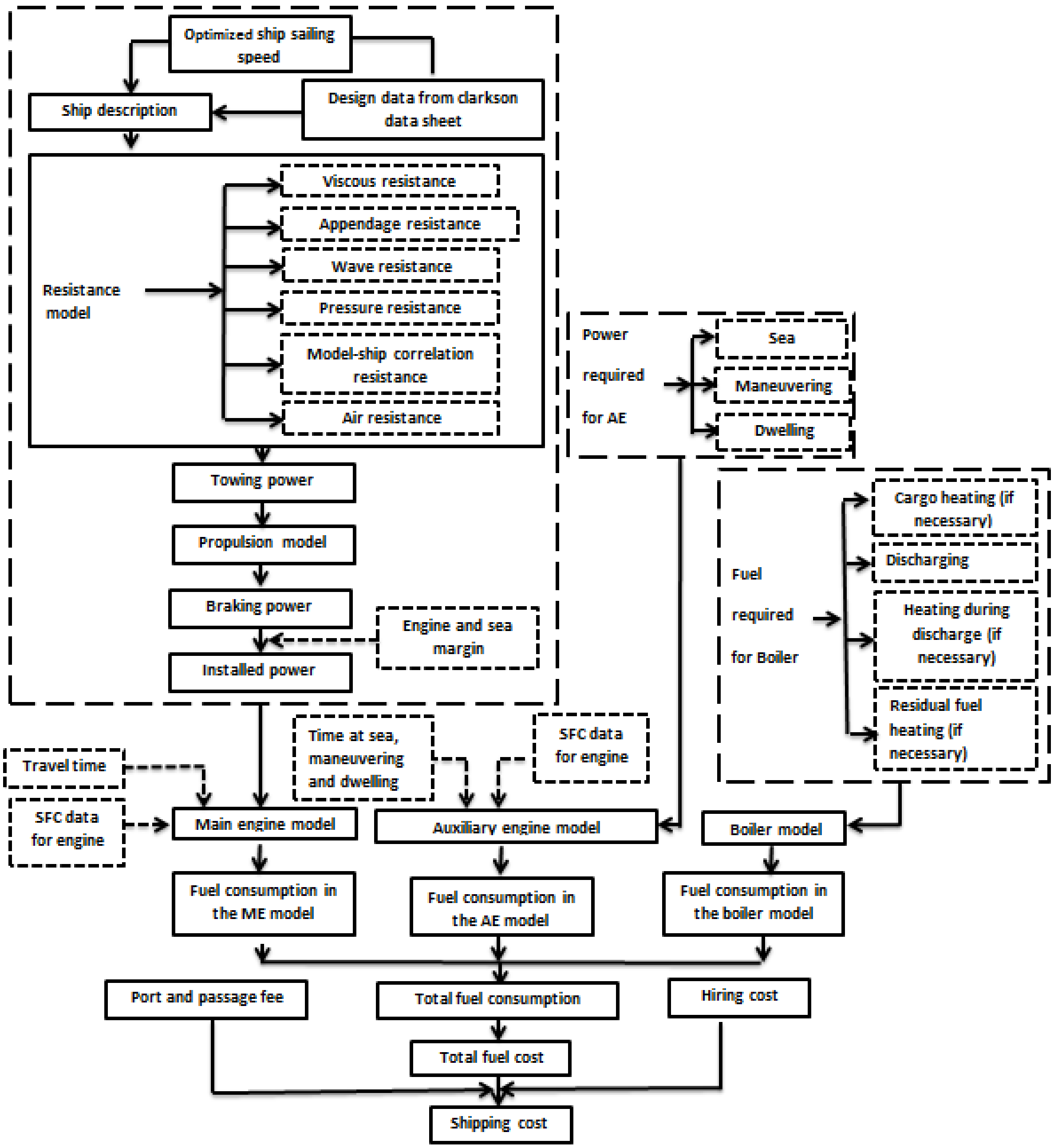

Figure 4: Shipping cost calculation method

Finally, total fuel cost, hiring cost, and port and passage fees are added to calculate the shipping cost per barrel SCO and dilbit. The shipping cost is calculated at different vessel speeds in order to determine the optimized speed, that is, the speed at which cargo shipping costs are lowest.

2.3 Developed models

2.3.1 SAGD

2.3.1.1 Plant description

Over 80% of Alberta's oil sands are below the earth's surface and are recovered using an in situ technique such as SAGD [73]. Existing and proposed projects using SAGD range from 30-60 kbd (single phase) [74]. The study model plant in this study has a capacity of 40 kbd [36], scales well for both large and small facilities, and has a steam-oil ratio (SOR) of 2.87, which is the aggregated production-weighted SOR over the seven-year period ending 2015[3]. The aggregated production-weighted SOR ranged from 2.61 to 3 during that time [75]. The plant in the developed model has a central processing facility (CPF) that includes an oil removal unit, a de-oiling unit, a cooling and separation unit, a water treatment unit, and a steam generator. 94 wells, grouped into six well pads, are assumed [36], as well as electric submersible pumps, which are considered to be the best choice for high production volumes [76]. The pumps are used to lift the emulsion from the reservoir. For steam generation, a combination of an evaporator and standard drum boilers is assumed over the traditional approach (once-through steam generation) because of their technical advantages, including greater reliability, high steam quality, reduced maintenance and operations requirements, less chemical handling, and ease of use [77].

In SAGD, a pair of horizontal well bores (an injector and a producer situated 4 to 6 m apart) is drilled into the oil sands, 80-1000 m deep, depending on the reservoir [78, 79]. In the CPF, steam generated from the drum boiler is injected into the well through the steam injection well. The steam heats the bitumen to a temperature at which it can flow by gravity into the producing well along with the condensed water. The emulsion from the reservoir is pumped to the CPF and cooled by sets of exchangers.

[3] 2015 data are for the months of January and February only

Table 2: SAGD model specifications

Parameters	Value	Comments	References
Well head pressure (kPa)	2200	Project-specific and 1100-4500 kPa	[79, 80]
Bottom-hole pressure (kPa)	1200	Project-specific and 390-4500 kPa	[79, 81, 82]
Pump efficiency (%)	70	Optimal operating range	[76]
Horizontal depth (m)	800	Project-specific and 550-1000 m	[31, 79]
Vertical well depth (m)	200	Project-specific and 80-1000 m	[31, 79]
Drum boiler efficiency (%)	97		[83]
iSOR	2.87	Weighted average SOR over 7 years	
Efficiency of gas turbine (%)	42.5		[36]
Efficiency of HRSG exhausts recovery (%)	65		[36]
Efficiency of HRSG direct firing duct burner (%)	90		[36]
Steam loss in reservoir (%)	10%	5-10%	[83]
Blow down loss from steam generator (%)	2%	1-3%	[84]

After the first stage of cooling, diluent is added in order to facilitate the separation of bitumen from water (since bitumen and water have almost the same density). Once diluent is added, it flows to the free-water knockout vessel where it is separated by gravity. The water flows to the de-oiling unit that includes a skim tank, an induced gas flotation (IGF) cell, and an oil removal filter (ORF) where sediment and oil are removed from the produced water. The water is treated so that it can be used again to produce steam. The parameters considered to estimate power and natural gas consumption are detailed in Table 2. This study explores two operations, one without cogeneration (a stand-alone operation) and one with cogeneration. A detailed schematic of the flow model for cogeneration systems is shown in Figure 5.

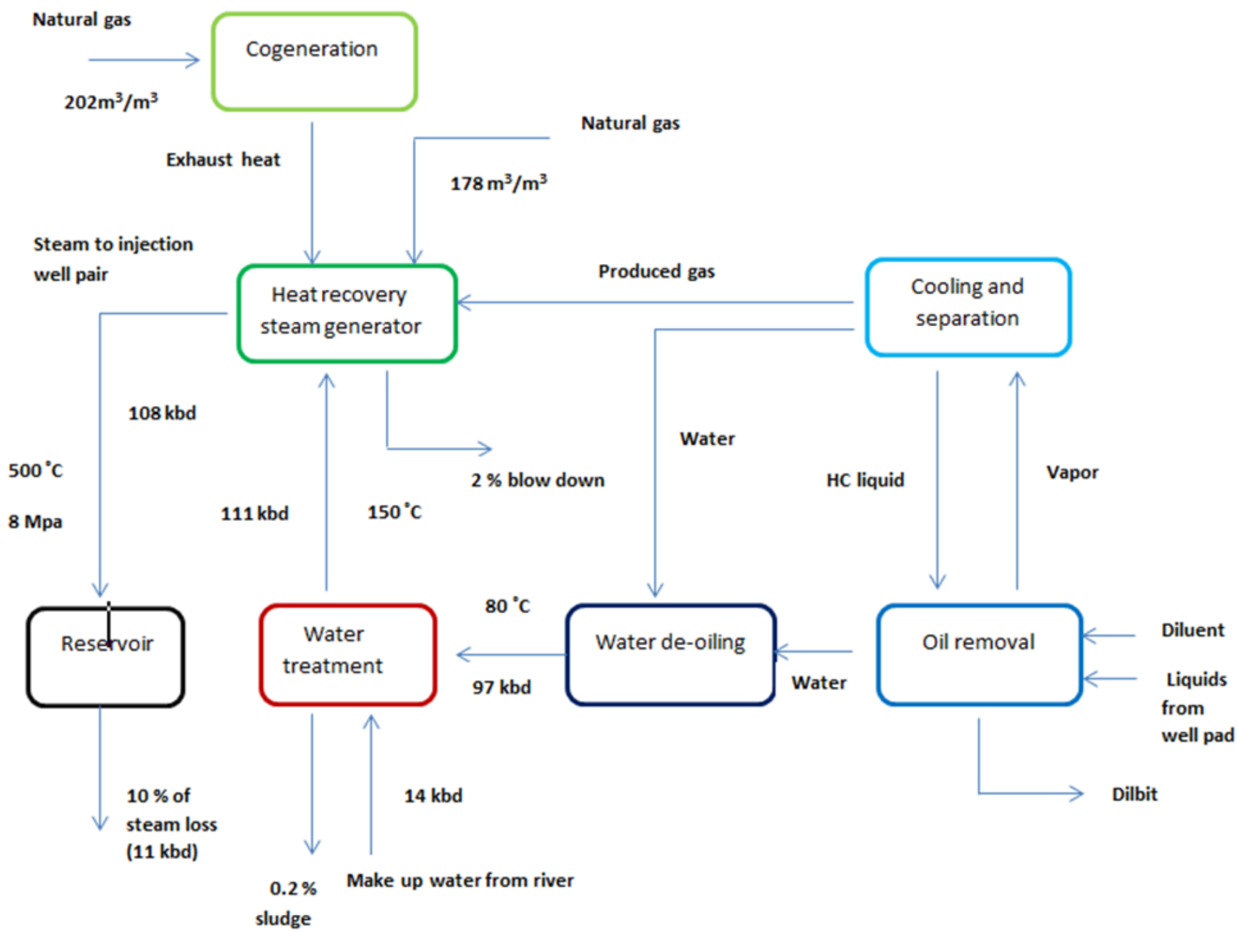

Figure 5: SAGD flow model with cogeneration

The operation without cogeneration uses a natural gas-fired drum boiler to generate steam on site and also purchases electricity from Alberta's grid. A cogeneration operation uses a natural gas-fired drum boiler integrated with a gas turbine and sells excess electricity to the grid. Because most SAGD operations are of this sort [85], our study only evaluates cogeneration operation using a gas turbine.

2.3.1.2 Cost model

The major costs considered for bitumen production are capital, operating and maintenance (O&M), natural gas, and electricity-related costs. Based on an earlier study [36], the capital costs used to develop the economic model include: the purchase of the land to build a plant;

permits/legal costs; plant operating equipment; construction costs; and financing/commissioning.

Table 3: Cost model SAGD specifications

Industrial parameters	Value	Comments/Reference
Plant capacity (kbd bitumen production)	40	Scales well for large and small facilities [36]
Initial capital cost for SAGD without cogen (M$)	890	Calculated using the capacity factoring method mentioned in [86] (see Eq. 8 in Appendix A). Capital investment is assumed to be 50%/year from start of construction to operation
Initial capital cost for SAGD with cogen (M$)	1250	Calculated using the capacity factoring method mentioned in [86] (see Eq. 8 in Appendix A). Capital investment is assumed to be 50%/year from start of construction to operation
Price of natural gas ($/GJ)	4.76	[36]
Electricity ($/kWh)	0.07	[87]
Discount rate	15%	Assumed
Capacity factor	93%	[83]
Scale factor	0.7847	Developed using data from literature [88, 89]
O&M cost (% of initial capital cost)	6%	[36]

Industrial parameters	Value	Comments/Reference
Plant life	25 yrs.	[36]

A large amount of natural gas is consumed in SAGD to generate steam. The cost of natural gas is considered separately in order to evaluate its impact on production costs. The operating and maintenance (O&M) costs are a significant portion of production costs and include equipment repairs, employee wages, contracted services, fees, inspection costs, and insurance [36]. Electricity purchase, administrative costs, and well pair maintenance are included in O&M costs [90]. Several O&M to capital costs ratio ranges are found in the literature, from 2.09% [91] to 8.8% [88]. A middle range value of 6% is selected in this study. The inputs for the development of the model are given in Table 3.

2.3.2 Upgrader

2.3.2.1 Plant description

Most large-scale commercial upgrading technologies use either thermal cracking-coking or hydrogen-based cracking-hydro conversion [63, 64, 92]. This study considers 100 kbd SCO productions (base case) for both the upgrading technologies. Capacities below this would not give an acceptable economic return in the oil industry [93], although Nexen/OPTI's Long Lake project started at 72 kbd [94] as it is a specific case. Delay coker and hydroconversion are the upgraders commonly used in the refineries. Generally, upgrading involves converting long chain hydrocarbons to smaller chain hydrocarbons. Increasing the hydrogen-carbon ratio is known as primary upgrading, and reducing the sulfur content to below 0.5% is known as secondary upgrading [30, 63]. A delayed coking upgrader has an atmospheric distillation unit (ADU), a vacuum distillation unit (VDU), a coking unit, a naphtha hydrotreater (NH), a diesel hydrotreater (DH), a gas oil hydrotreater (GH), a steam methane reforming unit (SMR), a plant fuel system, and a sulfur removal unit. When the coker unit is replaced by a hydrocracker unit, the new unit is referred to as a hydroconversion upgrader (HCU). Dilbit is heated by steam and a gas-fired heater in the ADU from 275˚F to 720˚F [95] to separate diluent, naphtha, diesel, and atmospheric residue (AR). The separated naphtha and diesel are treated in the hydro treating unit. The AR is sent to the VDU and heated further to yield light vacuum gas oil (LVGO), heavy vacuum gas oil (HVGO), and vacuum residue (VR).

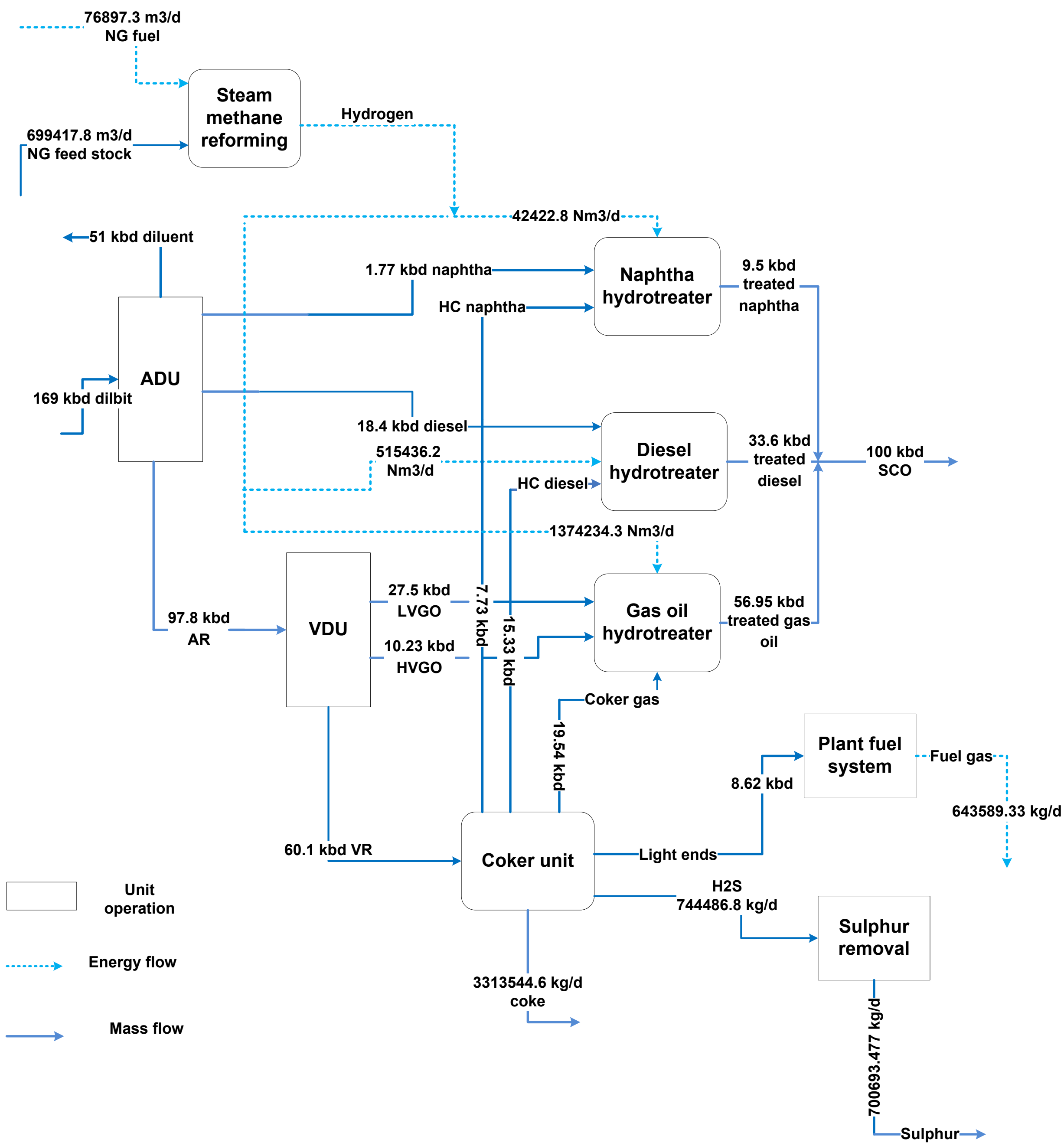

Figure 6: Flow model of delayed coking upgrader

The VR from the VDU is heated in the coking unit to approximately 500˚C [95], at which high-carbon residue molecules are deposited in the drum as coke and the lighter hydrocarbons produced are treated in the hydro treating unit. In the HCU, the heavy feed is cracked at a lower temperature of 350-430˚C under the high hydrogen partial pressure of 6000-1000 kpa [96]. The products from the NH, DH, and GH yield SCO. Both upgraders use SMR, and natural gas is used both a feedstock and fuel to meet hydrogen requirements [97]. This study explores the impact of cogeneration on the upgrading costs of SCO for both a DCU and an HCU. A detailed flow model of each is shown in Figures 6 and 7.

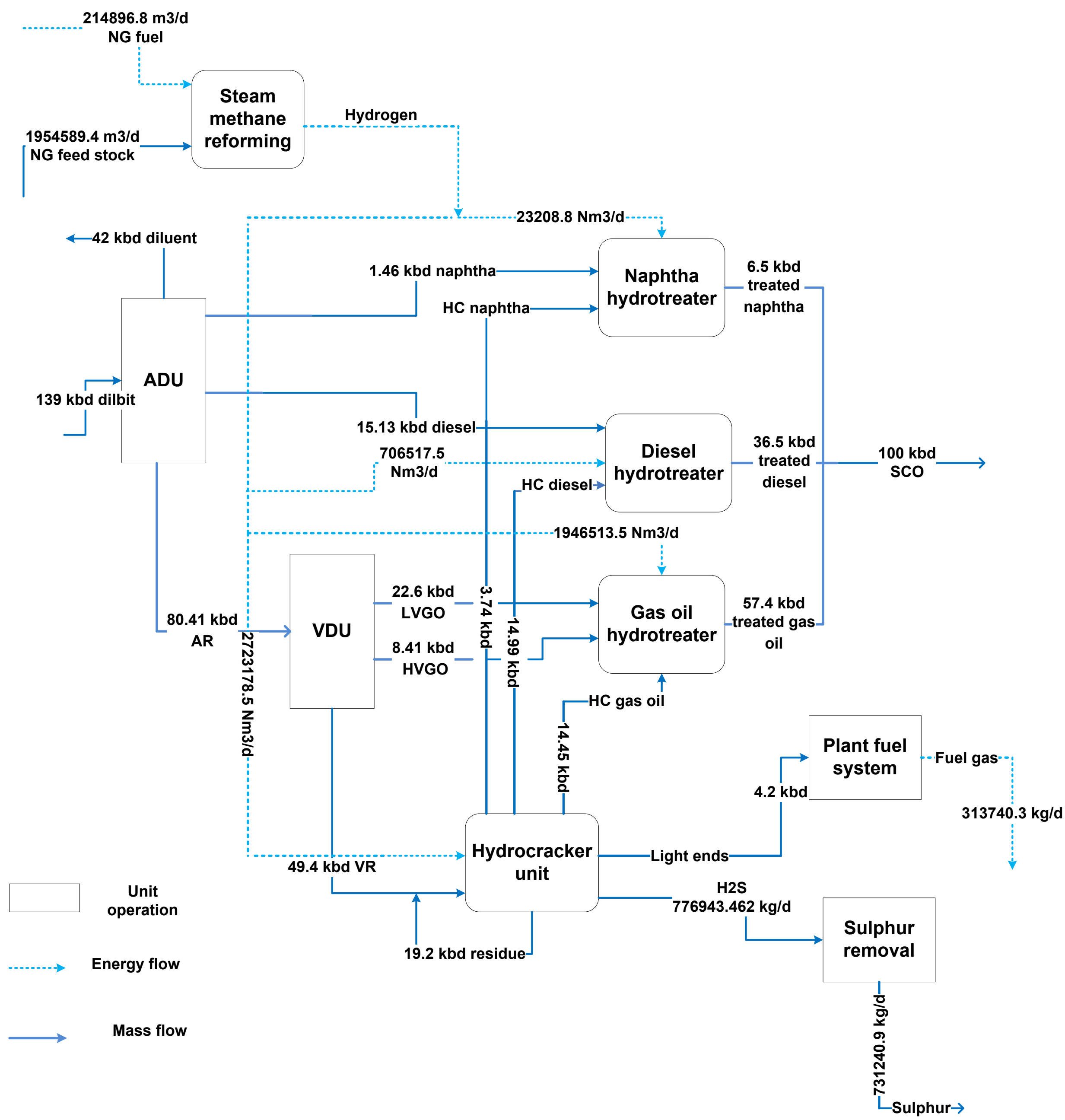

Figure 7: Hydro-conversion upgrader flow model

2.3.2.2 Cost model

The model developed to evaluate the upgrading costs includes capital, O&M, electricity, and natural gas costs. The capital costs include the costs involved in plant construction to start the operation and the equipment needed to run the plant. A four-year construction period is assumed [98] as well as equal initial capital investment each year. Several O&M cost to capital ratio ranges are found in the literature (from 4.0% [99] to 7.5% [100]), and 4% is assumed in this study. O&M costs include electricity purchase, administration costs, and ongoing facility maintenance costs [100]. Any revenue generated from excess electricity sales by the cogeneration plant in both the HCU and the DCU are accounted for in the upgrading cost calculation. Table 4 summarizes the economic specifications for the upgrading plant.

Table 4: Economic model specifications of the upgrader

Industrial parameters	Value	Comments/Reference
Plant capacity (kbd SCO production)	100	Considered minimum capacity for economies of scale [93]
Initial capital cost for a DCU without cogeneration (M$)	4800	Calculated using the capacity factoring method mentioned in [86] (see Eq. 8 in Appendix A). Assumed equal capital investment in the first four years
Initial capital cost for a DCU with cogeneration (M$)	4900	Calculated using the capacity factoring method mentioned in [86] (see Eq.8 in Appendix A). Assumed equal capital investment in the first four years
Initial capital cost for an HCU without cogeneration (M$)	6600	Calculated using the capacity factoring method mentioned in [86] (see Eq.8 in Appendix A). Assumed equal capital investment in the first four years

Industrial parameters	Value	Comments/Reference
Initial capital cost for an HCU with cogeneration (M$)	6800	Calculated using the capacity factoring method mentioned in [86] (see Eq.8 in Appendix A). Assumed equal capital investment in the first four years
Price of natural gas ($/GJ)	4.76	[36]
Electricity ($/kWh)	0.07	[87]
Discount rate	15%	Assumed
Capacity factor	89%	[100]
Scale factor	0.55	Developed using data from the literature [88, 101]
O&M cost (% of initial capital cost)	4%	[98]
Plant life (yr.)	25	Assumed same as SAGD

2.3.3 Transportation by pipeline

2.3.3.1 Model description

The study assesses several transportation scenarios for dilbit, SCO, and diluent. A pipeline designed to transport 300 kbd of crude oil and refined products was assumed; this distance is the same as that of an existing pipeline (Trans Mountain) [65] from production site to sea port. For the transportation of dilbit, an average distance of 500 km between the extraction site and the upgrader in Edmonton and 1647 km from the production site to the sea port are considered. The transportation of dilbit over 500 km includes diluent return, at a capacity of 90 kbd [102], while for the scenario without diluent return it was assumed that diluent is used in the upgrading process. For the transportation of SCO from upgrader to sea port, a distance of 1,147 km is used, as it is the existing pipeline distance. For the sake of simplicity, the study does not include elevation losses. Head loss due to friction is calculated using fluid viscosity, the Reynolds number, friction factor, pipe length, pipe roughness, etc., for different crude grades and transportation distances.

Table 5: Economic and technical specifications of transportation models

Crude feed	Dilbit	SCO	Diluent	Comments/References
Capacity (kbd)	300[2]	300[2]	90[3]	
API	22	32	55	[42]
Kinematic viscosity (cSt)	200	10	1.3	[42]
Pump efficiency (%)	70	70	70	[42]
Distance (km)	500[4], 1647[5]	1147[6]	500[4]1647[5]	
Pipeline diameter ID (m)	0.61	0.61	0.37	Calculated using the governing fluid flow equation (see Eq. 1 in Appendix A) taking velocities in the range of 1.5-3.0 m/s
Thickness (m)	0.0127	0.0127	0.0127	The same value is assumed for all cases

Crude feed	Dilbit	SCO	Diluent	Comments/References
Absolute roughness (mm)	0.046	0.046	0.046	[103]
∆P (bar)	50	50	50	[104]
Discount rate (%)	12	12	12	Assumed
Inflation rate (%)	6.6	6.6	6.6	Assumed

[2] Existing Trans Mountain Pipeline capacity

[3] Existing capacity of Polaris Pipeline

[4] 500 km is considered from FortMcMurray to Edmonton

[5] 1647 km is considered from FortMcmurray to the Westridge terminal in B.C

[6] Trans Mountain Pipeline is 1147 km

The Darcy-Weisbach equation was used to calculate head loss (see Eq. 2 in Appendix A). The pipeline diameter was determined using the governing fluid flow equation shown in Eq. 1 in Appendix A, with a velocity between 1.5 and 3.0 m/s. Economic and technical model specifications are shown in Table 5.

2.3.4 Shipping

2.3.4.1 Model description

A data-intensive model was developed to evaluate the shipping costs of SCO and dilbit from the Westridge terminal in Vancouver to the Asia-Pacific region, specifically to ports in China, Japan, and India. Shipping costs are calculated based on a time charter, wherein the charterer leases the tanker for a specific time period and pays for fuel costs, port and passage fees, and hiring costs. This method is used by most crude oil carriers. It was assumed that both the SCO and dilbit carriers in the base model use an Aframax tanker [105] with a cargo capacity of 729,000 barrels. At present, the Westridge terminal can handle the largest tanker size, i.e., an Aframax tanker. However, given future scenarios, the shipping costs of SCO and dilbit for other tanker sizes such as the very large crude carrier VLCC) [105] and the Suezmax [105] were included. SCO and dilbit carrier specifications for the given capacity are shown in Table 6.

Table 6: Specifications of SCO and dilbit carriers

	Nomenclature	Value	Unit
Design ship speed[7]	V	6.69	m/s
Vessel's Specifications[8]			
Cargo volume	V_c	729,000	barrel
Displacement	Δ	123,066	tons
Deadweight tonnage	dwt	105,927	tons
Gross tonnage approximate	GT	57,177	tons
Light displacement	L_D	17,139	tons
Overall length	L_{OA}	243.98	m
Length between perpendiculars	L_{PP}	234	m
Breadth	B	42	m
Design draught	D_{design}	14.92	m
Depth	T	21	m
Air draft	A	43	m
Longitudinal center of buoyancy	l_{cb}	2.34	m
Coefficients[9]			
Block coefficient	C_b	0.82	
Midship section coefficient	C_m	0.98	
Water plane coefficient	C_w	0.92	
Prismatic coefficient based on waterline length	C_p	0.84	

[7] Designed ship speed refers to the speed at which the shipping costs is lowest

[8] Vessel specifications are taken from the Clarkson data sheet [66]

[9] The midship section coefficient is taken from MAN Diesel & Turbo [106] and other coefficients are calculated using Eq.16-18 in Appendix C

The shipping costs of SCO and dilbit were calculated to set a base case for the vessel specifications shown in Table 6 at an optimized speed of 6.9 m/s. Seven scenarios were developed based on main and auxiliary engine fuel use and on propulsion system type in order to evaluate the most economical shipping pathway.

2.3.4.2 Resistance and installed power estimate

The calm water resistance was calculated using the method described in section 2.1 and added air resistance to calm water resistance to calculate total resistance of the SCO and dilbit carriers. The total resistance was estimated for the vessel specifications given in Table 6 at various speeds (shown in Appendix A, Figure S1). The resistance model developed to calculate the total installed power of the engine has some limitations:

- It is valid only for a Froude number below 0.24 [107].
- It is valid only for certain prismatic coefficient ranges, i.e., $0.73 \leq C_p \leq 0.85$ [107].

The total calm water resistance plus air resistance was calculated for the optimized speed of the vessel to be 97.6 MT. Using Eq.15 (shown in Appendix A), the total calm water resistance, towing power, braking power, and propeller efficiency of the total installed power of the engine to be 10.4 MW was calculated for both SCO and dilbit carriers.

Based on the value of the calculated installed power, the engines were selected from MAN B&W's engines guidelines [108] summarized in Table 7.

Table 7: Engine configurations and SFOC data for the base model

	Abbreviations	Aframax tanker	Fuel	Rpm	Unit
Engine types					
Main engine model[10]		1 x MAN S60MC8	HFO	105	
Auxiliary engine model[11]		1x aux. diesel gen 9L28/32H	MDO	750	
SFOC data					

	Abbreviations	Aframax tanker	Fuel	Rpm	Unit
Main engine SFOC[10]	SFO_m	156			g/kWh
Auxiliary engine SFOC[11]	SFO_{aux}	191			g/kWh

[10] Main engine models and SFOC data are selected from MAN B&W Diesel [108]

[11] Auxiliary engine models and SFOC data are selected from MAN B&W Turbo [109]

The shipping costs are calculated based on the selected engine and compared for China, Japan, and India. The average inter-port distance is estimated taking major port distance of China, Japan, and India using the Portworld Distance Calculator [110].

2.3.4.3 Cost model

The shipping cost is made up of fuel, hiring, and port and passage fees, as explained in section 3.4.1. The fuel types considered for the base case model are heavy fuel oil (HFO) and marine diesel oil (MDO) for the main and auxiliary engines, respectively. The hiring cost is taken as CAD$ 25,610 per day [111]. The economic parameters used in the shipping model base case are shown in Table 8.

Table 8: Economic parameters

Sailing parameters	Base case	Units	References
Japanese ports	4,450	nautical mile	[110]
Chinese ports	5,193	nautical mile	[110]
Indian ports	9,090	nautical mile	[110]
Speed of SCO/dilbit carrier	6.9	m/s	Optimal speed of carriers
Cargo loading and unloading rate	9,000	m^3/hr	[66]
Cargo properties			

Sailing parameters	Base case	Units	References
Density of SCO	857	kg/m^3	[112]
Viscosity of SCO	10	cST	[71]
Density of dilbit	922	kg/ m^3	[113]
Viscosity of dilbit	200	cST	[71]
Fuel oil cost (dollars per ton)			
HFO	603	$/ton	[114]
MDO	891	$/ton	[115]
SCO/dilbit carrier hire cost	25,610	$/day	[111]

2.4 Results and discussion

2.4.1 SAGD

In this section, the total energy consumed and the results from the discounted cash flow analysis for SAGD are reported. The production cost includes mainly natural gas, O&M, and capital costs, and energy consumption is primarily natural gas. The overall production cost is influenced mainly by natural gas consumption, followed by O&M and capital costs for SAGD with and without cogeneration. The natural gas cost accounted for 52% and 47% of overall production costs of SAGD with and without cogeneration, respectively. Table 9 shows the energy consumption and production costs of SAGD with the variability in cogeneration system. Natural gas consumption with a SOR of 2.87 for SAGD with and without cogeneration is 1.82 and 1.04 GJ/bbl bitumen, respectively. However, it is important to mention that these values may vary depending on the SOR and the efficiency of the process. The evaporating unit consumes a significant amount of electricity [77, 116]. This study calculates the consumption of 7.9 KWh/bbl of bitumen.

Table 9: Estimated SAGD costs

SAGD without cogeneration	Value
Natural gas consumption (GJ/bbl bitumen)	1.04

SAGD without cogeneration	Value
Total natural gas cost (MC$/yr.)	74.7
Electricity consumed (kWh/bbl bitumen)	8
O&M cost (MC$/yr.)	53.4
Production cost (C$/bbl bitumen)	21.6[12]
SAGD with cogeneration	
Natural gas consumption (GJ/bbl bitumen)	1.82
Total natural gas cost (MC$/yr.)	130.3
Total electricity produced (kWh/bbl bitumen)	143.1
Revenue generated from excess electricity sold (MC$/yr.)	128.4
O&M cost (MC$/yr.)	75
Production cost (C$/bbl bitumen)	20.8[12]

[12] This figure does not include drilling and diluent costs

The linear correlation estimated for the instantaneous steam oil ratio (iSOR- measures the current or instantaneous rate of steam which is required to produce one barrel of bitumen) and electricity consumption is shown in [31, 43]. The estimated production costs (C$/bbl bitumen) for SAGD with and without cogeneration are C$20.8 and C$21.6, respectively. The production costs for SAGD with cogeneration are lower due to the revenue generated from the produced excess electricity. In 2006, the NEB [39] estimated the operating and supply costs for SAGD as C$10-14 and C$18-22, respectively, but this study does not consider variations in cogeneration system and technical parameters. However, the values estimated by the NEB are within the range of values reported in this study (section 4.6.1).

2.4.2 Upgraders

The energy consumed in the upgrader unit is in the form of natural gas, electricity, and fuel gas. In the units without cogeneration, the HCU consumes 72.0% more natural gas than the DCU (0.22 GJ/bbl of bitumen is required by the DCU). This is because additional natural gas is required in the HCU to produce hydrogen. The DCU consumes an estimated 8.3 kWh electricity/bbl of bitumen and the HCU uses an estimated 12.8 kWh electricity/bbl of bitumen. More electrical energy is consumed in the HCU because it requires more hydrogen in the hydrocracker unit, thus yielding high SCO [71]. The HCU and the DCU produce 313,740 and 643,589 kg flue gas/day, respectively, for a 100 kbd SCO production capacity. The upgrading costs of the HCU and the DCU with and without cogeneration (C$/bbl SCO) estimated in this study are C$54.04 and C$52.32, C$36.96 andC$36.48, respectively. It costs less to produce SCO in the DCU than the HCU both because the HCU has a higher capital cost and, as noted above, the HCU consumes more natural gas and electricity than the DCU, which significantly increases energy costs. Initial capital and O&M costs are the two major components of the upgrading cost. In 2006, the NEB estimated the upgrading cost as C$39 per barrel of SCO [39]. This value is within the range of upgrading cost for DCU presented in section 4.6. The estimated energy consumption and upgrading costs for both upgraders (DCU and HCU) are presented in Tables 10 and 11.

Table 10: Estimated DCU costs

DCU without cogeneration	**Value**
Natural gas consumption (GJ/bbl bitumen)	0.22
Total natural gas cost (MC$/yr.)	44.1
Electricity consumed (kWh/bbl bitumen)	8.3
O&M cost (MC$/yr.)	192
Flue gas produced (kg/day)	643589
Upgrading cost (C$/bbl SCO)	36.48
DCU with cogeneration	
Natural gas consumption (GJ/bbl bitumen)	0.27
Total natural gas cost (MC$/yr.)	54
Total electricity produced (kWh/bbl bitumen)	14.95
Revenue generated from excess electricity sold (MC$/yr.)	17.84
O&M cost (MC$/yr.)	196
Upgrading cost (C$/bbl SCO)	36.96

Table 11: Estimated HCU costs

HCU without cogeneration	**Value**
Natural gas consumption (GJ/bbl bitumen)	0.79
Total natural gas cost (MC$/yr.)	131
Electricity consumed (kWh/bbl bitumen)	12.80
O&M cost (MC$/yr.)	264
Flue gas produced (kg/day)	313740
Upgrading cost (C$/bbl SCO)	52.32
HCU with cogeneration	
Natural gas consumption (GJ/bbl bitumen)	0.83
Total natural gas cost (MC$/yr.)	139
Total electricity produced (kWh/bbl bitumen)	26.62
Revenue generated from excess electricity sold (MC$/yr.)	30.5
O&M cost (MC$/yr.)	272
Upgrading cost (C$/bbl SCO)	54.04

2.4.3 Transportation by pipeline

Different pipeline transportation options were considered based on the system boundaries developed. The energy consumed to transport both SCO and dilbit via pipeline is in the form of electricity. This is the only energy used to overcome the friction losses and drive the inlet and booster station pumps. In a work by Tyler [18], the electricity consumed accounted for 96% of the overall energy inputs at the operation phase while construction of pipeline equipment and facilities were 4%. In this study, only the energy consumed at the operation phase is considered. The capital costs associated with the pipeline depend on market distance and production scales. The transportation costs of SCO and dilbit were considered for market distance of 1–3000 km and capacity of 100,000 –750,000 bbl/day in a work by Verma et al. [45]. An increase in transportation distance increases the material, labor, and booster station costs, etc., and hence overall costs. SCO and dilbit transportation costs for different scenarios are given in Table 12.

Table 12: SCO and dilbit transportation costs for different scenarios

Scenarios	Transportation cost per barrel
Dilbit transportation (500 km) without diluent return (C$/bbl bitumen)	2.15
Dilbit transportation (500 km) with diluent return (C$/bbl bitumen)	2.99
Dilbit transportation (1647 km) without diluent return (C$/bbl bitumen)	6.78
Dilbit transportation (1647 km) with diluent return (C$/bbl bitumen)	9.43
SCO transportation (1147 km) (C$/bbl SCO)	2.74

2.4.4 Shipping

2.4.4.1 Fuel consumption and shipping cost to the China port

The shipping costs to the China port were calculated at an optimized speed of 6.9 m/s (see Figure 8). This is the speed at which the shipping costs are minimum; it was determined as shown in this figure after assessing the vessel speed at a number of reiterations. SCO and dilbit shipping costs were calculated based on an Aframax tanker with a 729 kbd capacity as C$2.78/bbl SCO and C$3.19/bbl dilbit, respectively. The fuel and hiring costs are the two major components influencing shipping costs. Although the hiring cost decreases with increases in vessel speeds above 6.9 m/s, the power required for the engine increases so rapidly that both fuel consumption and shipping costs rise considerably (see Figure 8). However, when the speed drops below the optimized value, the hiring cost has a significant effect on shipping cost. This is because decreasing the velocity increases the number of days to reach the destination port, thereby increasing both the hiring and the shipping cost.

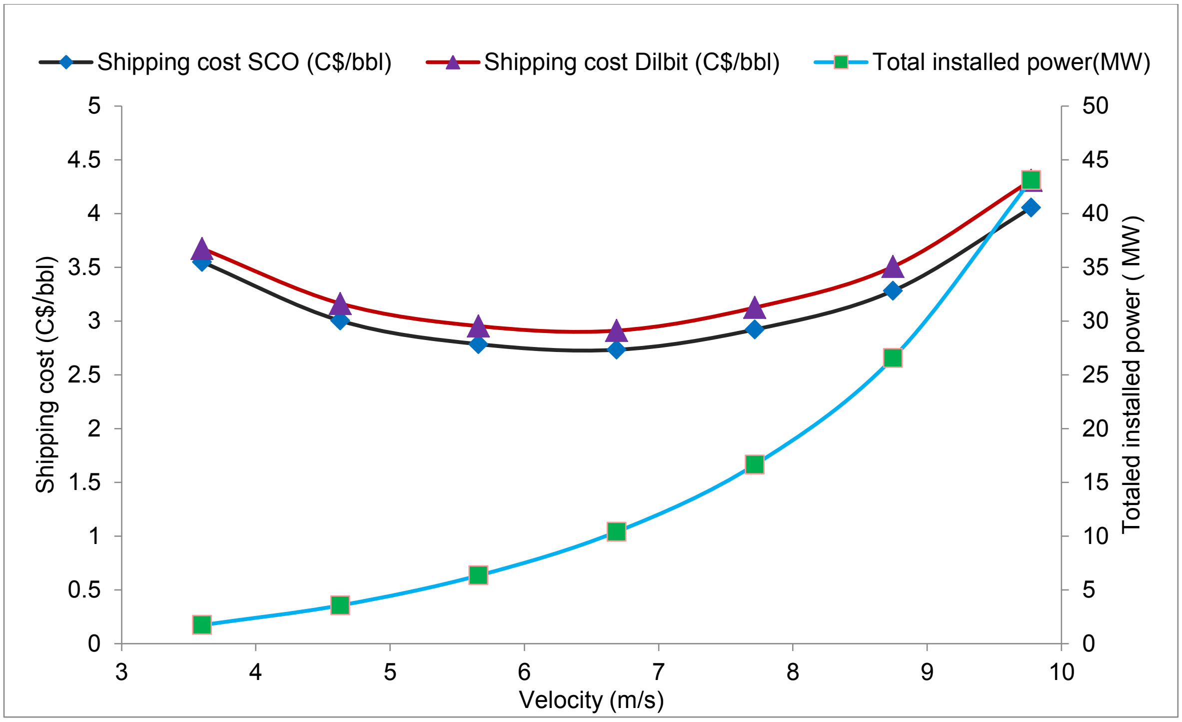

Figure 8: Optimized SCO and dilbit carrier speeds

The components influencing shipping costs, i.e., the charges associated with HFO, MDO, hiring, and port and passage fees, are shown in Figure 9. Dilbit shipping costs are higher than SCO shipping costs. This is because more fuel is consumed to heat cargo (i.e., to reduce dilbit viscosity) both during the voyage and at discharge, as shown in Figures 10 and 11. Total HFO consumption for the main engine is 980 tons per voyage for both SCO and dilbit carriers. Power from the main engine is used to overcome the calm water and air resistance of the vessels. The auxiliary engine requires 233 tons/voyage of MDO. Fuel consumption for the main engine, auxiliary engine, cargo heating, and discharging are accounted for from the Westridge terminal in Vancouver to the Chinese port. The fuel and hiring costs are 53% and 43% of the shipping cost of dilbit, respectively, and 45% and 49%, respectively, for SCO. The port and passage fees have minimal impact on the shipping cost for either cargo.

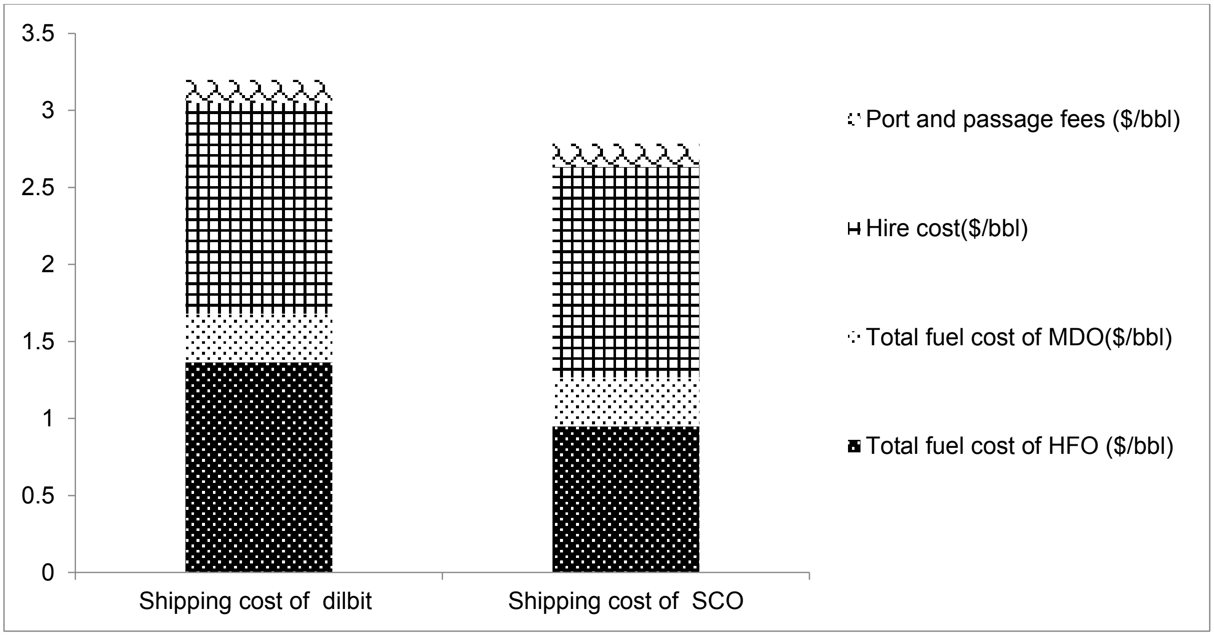

Figure 9: Shipping costs per barrel of SCO and dilbit from the Westridge terminal in Vancouver to the Chinese port

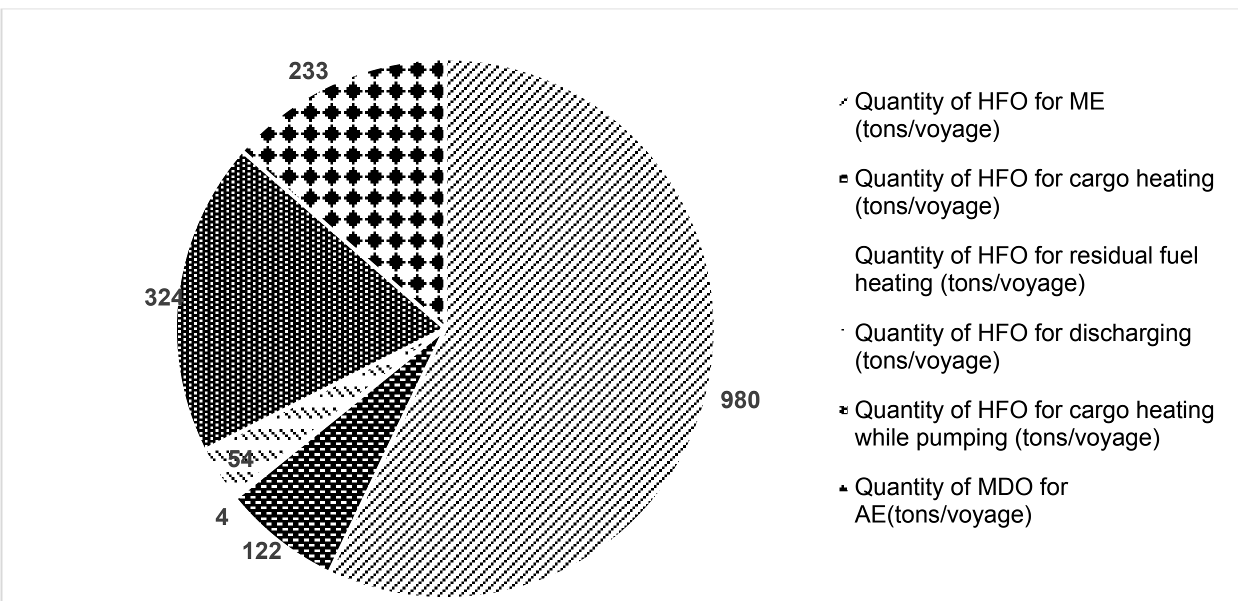

Figure 10: Fuel consumption to ship dilbit from the Westridge terminal in Vancouver to the Chinese port

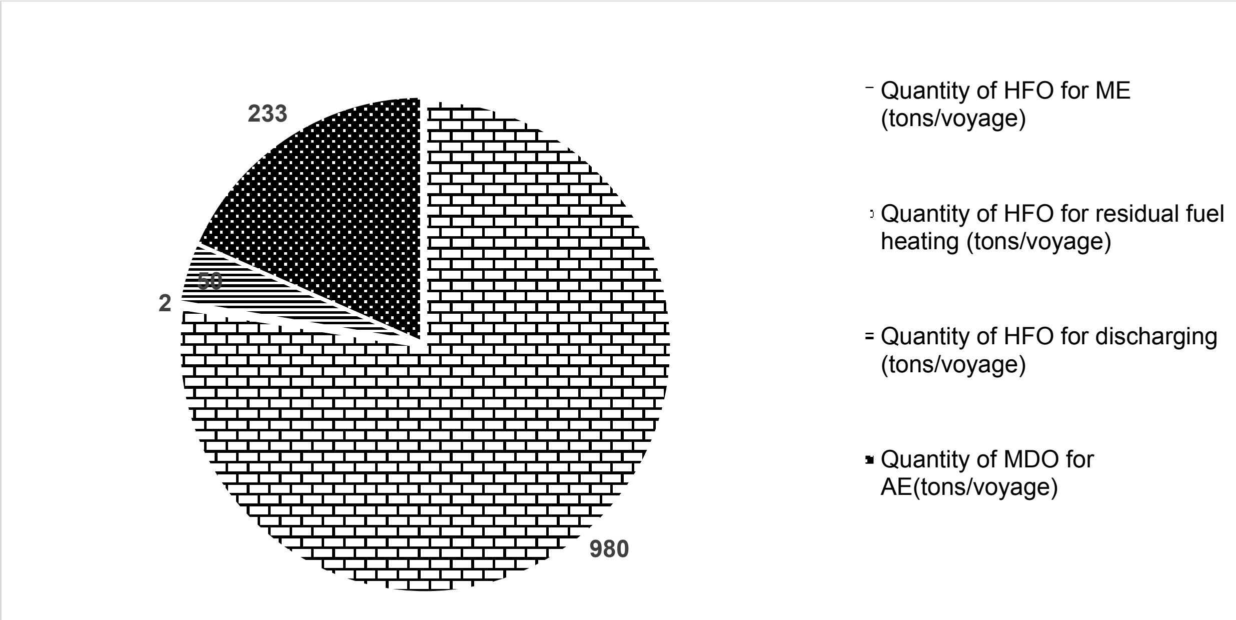

Figure 11: Fuel use to ship SCO from the Westridge terminal in Vancouver to the Chinese port

2.4.4.2 Comparison of shipping cost for China, Japan and India

Figures 12 and 13 show SCO and dilbit shipping costs from Vancouver to ports in China, Japan, and India. The costs are evaluated at the optimized speed of 6.9 m/s for an Aframax tanker. The port in Japan has the shortest average distance of 4,450 nautical miles (8,241.4 kilometers) and a sailing time of 14 days. For China and India, the average number of days is 17 and 29. The shipping costs per barrel SCO and dilbit to Japan are C$2.43 and C$2.84, respectively, to China are C$2.78 and C$3.20, respectively, and to India are C$4.66 and C$5.08, respectively. Japan's shipping costs are the lowest because its inter-port distance is the shortest, and thus fuel consumption and the number of hiring days are the lowest of the three destinations.

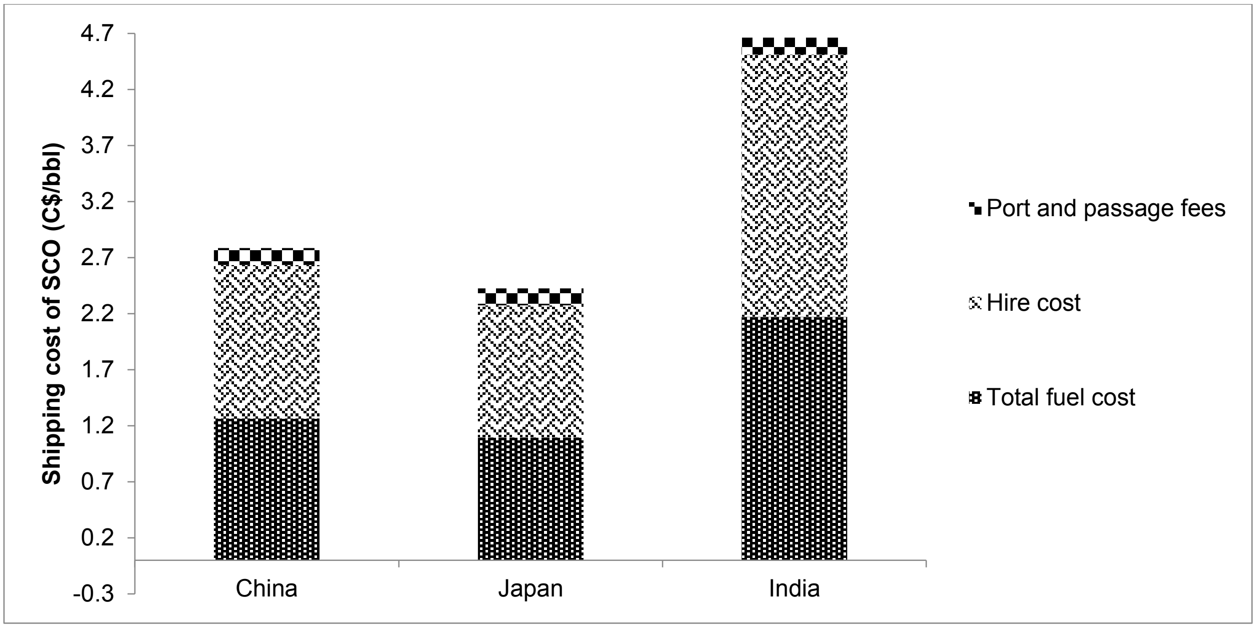

Figure 12: SCO shipping costs to China, Japan, and India

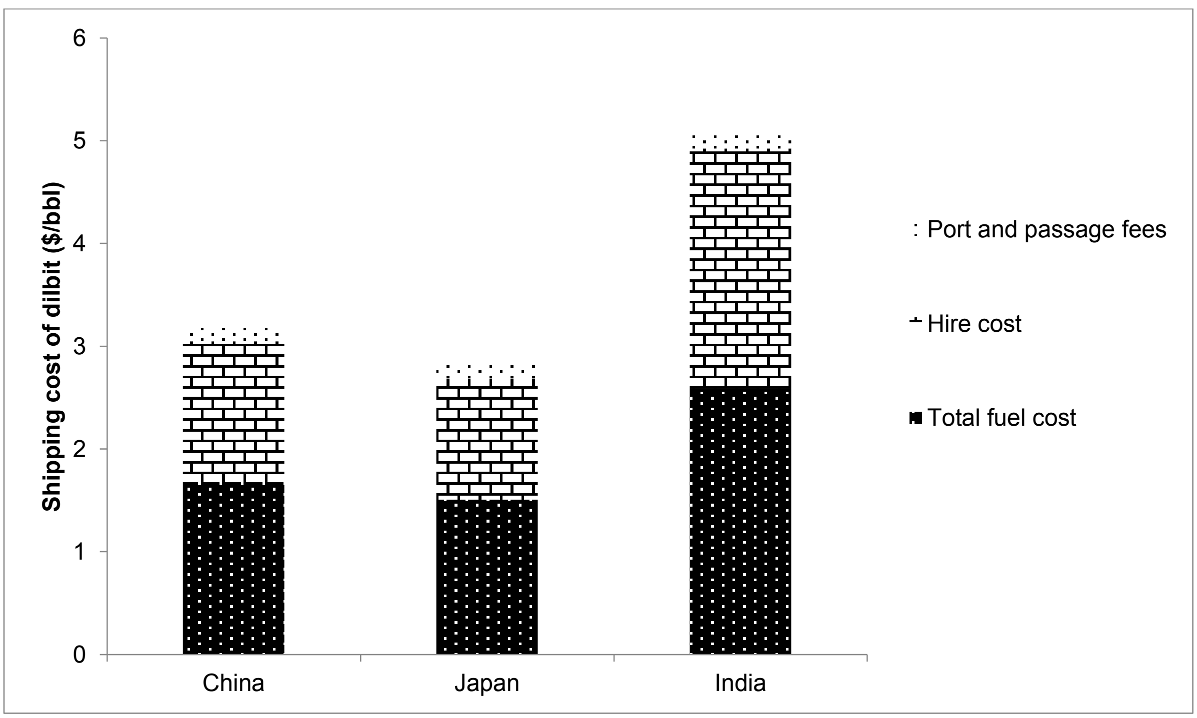

Figure 13: Dilbit shipping costs to China, Japan, and India

2.4.5 Supply chain pathways

Four pathways were developed with variations in cogeneration systems in both the SAGD and the upgrader plants, and in diluent return conditions in pipeline transportation. These pathways represent existing and future oil sands projects. The pathways were designed based on the two most common upgraders, the DCU and the HCU, and considered that dilbit is upgraded in Canada or in China. It is possible to send SCO to the refineries in India based on their capability to handle the product of API value ranged 32.0- 35.5 provided in [8], though the utilization rate of their refineries was more than 100% in 2010. A Canadian oil sands product in the form of SCO is also transported to Japan as their refineries might be able to process it. SCO and dilbit shipping pathways include the base case in which HFO and MDO are used as a fuel in the main and auxiliary engines, respectively, with travel from the Westridge terminal in Vancouver to the port in China. Details of the pathways are shown in Figure 14.

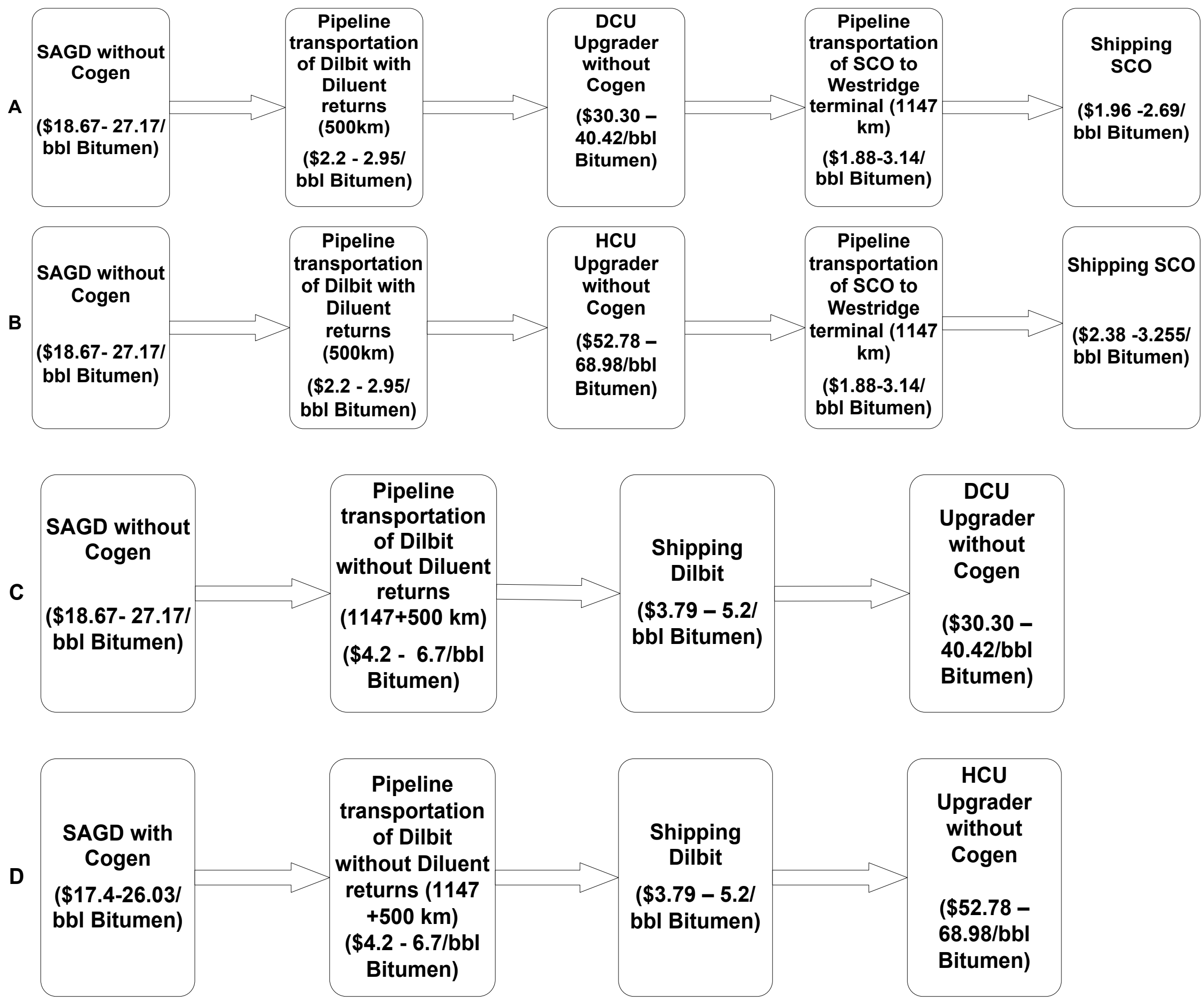

Figure 14: Canadian oil sands supply chain routes: A): Pathway 1- SAGD bitumen is upgraded in delayed cokers and the produced SCO is transported by pipeline (1147 km) and shipped to the port in China. (B): Pathway 2- Bitumen recovered in SAGD is upgraded through hydroconversion and the produced SCO is transported by pipeline

(1147 km) and shipped by ocean tanker to the port in China. (C): Pathway 3- Bitumen recovered in SAGD is transported and shipped as dilbit to China and upgraded there in delayed cokers. (D): Pathway 4- SAGD bitumen is transported and shipped as dilbit to China and upgraded there through hydroconversion.

2.4.5.1 Pathway comparison

Supply chain costs from the production site in Alberta to a destination in China range from C$52.48-107.75, as shown in Figure 15. For the default case, supply chain costs range from C$60.70-86.83. These wide ranges are mainly due to the differences in HCU and DCU upgrading costs. Of all the pathways, pathway 1 has the lowest supply chain costs, ranging from C$52.48-75.48/bbl bitumen. The average free on board (FOB) price of imported crude oil in China in 2009 was US$61.95/bbl [117].

The supply chain costs of SCO and dilbit were also evaluated to ports of Japan and India (see Table 13). The costs are lowest to Japan because, as mentioned earlier, shipping costs are lowest to this country because it has the shortest shipping distance of the countries considered here.

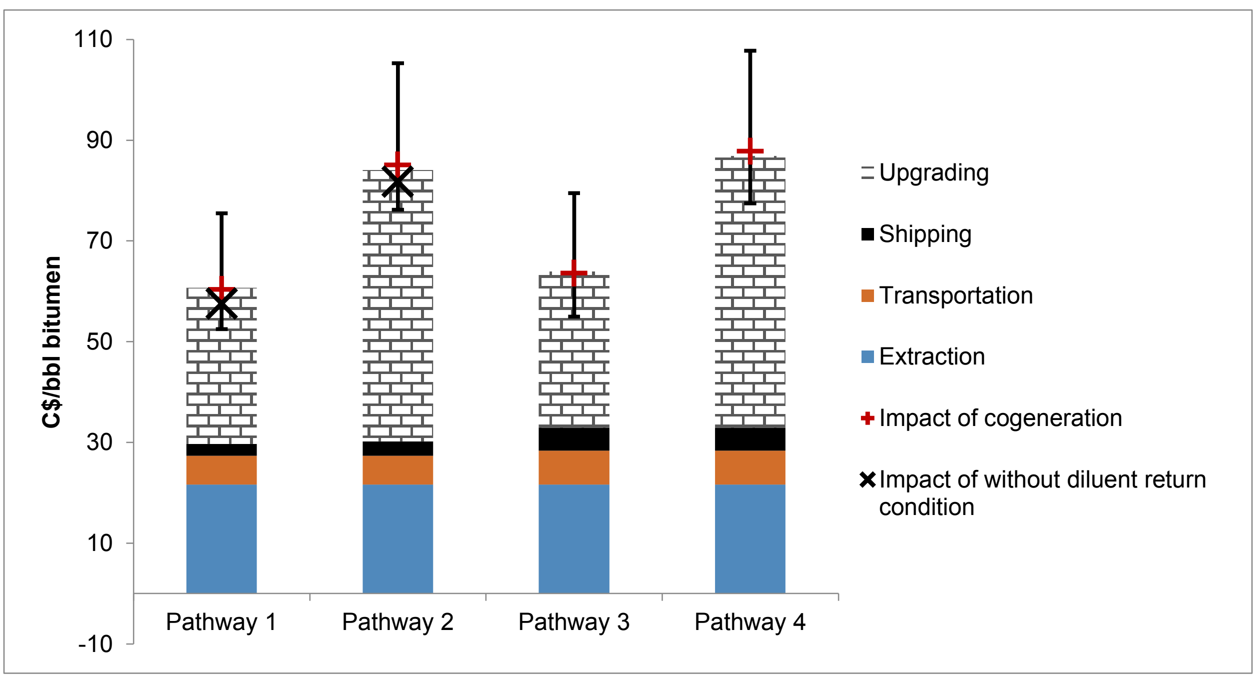

Figure 15: Supply chain costs in the delivery of Canadian oil sands products to China

Table 13: Supply chain costs for China, Japan, and India

Countries	Total supply chain cost (C$/bbl Bitumen)
China	60.70–86.82
India	62.29–89.51
Japan	60.40–86.34

2.4.5.2 Shipping scenario comparison

Seven scenarios were developed based on fuel use in the main and auxiliary engines and on propulsion system types in order to evaluate the most economic shipping pathway (see Table 14). An Aframax tanker with a capacity of 729 kbd (for both SCO and dilbit) was used for the base shipping model.

Table 14: Shipping scenarios

Engine types[13]	Installed power (MW)	Fuels	Scenario
Fuel use in main and auxiliary engines			
Main engine: 1 x MAN S60MC8	10.4	MDO	1
Auxiliary engine: 1 x Aux. Diesel Gen 9L28/32H		MDO	
Main engine:1 x MAN B&W 7S50ME-C8.2-GI-TII	11.6	LNG	2
Auxiliary engine: 1 x Aux. Diesel Gen 9L28/32H		MDO	
Main engine: 1 x MAN S60MC8	10.4	HFO	3
Auxiliary engine: 1 x Aux. Diesel Gen 9L28/32H		HFO	
Main engine: 1 x MAN S60MC8	10.4	MDO	4
Auxiliary engine: 1 x Aux. Diesel Gen 9L28/32H		HFO	

Engine types[13]	Installed power (MW)	Fuels	Scenarios
Main engine: 1 x MAN B&W 7S50ME-C8.2-GI-TII	11.6	LNG	5
Auxiliary engine: 1 x Aux. Diesel Gen 9L28/32H		HFO	
Propulsion system			
Main engine: 1 x MAN S60MC8	10.4	HFO	6
Auxiliary engine: 1 x Aux. Diesel Gen 9L28/32H		MDO	
Main engine: 1 x Wartsila 12V50DF	11.4	HFO	7
Auxiliary engine: 1 x Aux. Diesel Gen 9L28/32H		MDO	

[13] Engines configurations are taken from MAN product guides and a Wartsila product guide [108, 109, 118, 119]

For each scenario, installed engine power was calculated based on the same capacity using the method described in section 2.1.

For scenario 7, an electric propulsion system is assumed; in this system, the propeller is powered by a four-stroke medium speed engine. In the other scenarios, it is assumed a mechanical propulsion system is used and power is provided by two-stroke slow speed engine. A four-stroke engine loses power in the generators, transformers, motors, gear box, and shaft [120], whereas a two-stroke engine loses power in the shaft and gear box. Thus more power is required to drive the propeller in electric propulsion systems since they are less energy efficient. For scenarios 2 and 5, it was assumed that liquefied natural gas (LNG) is the fuel used in the gas injection (GI) engine. To estimate the installed power of the main engine using LNG, following assumptions were made:

- SCO and dilbit carriers using liquefied natural gas (LNG) as fuel in the main engine are designed for the same capacity (729,000 barrels) with sufficient space for LNG tanks without losing any space for the cargo.
- Since GI engine systems work like two-stroke engines, the efficiency is the same for both.
- Boil-off gas is not considered for the model since there is very little boil-off gas.

It is important to mention that currently no vessels use LNG as fuel in the main engine in crude oil transportation. Figure 16 shows the shipping cost per barrel SCO and dilbit for the seven scenarios. Scenarios 3 and 6 are existing situations. In these, port emissions restrictions determine how fuel is used in the main and auxiliary engines. For example, HFO can be used as a fuel for the main engine and HFO and MDO can be used for auxiliary engine. Shipping costs per barrel SCO and dilbit for scenarios 3 and 6 are C$2.68 and C$3.10 and C$2.78 and C$3.19, respectively. However, shipping costs for both cargos in scenario 7 are high compared to the existing scenarios. This is because the four-stroke engine is less efficient than the two-stroke engine and thus consumes more fuel in the main engine. Scenarios 1 and 4 have the highest shipping costs per barrel SCO and dilbit because MDO costs considerably more than HFO. The most economical scenario is 5, where LNG and HFO are used as fuel in the main and auxiliary engines, respectively. This is because LNG costs (C$237/ton) [36] less than HFO (C$ 603/ton) [121]and MDO (C$ 891/ton) [115]. The shipping costs per barrel SCO and dilbit for scenario 5 are C$2.04 and C$2.20, respectively.

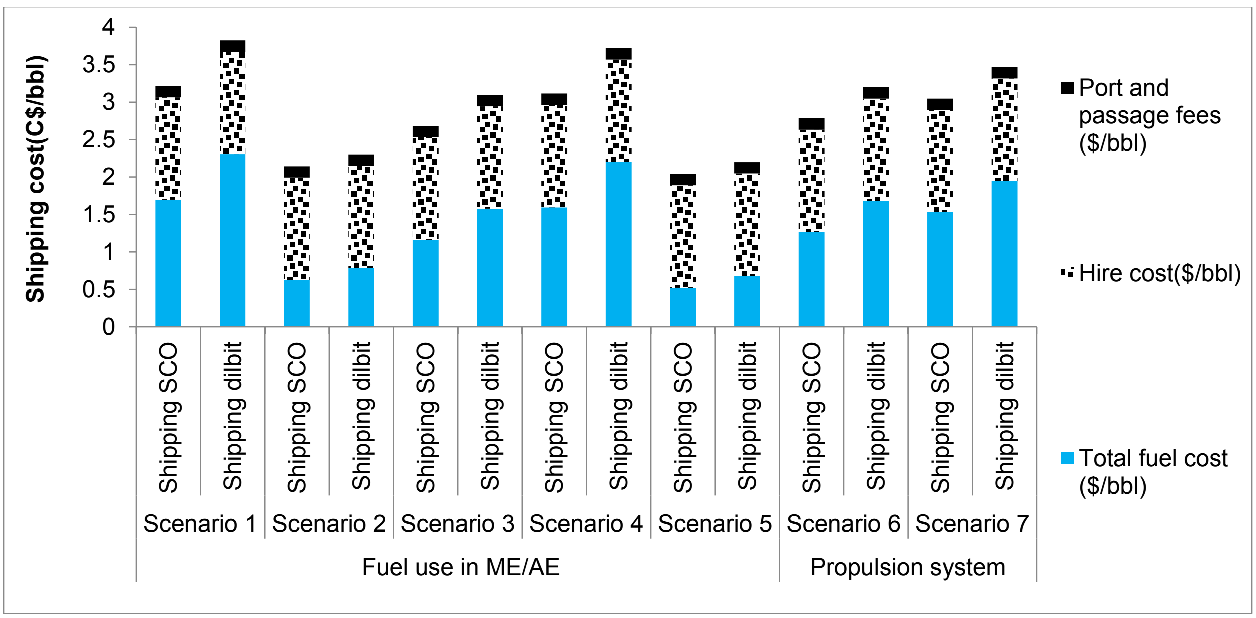

Figure 16: Shipping costs, scenarios 1-7

2.4.6 Sensitivity analysis

2.4.6.1 SAGD

The sensitivity of production costs was investigated in a SAGD plant in terms of iSOR, volume of produced gas, capital cost, natural gas cost, O&M cost, steam pressure, boiler efficiency, and capacity. Some other parameters, such as the efficiency of the gas turbine, HRSG exhaust recovery efficiency, HRSG firing duct efficiency, and electricity price, are included to observe the impact on production costs of SAGD with cogeneration. As shown in Figure 17, capital cost and capacity are the parameters to which production costs are most sensitive. With an increase in capacity by 20%, production costs decrease by 21% and 12%, while a 20% increase in capital cost increases production costs by 19.2% and 14%, respectively, for SAGD with and without cogeneration.

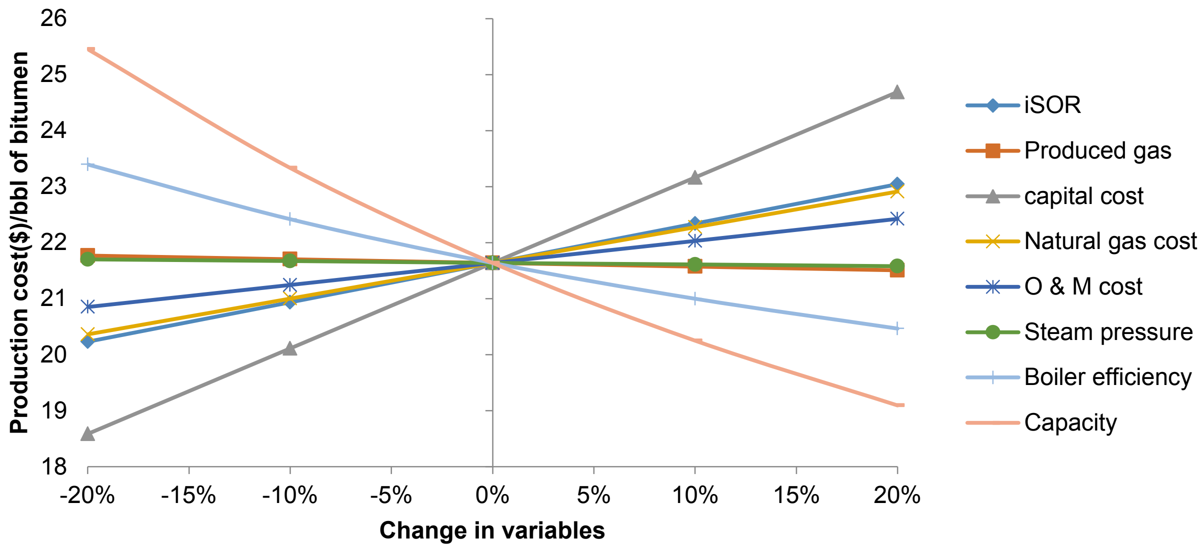

Figure 17: The sensitivity of key parameters on a SAGD plant without cogeneration

Increasing the iSOR increases natural gas consumption, which ultimately increases production costs. Parameters such as produced gas, steam pressure, O&M cost, HRSG firing duct efficiency, and HRSG exhaust recovery efficiency have little effect on production cost.

A Monte Carlo simulation was performed in order to evaluate the impact of different variables on the production costs for SAGD with and without cogeneration. All the uncertain input variables of the SAGD model were identified and the highest and the lowest ranges of these variables were defined. A random sampling was performed by using uncertain input variables from the SAGD model to generate production costs per barrel bitumen with their occurrence probability measures.

As shown in Figure 18, production costs per barrel bitumen from SAGD with and without cogeneration are from C$17.44-26.03 and C$18.67-27.17, respectively, for 90% probability. Production costs with cogeneration are below those without cogeneration due to the additional revenue generated with cogeneration from the excess electricity sold to the Alberta grid.

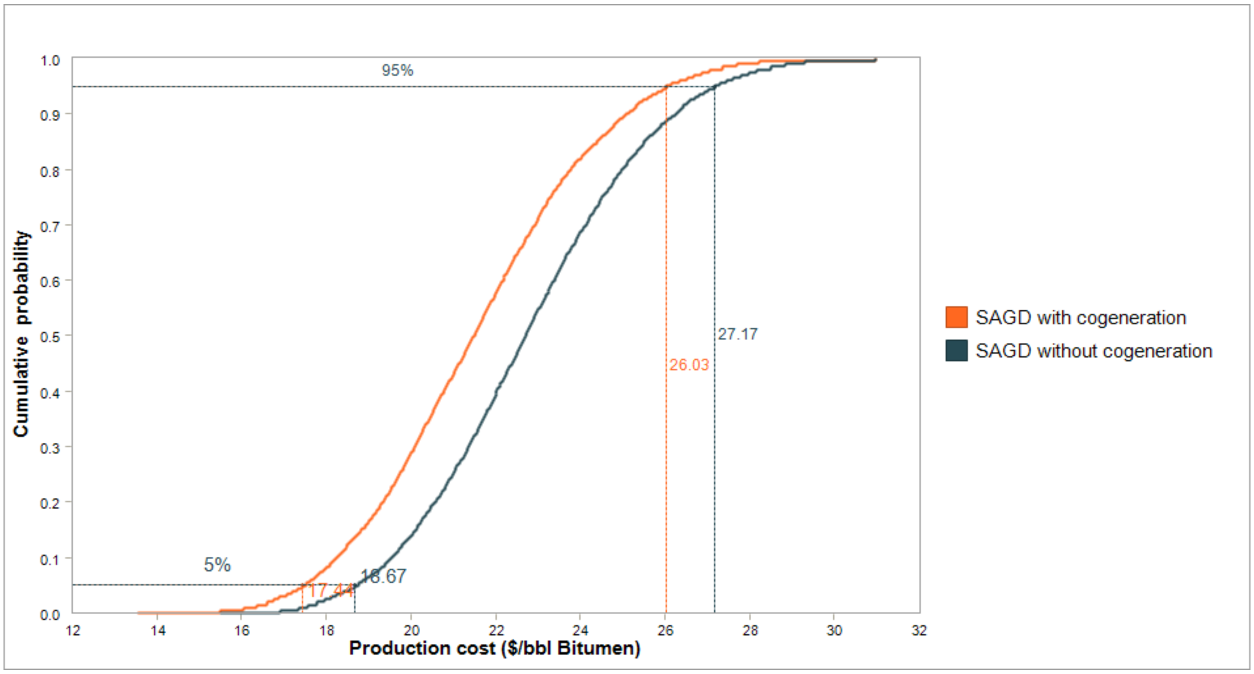

Figure 18: Ascending cumulative probability plot for production cost per barrel bitumen

2.4.6.2 Upgrader

The sensitivity of the upgrading cost was analyzed in terms of different parameters such as capital costs, natural gas costs, O&M costs, steam boiler efficiency, NG heater efficiency, heat exchanger efficiency, and capacity by changing their values by +/- 20% for a DCU and an HCU and using no cogeneration as the base case. Upgrading costs were most sensitive to changes in capacity and capital costs for both operations, as shown in Figure 19. A 20% decrease in capacity reduces upgrading costs by C$8.03 and C$5.85 with an HCU and a DCU, respectively. However, with a 20% increase in capital costs, upgrading costs using an HCU and a DCU increase by 18.46% and 19.25%, respectively. Other parameters, such as natural gas costs, heat exchanger efficiency, NG heater efficiency, and steam boiler efficiency, have small impacts on upgrading costs.

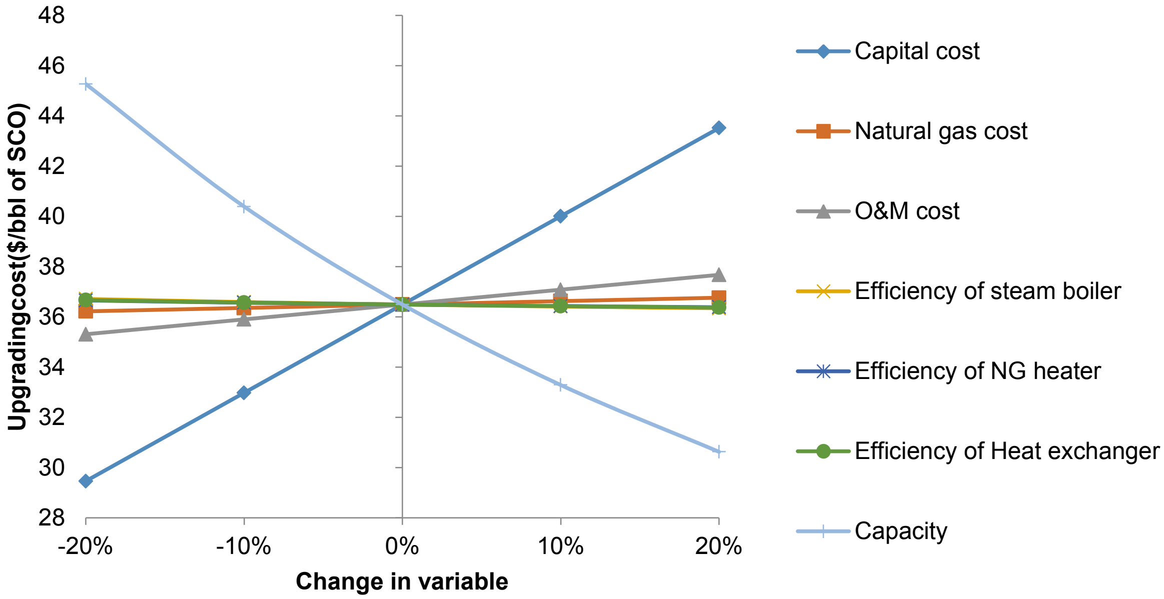

Figure 19: Sensitivity of key parameters on a DCU without cogeneration

In order to evaluate upgrading cost ranges for the DCU and HCU with and without cogeneration, a Monte Carlo simulation was performed. All the uncertain variables like capital cost, natural gas cost, operating and maintenance cost, etc., of the upgrader were identified and a triangular distribution was assigned to each variable defining a maximum and minimum value because of lack of data of all variables in public domain. From the ascending cumulative probability plot shown in Figure 20, the upgrading costs per barrel SCO for DCUs and HCUs with and without cogeneration are from C$36.18-48.09 and C$35.63-47.53, and C$53.35-68.62 and C$51.25-66.68, respectively, for 90% probability. Upgrading with an HCU is higher than with a DCU because an HCU is both highly capital intensive and has high operating and maintenance costs.

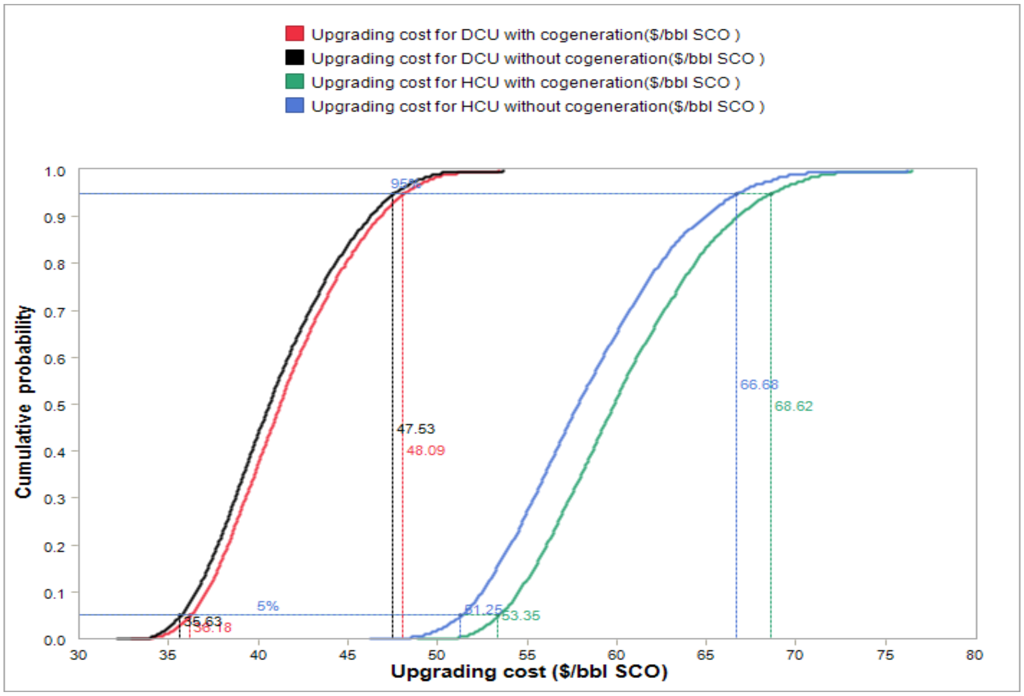

Figure 20: Ascending cumulative probability plot for upgrading cost per barrel SCO

2.4.6.3 Transportation

To measure the effects of key parameters on the transportation costs of SCO and dilbit, two corresponding sensitivity analyses were carried out. The first was for transporting dilbit 500 km with diluent return and the second was for transporting SCO 1147 km, both at a 300 kbd capacity. When the pipeline lifetime decreases by 20%, the transportation costs of dilbit and SCO increase by 35% and 38%, respectively. A 20% increase in capital costs increases the transportation costs of dilbit and SCO by 14% and 19%, respectively.

As illustrated in Figure 21, pipeline lifetime and capital costs have the largest influence transportation costs. Other parameters, like capacity and velocity, have moderate impact, while pump efficiency and electricity cost have less impact than other parameters.

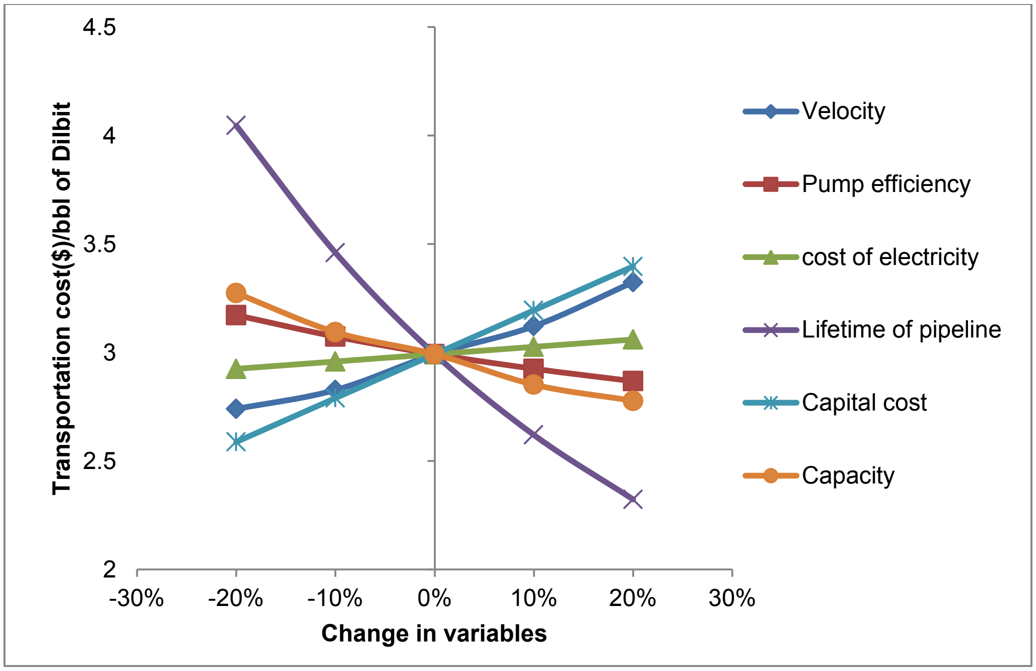

Figure 21: Sensitivity of key parameters on dilbit transportation with diluent return (500 km)

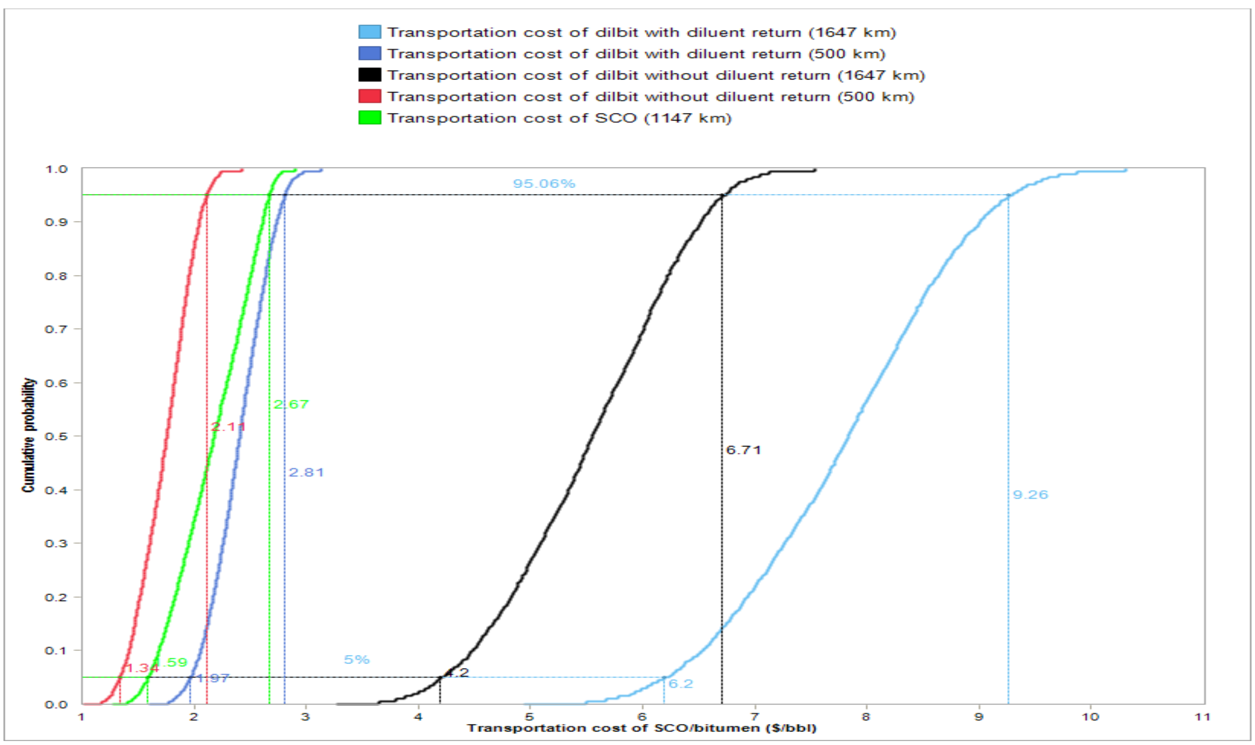

Figure 22: Ascending cumulative probability plot for transportation model

In order to evaluate transportation cost ranges with their occurrence probability measures, all the uncertain variables were identified such as velocity, pipeline life, etc., in the transportation model and defined the maximum and the minimum ranges of each variable. A Monte Carlo simulation by generating random samples using uncertain variables from the transportation model was performed. Figure 22 shows transportation cost ranges with 90% probability occurrence for different scenarios in the transportation model.

2.4.6.4 Shipping

A sensitivity analysis in order to evaluate the impact of key parameters such as hiring cost, fuel cost, capacity, efficiency of boiler, etc., on the shipping costs of SCO and dilbit by changing their values by +/-20%. Figure 23 shows that the shipping cost of dilbit is most sensitive to changes in capacity, fuel cost, and hiring cost. The shipping cost of SCO follows the same pattern (see Appendix A, Figure S8).

A 20% decrease in capacity increases the shipping costs of SCO and dilbit by 23% and 22%, respectively, and a decrease in HFO and hiring costs by 20% decreases the shipping costs of SCO and dilbit by 9% and 8%, respectively. Other parameters, such as heat exchanger efficiency, pump efficiency, boiler efficiency, port and passage fees, and discharge rate, have little impact on the shipping costs of either SCO or dilbit.

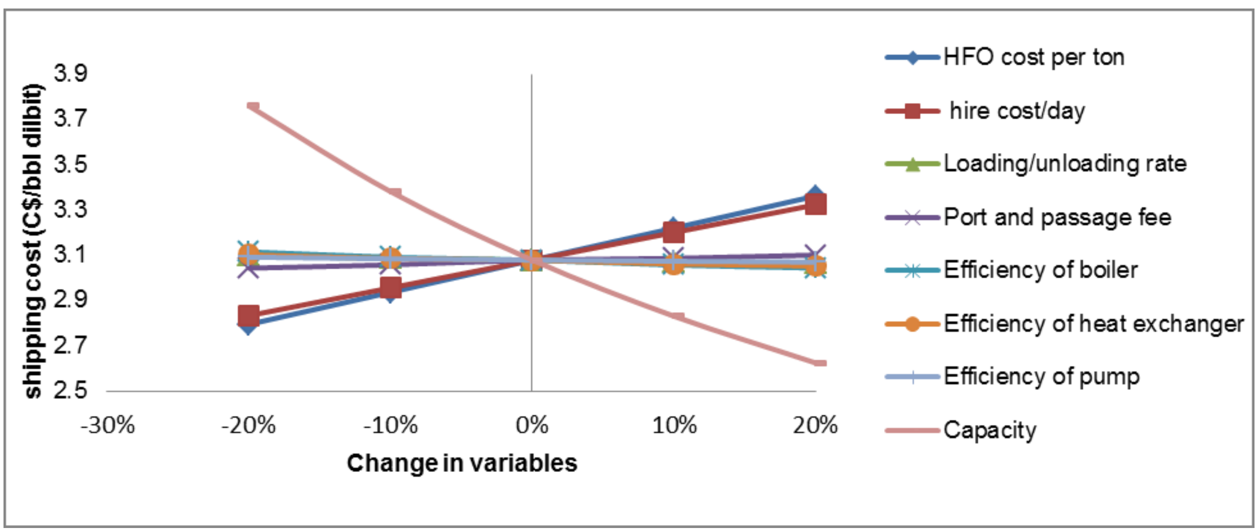

Figure 23: Sensitivity analysis of key parameters on the shipping cost of dilbit

A Monte Carlo simulation was performed by generating random samples with their probability occurrence in order to evaluate SCO and dilbit shipping cost ranges for different scenarios.

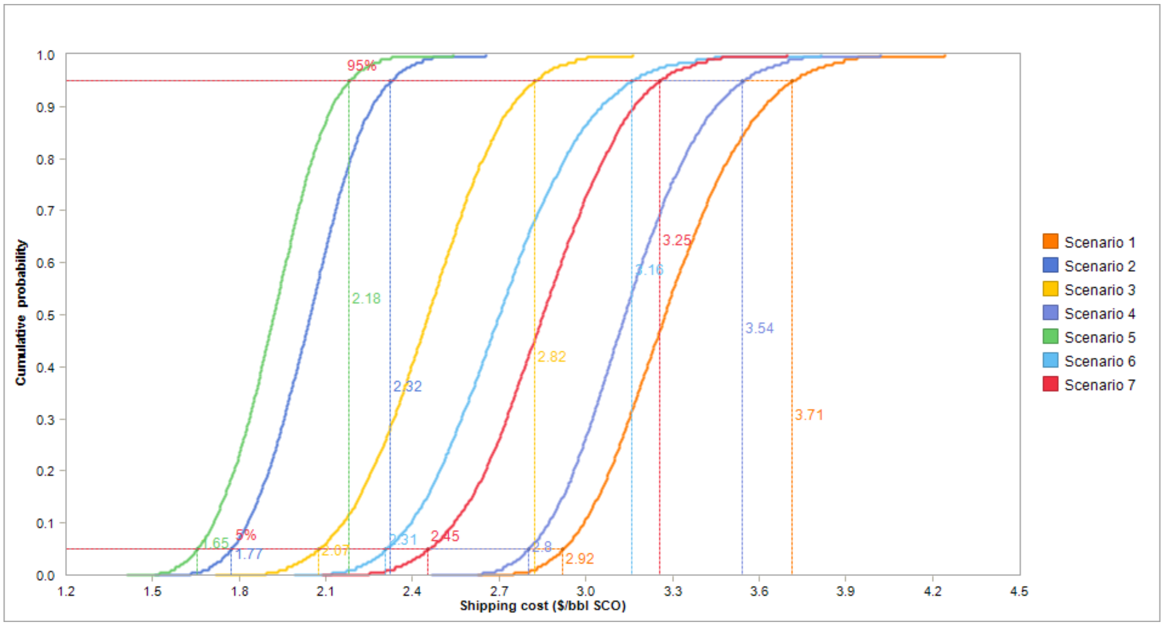

Figure 24: Ascending cumulative probability plot for seven scenarios of shipping SCO from the Westridge terminal to China

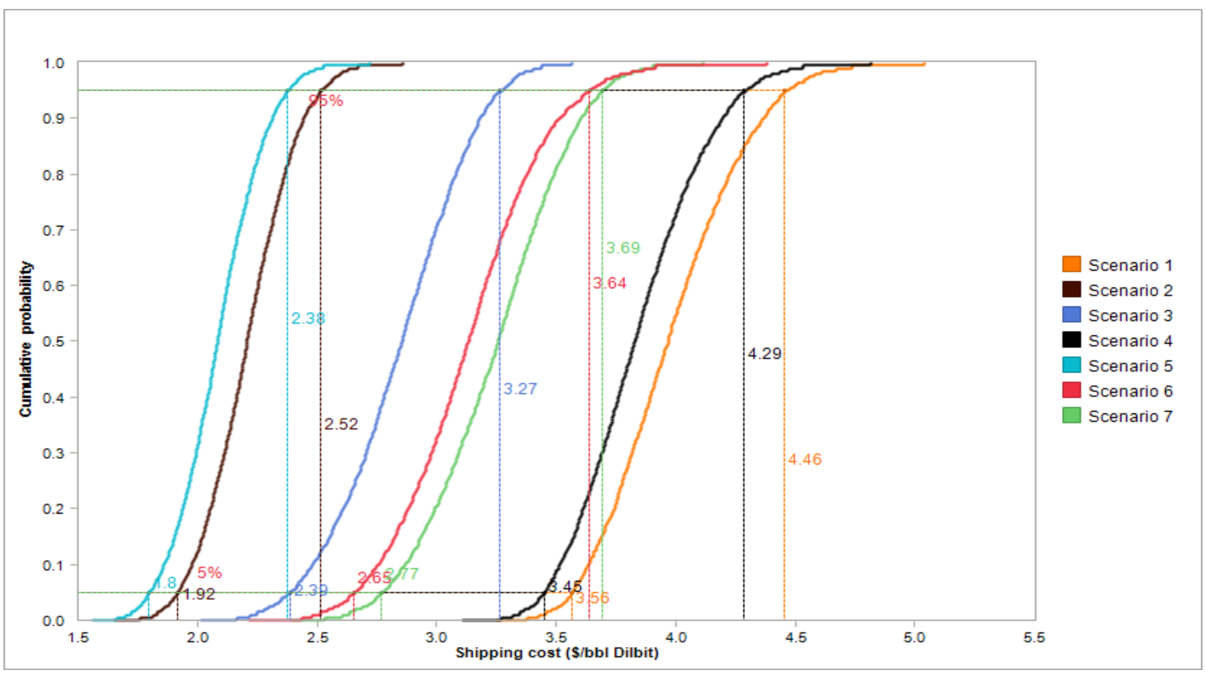

Figure 25: Ascending cumulative probability plot for seven scenarios of shipping dilbit from the Westridge terminal to China

First, all the uncertain parameters of the shipping model such as fuel cost, hiring cost, loading/unloading rate, port and passage fees, capacity, etc., were identified and then assigned a triangular distribution to each variable because of lack of information in public domain on how the variables will vary. Figures 24 and 25 show shipping cost ranges per barrel SCO and dilbit for different scenarios with 90% probability. Of all the scenarios, scenario 5 is the most economical; costs range from C$1.65-2.18/bbl SCO and C$1.8-2.38/bbl dilbit, respectively. The main engine uses LNG and the auxiliary engine uses HFO in this scenario. Scenario 1, in which MDO is used as a fuel in the main and auxiliary engines, has the highest shipping costs. This is due to the relatively high price of MDO compared with LNG.

2.5 Conclusion

In this study, the results of a detailed data-intensive techno-economic model to estimate production (SAGD), transportation (SAGD-upgrader-port in Vancouver), upgrading, and shipping costs of Canadian oil sands products are presented. This model was used to develop four pathways (two for SCO and two for dilbit) from production site to potential sea port destinations in the Asia-Pacific region. Supply chain costs (C$) per barrel of bitumen to China, Japan, and India range from 61-87, 60-86, and 62-90, respectively, depending on the pathway. The results also show that overall supply chain costs of Canadian oil sands products are influenced most by production and upgrading costs. Of the seven shipping scenarios, the most economical is scenario 5 (C$2.04/bbl SCO and C$2.20/bbl dilbit), where LNG and HFO are used as fuel in the main and auxiliary engines, respectively. The sensitivity analyses indicate that production and upgrading costs are mostly influenced by capital cost, while pipeline lifetime and capacity significantly impact transportation (pipeline) and shipping costs, respectively. The results of this study will serve as a decision-making tool for policy makers, government, and industry, and help achieve the most economic pathway for diversifying markets in the Asia-Pacific region.

Chapter 3[1]

A well-to-wheel life cycle assessment (LCA) of greenhouse gas emissions from Canadian oil sands supply chain for transportation fuels in China

3.1 Introduction

The quest to improve trade opportunities between Canada and China has extended to Canadian oil sands products. It is important to have an ecological framework that ensures a pathway with minimal emissions to strengthen the trade relationship in an environmentally friendly way. There are no studies in the literature that assess the life cycle emissions associated with the transportation of Canadian oil sand products for use as transportation fuel in China. Few studies investigate the conventional and non-conventional crudes imported from Canada to the U.S. One study [44] reviewed energy use and GHG emissions for different types of fossil fuel in China to identify the better choice in terms of the advantages in life cycle fossil use and GHG intensity. GREET (the Greenhouse Gases, Regulated Emissions, and Energy Use in Transportation Model) [41] and GHGenius [40] were used to quantify WTW GHG emissions for transportation fuels derived from crude oil. None of these studies address the WTW GHG emissions from Canadian oil sands products used in China as transportation fuels. Therefore, this work focuses understanding the environmental impact of imported crudes (Saudi Arabian crudes) as well as those that can occupy the future Chinese oil market (Canadian oil sands products). In order to strengthen the long-term trade relationship in an environmentally friendly, it is important for Canada to supply its oil sands products at relatively low emissions.

This chapter is aimed at evaluating the total well-to-wheel (WTW) life cycle (LC) emissions from Canadian oil sands products used for transportation fuel (gasoline, diesel, and jet fuel) in China. An LCA model was developed from recovery and extraction to the end use of products in China for two supply chain products: dilbit and SCO. This LCA model was run to develop all the possible pathways of Canadian oil sands supply chain products to China that are likely to be applied by industry in future. The LC inventory was analyzed for each stage of operations using their relevant inputs. This chapter includes the assumptions and methodology used to develop the life cycle assessment (LCA) model. Surface mining and steam assisted gravity drainage (SAGD) are the two methods assumed in this study for the recovery and extraction of the

[1] This version of chapter has been submitted to International Journal of Life Cycle Assessment for publication: Sapkota K., Oni O. A., Kumar A. *A well-to-wheel life cycle assessment (LCA) of greenhouse gas emissions from Canadian oil sands supply chain for transportation fuels in China. International Journal of Life Cycle Assessment, 2017 (in review)*

bitumen. GHG emissions from diesel, natural gas and electricity consumption of these operations are taken from Nimana et al. [31] and used to quantify the total LC emissions from transportation fuels in China. Canadian oil sands products are transported in the form of synthetic crude oil (SCO) and dilbit by pipeline. GHG emissions were calculated using the total energy required for pumping and the weighted average of the Canadian and U.S. provincial electricity grid emission factors [122, 123]. Two upgraders, delayed coking and hydroconversion, are used to produce SCO from bitumen, and pathways were constructed using these upgraders depending on whether the bitumen will be upgraded in Canada or China. Findings from Nimana et al. [30] on the GHG emissions from upgraders were used to develop the WTW GHG emissions of the transportation fuels considered in this study. In this study, dilbit and SCO are shipped from a Vancouver port to a China port by Aframax tanker. Total GHG emissions from shipping by ocean tanker were obtained from the calculated power and emissions factor for each engine. Eight potential pathways were developed using the emissions from each stage of operations. Finally, sensitivity and uncertainty analyses were conducted to observe the effects of technical parameters on shipping. The overall goals of this study are:

- To conduct a comprehensive well-to-wheel (WTW) life cycle assessment (LCA) of Canadian oil sands products supply chains.
- To quantify the comparative energy inputs and GHG emissions from Canadian oil sands products for use as transportation fuels in China.
- To apply the LCA model to compare the LC GHG emissions among various possible oil sands product pathways.
- To identify the pathway with the highest and lowest GHG emissions in the use of transportation fuels in China from Canadian oil sands products.

3.2 Methodology

The fundamental framework used in this study to evaluate the LC emissions from transportation fuels is made up of the system boundary, functional unit, a life cycle inventory analysis, environmental impacts, and life cycle interpretation as per the methodology described in ISO14000 series [124]. This ISO standard was adopted to calculate the GHG emissions in all possibility pathways.

First, an LCA model of the WTW GHG emissions from recovery and extraction to end-use products in China was developed. The overall pathway is shown in the Figure 26. Second, eight oil sands market pathways were developed in the model.

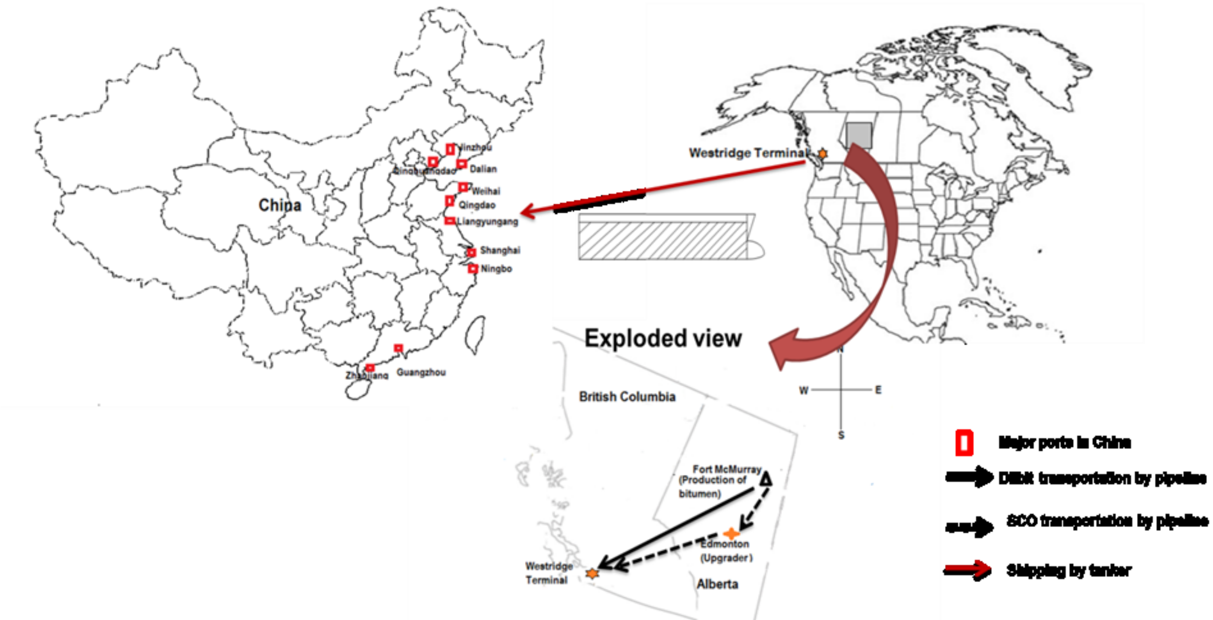

Figure 26: Map overview of Canadian oil sands products supply chain to China.

3.2.1 LCA Goal and scope

The goal of this study is to evaluate the life cycle environmental impacts of using transportation fuels in China derived from Canadian oil sands products. These aims are meant to highlight the most GHG-intensive stage in total WTW GHG emissions and identify possible areas of improvement. The scope is shown in detail in Figure 27 (A-B). The scope of this study includes all the stages throughout the entire LC from recovery and extraction of bitumen to the end use in China.

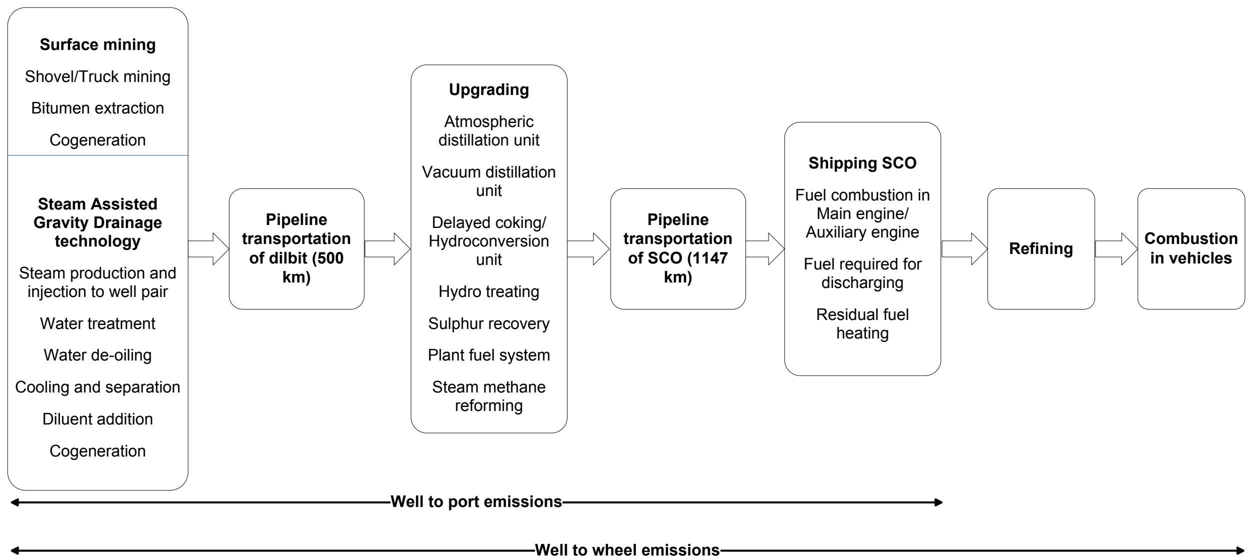

(A) Scope 1 of entire LC

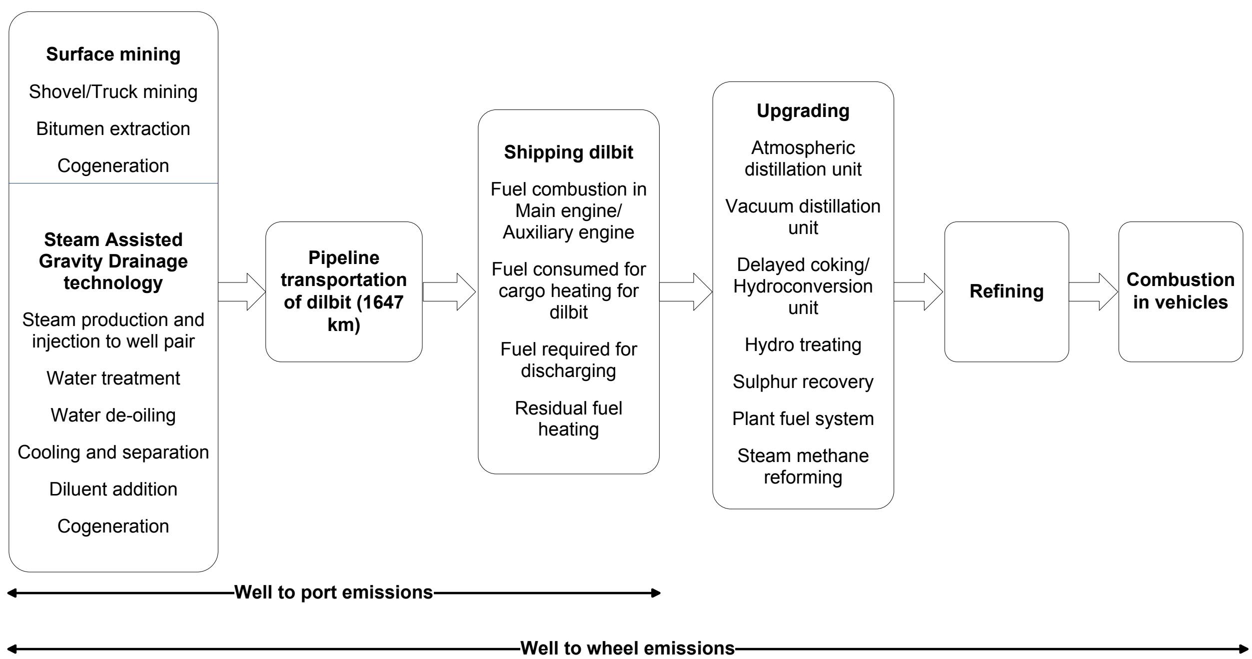

(B) Scope 2 of entire LC

Figure 27: WTW diagrams of Canadian oil sands products' life cycles that show the unit operations of recovery, extraction, upgrading, transportation, shipping, refining, and combustion as well as the subunit operations in each.

3.2.1.1 System boundary

Figure 28 (A-H) shows the LCA system boundaries of the WTW stages of all possible routes for the use of Canadian oil sands products as transportation fuels in China. The detail description of these pathways is shown in Table 15. WTW stages include extraction, transportation, upgrading, shipping, refining and combustion. The transportation of products from refinery to fuel tank is not included because of the difficulty in tracing the routes of transportation fuels to retail stores in China. The upgrader and refinery in China are assumed to be close to the sea port. Thus, their corresponding distances are left out. Many products, like coke and fuel oil, are produced throughout the LC pathways. Major products like gasoline, diesel, and jet fuel are produced in refineries along with coke and fuel oil as co-products while only coke is formed in the upgrader. Figure 28 (A-H) clearly shows produced coke and fuel oil as a co-products set inside the system boundary. The excess electricity from cogeneration in the oil sands is exported to the Alberta grid (and appropriately credited) and is considered to be outside the system boundary. Flaring, fugitives, land use, equipment, and infrastructure construction emissions are not included in this research. This research focuses on gasoline, diesel, and jet fuel production as LC end products.

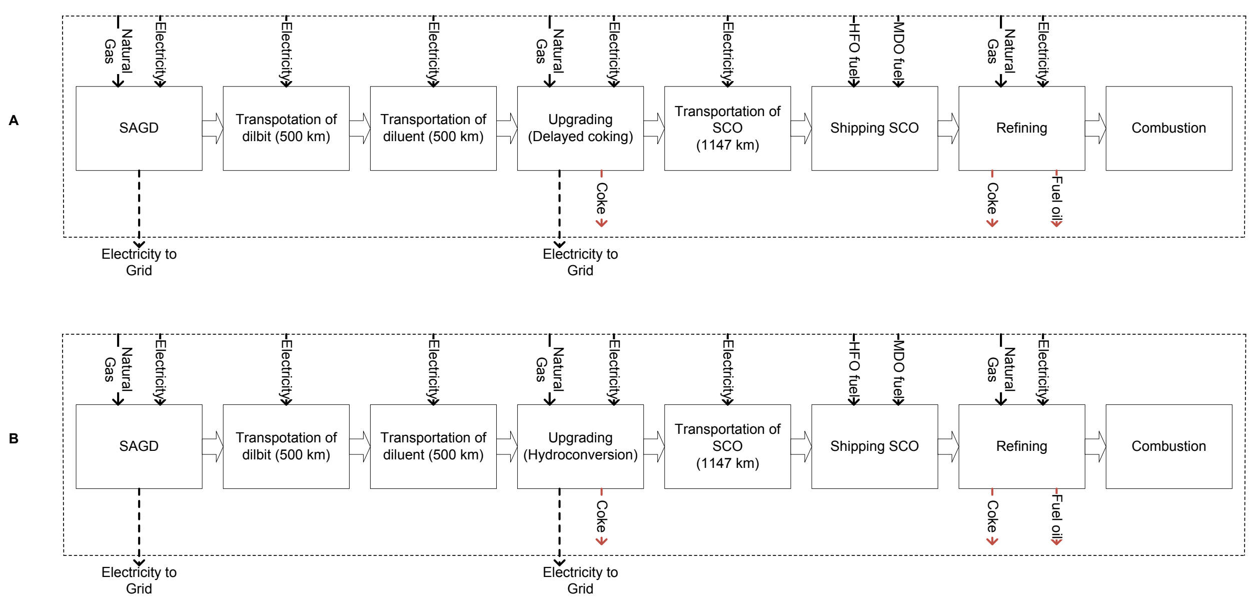

C

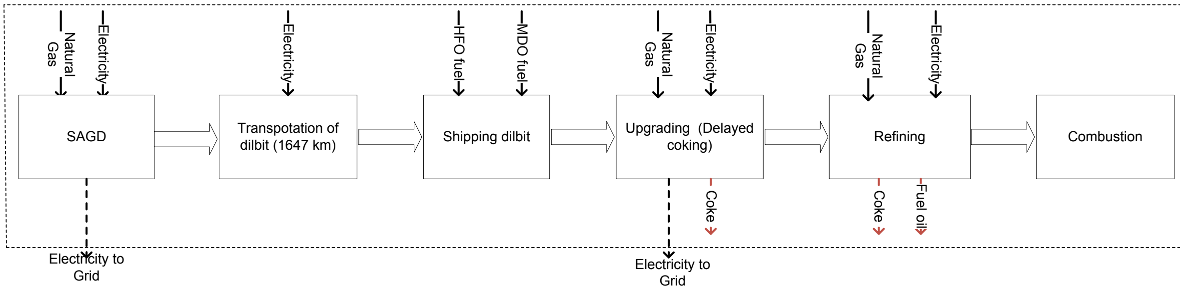
Natural Gas
Electricity
Electricity
HFO fuel
MDO fuel
Natural Gas
Electricity
Natural Gas
Electricity
SAGD
Transpotation of dilbit (1647 km)
Shipping dilbit
Upgrading (Delayed coking)
Refining
Combustion
Coke
Coke
Fuel oil
Electricity to Grid
Electricity to Grid

D

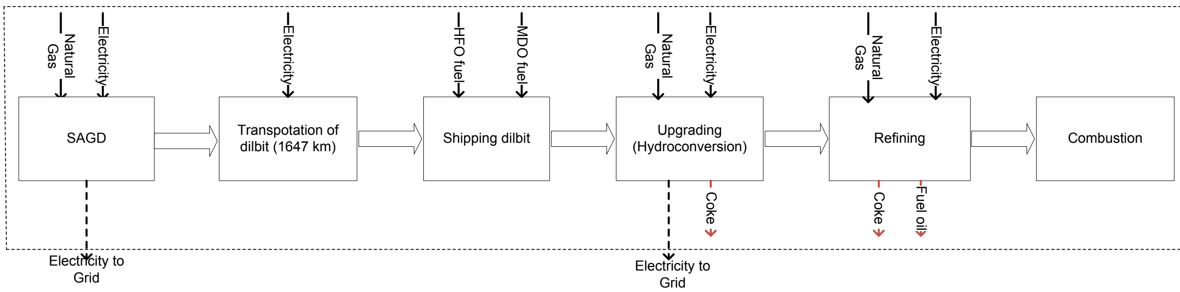
Natural Gas
Electricity
Electricity
HFO fuel
MDO fuel
Natural Gas
Electricity
Natural Gas
Electricity
SAGD
Transpotation of dilbit (1647 km)
Shipping dilbit
Upgrading (Hydroconversion)
Refining
Combustion
Coke
Coke
Fuel oil
Electricity to Grid
Electricity to Grid

E

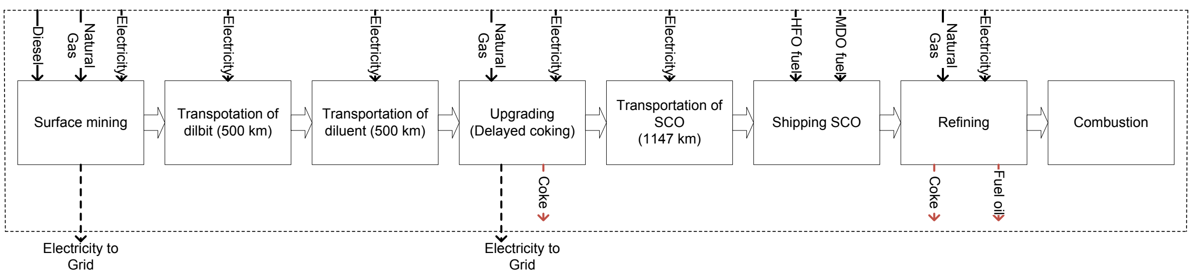
Diesel
Natural Gas
Electricity
Electricity
Electricity
Natural Gas
Electricity
Electricity
HFO fuel
MDO fuel
Natural Gas
Electricity
Surface mining
Transpotation of dilbit (500 km)
Transportation of diluent (500 km)
Upgrading (Delayed coking)
Transportation of SCO (1147 km)
Shipping SCO
Refining
Combustion
Coke
Coke
Fuel oil
Electricity to Grid
Electricity to Grid

F

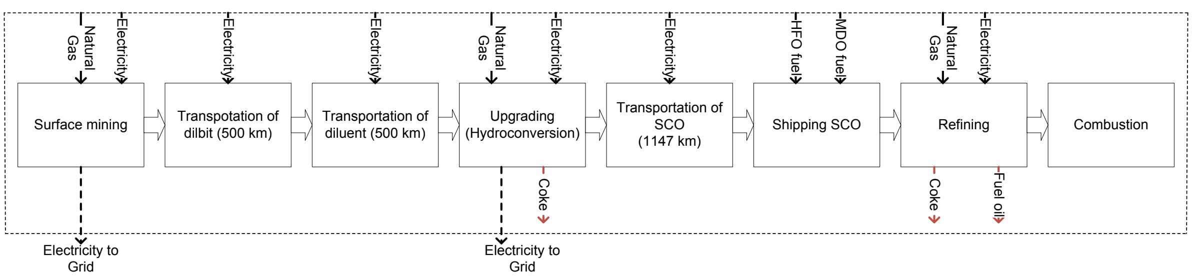
Natural Gas
Electricity
Electricity
Electricity
Natural Gas
Electricity
Electricity
HFO fuel
MDO fuel
Natural Gas
Electricity
Surface mining
Transpotation of dilbit (500 km)
Transportation of diluent (500 km)
Upgrading (Hydroconversion)
Transportation of SCO (1147 km)
Shipping SCO
Refining
Combustion
Coke
Coke
Fuel oil
Electricity to Grid
Electricity to Grid

G

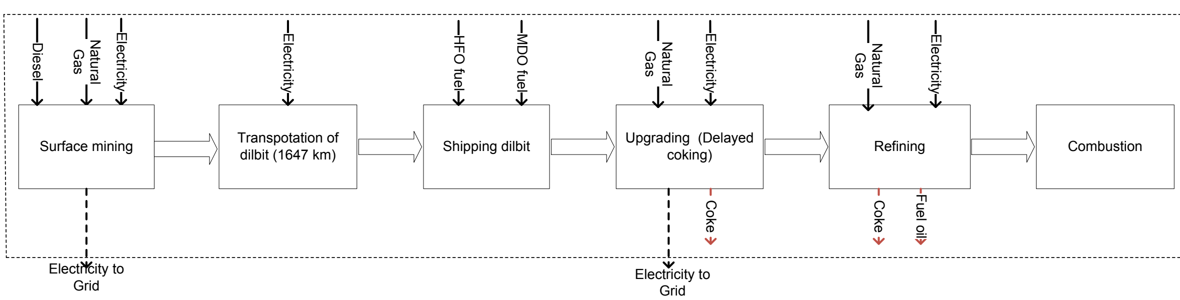
Diesel
Natural Gas
Electricity
Electricity
HFO fuel
MDO fuel
Natural Gas
Electricity
Natural Gas
Electricity
Surface mining
Transpotation of dilbit (1647 km)
Shipping dilbit
Upgrading (Delayed coking)
Refining
Combustion
Coke
Coke
Fuel oil
Electricity to Grid
Electricity to Grid

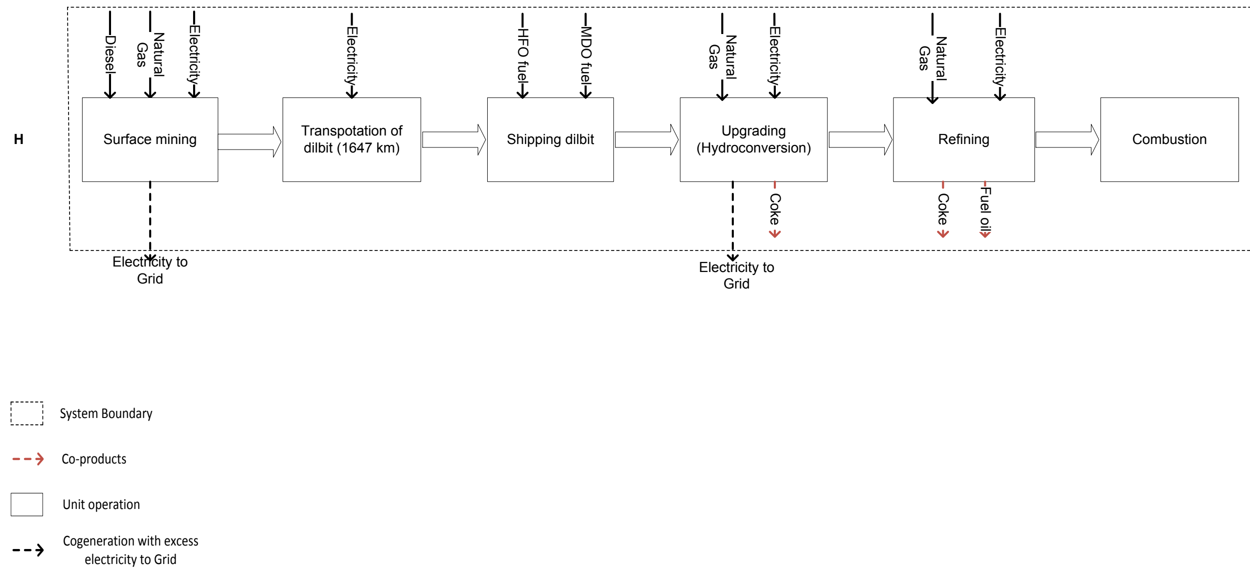

Figure 28: Canadian oil sands supply chain route to China (A): Pathway 1- Bitumen extracted from SAGD is transported by pipeline (500 km) and upgraded in delayed cokers; the produced SCO is transported by pipeline (1147 km), shipped to China, and refined there to produce gasoline and diesel. (B): Pathway 2- Bitumen obtained in SAGD is transported by pipeline (500 km) and upgraded in hydroconversion; the produced SCO is transported by pipeline (1147 km), shipped to China, and refined to gasoline and diesel. (C): Pathway 3- Bitumen recovered in SAGD is transported by pipeline (1647 km), shipped as dilbit to the destination port in China, and there upgraded in delayed cokers; finally, SCO is refined to diesel and gasoline. (D): Pathway 4- SAGD bitumen is transported by pipeline (1647 km), shipped as dilbit, and upgraded in hydroconversion, and the produced SCO refined to gasoline and diesel. (E): Pathway 5- Bitumen recovered in surface mining is transported by pipeline (500 km) and upgraded in delayed cokers, and the produced SCO is transported by pipeline (1147 km), shipped, and refined to produce gasoline and diesel. (F): Pathway 6- Surface-mined bitumen is transported by pipeline (500 km) and upgraded in hydroconversion, and the produced SCO is transported by pipeline (1147 km), shipped, and there refined to produce gasoline and diesel. (G): Pathway 7- Surface-mined bitumen is transported by pipeline (1647 km), shipped as dilbit to China, and upgraded in delayed cokers, and the produced SCO is refined to produce gasoline and diesel. (H): Pathway 8- Surface-mined bitumen is transported by pipeline (1647 km) and shipped as dilbit to be upgraded through hydroconversion in China; the produced SCO is refined to produce gasoline and diesel.

Table 15: Pathways of Canadian oil sands supply chain

Pathways of Canadian oil sands supply chain	Description	Assumptions/Comments
Pathway 1	Bitumen is extracted from the production site using SAGD. The dilbit is transported via pipeline (500 km) and upgraded in delayed coking upgrader. The produced SCO is transported by pipeline (1147 km) to the Westridge terminal in Vancouver where it is loaded in tanker and shipped to China, and there refined to produce gasoline and diesel.	Diluent is returned back to the production site (500 km).
Pathway 2	Bitumen is extracted from SAGD technology. The dilbit is transported by pipeline (500 km) and upgraded in hydroconversion. The produced SCO is transported by pipeline (1147 km) to the Westridge terminal where it is loaded in the SCO carrier and shipped to China. Finally, it is send to the refinery to be refined to gasoline and diesel.	Diluent is send back from the upgrader to the production site (500 km).
Pathway 3	Bitumen is recovered in SAGD. The dilbit is transported by pipeline (1647 km) to the Westridge terminal in Vancouver, where it is shipped as dilbit to the destination port in China. The dilbit is upgraded in delayed cokers in China. The SCO obtained from upgrader is refined to diesel and gasoline.	Diluent is assumed to be used in the refinery in China.
Pathway 4	SAGD bitumen is transported by pipeline (1647 km) to the Westridge terminal in Vancouver. The dilbit is loaded into the tanker and shipped as dilbit. The dilbit is upgraded in hydroconversion in China, and the produced SCO is refined to gasoline and diesel.	Diluent is used in the refinery in China.
Pathway 5	Bitumen is recovered in surface mining. The dilbit is transported by pipeline (500 km) and upgraded in delayed cokers. The produced SCO is transported by pipeline (1147 km) to the Westridge terminal where it is loaded into the tanker and shipped to China. Finally, SCO is refined in refinery to produce gasoline and diesel.	Diluent is returned back by pipeline to the production site (500 km).
Pathway 6	Surface-mined bitumen is transported by pipeline (500 km) to Edmonton. Hydroconversion upgrader is used to upgrade the dilbit, and the produced SCO is transported by pipeline (1147 km) to the Westridge terminal, loaded into the tanker and shipped to China. Finally SCO is refined to produce gasoline and diesel.	Diluent is returned back by pipeline to the production site (500 km).
Pathway 7	Surface-mined bitumen is transported by pipeline (1647 km) to the Westridge terminal where it is loaded into the tanker and shipped as dilbit to China. Delayed coking upgrader in China upgrade the dilbit, and the produced SCO is refined to produce gasoline and diesel.	Diluent is assumed to be used in refinery in China.
Pathway 8	Surface-mined bitumen is transported by pipeline (1647 km) to the Westridge terminal in Vancouver. The dilbit is loaded into the tanker and shipped as dilbit to the port in China where it is upgraded through hydroconversion; the produced SCO is refined to produce gasoline and diesel.	It is assumed that diluent is used in the process in refinery in China.

3.2.1.2 Functional unit

In this study, the functional unit considered for the full life cycle is one g-CO_2eq per mega joule of refined product. The life cycle GHG emissions in recovery and extraction, transportation, upgrading and shipping are presented in one kg-CO_2eq per unit volume of crude feed. The energy content of the fuels is calculated using their lower heating value (LHV). The emissions from other GHGs like CH_4 and N_2O are converted to carbon dioxide equivalents based on the 100-year global warming potential factors described in the Fifth Assessment Report of the Intergovernmental Panel on Climate Change 2013 [125].

3.2.2 LC Inventory analysis

3.2.2.1 General description

An LCA model for recovery and extraction to the end use of products in China was constructed for two supply chain products: dilbit and SCO. This LCA model was run to develop all the pathways likely to be applied by the Canadian oil sands industry in future to diversify the oil sands market in China. In an LC inventory analysis, the relevant inputs used in each unit operation of the WTW emissions are provided. The LC GHG emissions and energy use are quantified for each unit operation: recovery and extraction, transportation of SCO dilbit, diluent upgrading (DCU/HCU), shipping (SCO/dilbit), refining, and combustion.

3.2.2.2 Data collection and assumptions

This section includes the data collected for each unit operation in the system boundary. Each unit operation is described with its associated inputs and assumptions.

3.2.2.2.1 Recovery and extraction

The recovery and extraction of bitumen is the first stage in the LCA model of WTW GHG emissions. Surface mining and steam assisted gravity drainage (SAGD) are the two methods considered in this study for recovery and extraction. The main energy inputs in surface mining operations are diesel, natural gas, and electricity, and in SAGD, natural gas and electricity. Natural gas and electricity in surface mining heat water and drive pumps and floatation vessels, respectively, and diesel fuel runs the shovels and trucks. Natural gas in SAGD is consumed to produce steam. Its consumption depends on various parameters like the ratio of steam to oil (SOR), the quantity of gas produced during the extraction process, equipment efficiency, steam process conditions, and the temperature of the feed water that enters the boiler. Electricity is used in SAGD to power pumps, evaporators, and other equipment.

Nimana et al. [31] developed the model called FUNNEL-GHG-OS (FUNdamental ENgineering PrinciplEs-based ModeL for Estimation of GreenHouse Gases in the Oil Sands) to quantify the GHG emissions during recovery and extraction of bitumen from oil sands through SAGD and surface mining. The authors calculated the GHG emissions for all the unit and subunit operations of both methods. The GHG emissions figures used here for diesel, natural gas, and electricity consumption are taken from Nimana et al. [31] and were used to quantify the total LC emissions from transportation fuels in China. Readers are encouraged to review the work by Nimana et al. for more information.

3.2.2.2.2 Pipeline transportation

Canadian oil sands products are transported by pipeline in the form of SCO and dilbit. SCO is light crude and can be transported by pipeline easily. In order to transport bitumen, it is necessary to mix it with lighter hydrocarbons like naphtha or natural gas condensate. Pipeline transportation of dilbit is thus modeled assuming a composite of 70% bitumen and 30% diluent [126]. Energy use to transport dilbit and SCO and their GHG emissions primarily depend on market distance and production scale. The pipeline is designed with the capacity of 300,000 bbl/day of crude oil, which is the existing capacity of the Trans Mountain pipeline [65]. A distance of approximately 500 km is considered for the transportation of dilbit from the extraction site to the upgrader in Edmonton and 1647 km on average from the extraction site to the seaport in Vancouver. SCO is transported 1147 km to the sea port from the upgrader; this figure is the distance of the existing Trans Mountain pipeline [65]. The impact of variations in diluent return condition on WTW GHG emissions was investigated assuming a diluent pipeline capacity of 90,000 bbl/day [102] (a 70:30 ratio) over a distance of 500 km.

The main source of energy required to transport SCO and dilbit is assumed to be electricity. Electricity compensates head loss due to friction and drives the inlet and booster station pumps. Friction factor is determined from a Moody diagram using the Reynolds number and absolute roughness of new commercial steel pipeline taken from Subramanian [103]. The primary governing equation used to determine head loss due to friction is the Darcy-Weisbach equation (see Appendix B S2 eq. 2). Volumetric flow rate, head loss due to friction, pipeline length, crude density, and pump efficiency are the main input variables used to determine the power required to overcome friction. The velocity is calculated as 1.8 m/s based on the flow rate, which corresponds to the pipeline diameter of 0.61 m and was calculated using the continuity equation (see Appendix B S2 eq. 1). GHG emissions were calculated using the total energy required for pumping and the GHG emission factors estimated based on the weighted average of the

Canadian and U.S. provincial grid GHG emission factors [122, 123]. The key input variables and specifications of the transportation model are shown in Table 16.

Table 16: Input variables and specifications of the transportation model

Crude feed	Dilbit	SCO	Diluent	Comments/References
Capacity (kbd)	300[a]	300[a]	90[b]	
API	22	32	55	[42]
Kinematic viscosity (Cst)	200	10	1.3	[42]
Pump efficiency (%)	70	70	70	[42]
Distance (km)	500[c], 1647[d]	1147[e]	500[c], 1647[d]	
Pipeline diameter ID (m)	0.61	0.61	0.37	Calculated using governing fluid flow equation (Appendix B S2 eq. 1) assuming a velocity range of 1.8 m/s
Thickness (m)	0.0127	0.0127	0.0127	Same value is assumed for all cases
Absolute roughness (mm)	0.046	0.046	0.046	[103]
ΔP (bar)	50	50	50	[104]

[a] Existing Trans Mountain Pipeline capacity

[b] Existing capacity of Polaris Pipeline

[c] 500 km is considered from Fort McMurray to Edmonton

[d] 1647 km is considered from Fort McMurray to the Westridge terminal in B.C

[e] The Trans Mountain Pipeline is 1147 km

3.2.2.2.3 Upgrading

Bitumen obtained from Canadian oil sands first needs to be upgraded to SCO before it is sent to the refinery. Bitumen is upgraded in Canada or in China, depending on the pathway (as shown in Figure 1 [A-B]), and the upgraders are assumed to be of the same configuration in both countries. Two upgraders, delayed coking and hydroconversion, are used to develop the pathways. In a delayed coking upgrader, heavy feed is heated in a coking unit at 500˚C [95], while in hydroconversion the feed is cracked at a lower temperature of 350-430˚C under the high hydrogen partial pressure of 6000-15000 kPa [96]. The energy required to upgrade bitumen is mainly in the form of natural gas and electricity. Their consumption depends primarily on distillation properties, sulfur content, and the American Petroleum Institute (API) gravity of the feed and the products. The steam required in different unit operations of the upgrader is produced using natural gas and fuel gas. Process conditions, steam consumption, and electricity consumption are the main input data used to estimate the GHG emissions of the upgrading model. Nimana et al. [30] give more details in their paper.

Nimana et al. [30] used FUNNEL-GHG-OS to estimate energy consumption per barrel bitumen and life cycle GHG emissions for upgrading bitumen. They also used it to explore the impact of electricity cogeneration on the GHG emissions of oil sands upgrading operations. They used the emission factors for natural gas equipment from the GREET model [41]. An emission factor of 880 g-CO_2eq/KWh of Alberta's grid electricity was used, while in the cogeneration case, an emission factor of 650 g-CO_2eq/KWh of displaced electricity was used to quantify the GHG emissions [122]. The FUNNEL-GHG-OS model used the composition of fuel gas provided in a report by Netzer and associates [95] and estimated an emission factor of 2419.4 gCO_2eq/kg of fuel gas. The model ignored the fugitive, venting and flaring, land use, and equipment emissions. The results of this model were used to develop the WTW GHG emissions of the transportation fuels considered in this study.

3.2.2.2.4 Shipping

Once Canadian oil sands products reach the Westridge terminal, they are transported by ocean tankers. The facility at Westridge can handle nothing larger than Aframax tanker [105]. In this study, it is assumed that dilbit and SCO are shipped from Vancouver to ports in China using Aframax tankers with a capacity of 729,000 barrels. This capacity is the approximate average volume of the tanker. In order to estimate the shipping distance, the major ports in China were identified and the average inter-portal distance from the port of Vancouver was calculated using the Port World Distance Calculator [110]. The calculated average sailing time to China is 17 days. GHG emissions were evaluated at 6.9 m/s for an Aframax tanker [105]. This is the evaluated optimized speed at which shipping cost is lowest. Energy consumption and its GHG emissions depend on the type of propulsion system, velocity, type of fuel used, discharging rate, and efficiency of various systems. In this study, it was assumed that the power required to propel the Aframax tanker is provided by a mechanical two-stroke propulsion system. The required power is calculated using total calm water resistance and Holtrop and Mennen's approximate power prediction approach [67] along with the statistical power prediction method [68], speed, and propeller efficiency. The main engine (ME) is powered by heavy fuel oil (HFO) and the auxiliary engine (AE) burns marine diesel oil (MDO). Total GHG emissions were obtained by using the calculated power and emission factor for each engine. The input data used to quantify the GHG emissions are shown in Table 17.

Table 17: Parameters to estimate GHG emissions in shipping dilbit and SCO to China

	Nomenclature	Fuel	Value	Unit
Vessel specification[f]				
Cargo capacity	V_c		115,873	m^3
Deadweight tonnage	Dwt		105,927	tons
Length	L_{OA}		243.98	m
Breadth	B		42	m
Depth	T		21	m
Main engine model[g]		HFO	10.4	MW
Auxiliary engine model[h]		MDO	1.98	MW
CO_2 emission factor[i]			568	g/kWh
SFOC[2] data				
Main engine SFOC[g]	SFO_m		156	g/kWh
Auxiliary engine SFOC[h]	SFO_{aux}		191	g/kWh

[f] Vessels specifications are taken from the Clarkson data sheets [66].

[g] Power rating, emission factor, and SFOC are based on the main engine model (1 x MAN S60MC8). Its SFOC data are selected from MAN B&W Diesel [108].

[h] Power required, emission factor, and SFOC for auxiliary engine models are based on 1 x Aux. Diesel Gen 9L28/32H model and its SFOC data are selected from MAIN Diesel & Turbo [109].

[i] Average emission factor taken from MAN B&W Two-stroke Marine Diesel Engines and MAN Diesel & Turbo [127, 128].

[2] SFOC stands for Specific Fuel Oil Consumption, which depends on the ambient conditions and calorific value of fuel oil.

3.2.2.2.5 Refining

After upgrading, the SCO is sent to the refinery to produce transportation fuels: gasoline, diesel, and jet fuel. Different refineries consume different forms of energy depending upon configuration and feed properties. Many products like diesel fuel, jet fuel, gasoline, fuel oil, and liquefied petroleum gas are produced from the refinery. The main sources of energy are natural gas, fuel gas, electricity, and fuel oil. Due to the lack of data in the public domain for the parameters and process conditions of the refineries in China, a refinery model developed by Nimana et al. [30], simulating a typical deep conversion refinery in Aspen HYSYS, was used to quantify energy consumption and GHG emissions of a Chinese refinery model. Nimana et al. [32] used the default configuration, parameters, and conditions as used in Aspen HYSYS's refinery-wide sample model [129]. Since many products are produced from the refinery, allocation is necessary. This model allocated the refinery emissions on a sub-process level, that is, one based on the mass of the products. The model distributed the GHG emissions among the products for each subunit operation. The GHG emissions' values calculated by this model for the deep conversion refinery [130] were used to develop total LC GHG emissions.

3.2.2.2.6 Combustion

The combustion of the transportation fuels is the last stage of the LC emission pathway. The transportation fuels are burned in vehicle engines. Emissions vary with the type of vehicle used. The combustion of gasoline, diesel fuel, and jet fuel is considered for passenger cars and aircraft. The GHG emissions factors for the combustion of gasoline and diesel are taken from the GREET model [41].

3.3 Results and discussion

The WTW system boundary considered in this study includes emissions from extraction (SAGD/surface mining), pipeline transportation, upgrading, shipping, refining, and combustion. Nimana et al. earlier determined energy consumption and GHG emissions in the extraction, upgrading, and refining of Canadian oil sands products [30, 31]. In this study, the WTW life cycle emissions of the conversion of Canadian oil sands products to end uses in China was estimated and this was based on earlier studies.

3.3.1 GHG emissions of each stage of operation

The GHG emissions from extraction were found to be 7.17–14.23% of the total LC WTW emissions. SAGD emits more GHGs than surface mining, excluding land-use and fugitive emissions from tailings [31]. This is because more natural gas is required in SAGD for steam generation.

Transporting dilbit by pipeline emits more GHG emissions than SCO over the same distance because of the viscous nature of dilbit, which requires more energy to make it flow through the pipeline. However, the transportation of both SCO and dilbit by pipeline comprises a significantly small portion of total WTW LC emissions. A hydroconversion upgrader is more GHG-intensive than a delayed coker. This is because typically more energy is required for hydrogen production [43].

Table 18: GHG emissions of each stage

	GHG emissions		Units	Reference
	Range	Default		
Surface mining				
No cogeneration	223.2–302.9	257.9	$kgCO_2eq/m^3$ bitumen	[31]
With cogeneration[j]	186.9–203.6	199	$kgCO_2eq/m^3$ bitumen	[31]
SAGD				
No cogeneration	379.7–924.7[k]	460[k]	$kgCO_2eq/m^3$ bitumen	[31]
With cogeneration[j]	203–818.3[k]	203[k]	$kgCO_2eq/m^3$ bitumen	[31]
Upgrading				
Delayed coking				
No cogeneration		240.3	$kgCO_2eq/m^3$ bitumen	[30]
With cogeneration		208.6	$kgCO_2eq/m^3$ bitumen	[30]

	GHG emission Ranges	Default	Units	References
Hydroconversion				
No cogeneration		433.4	$kgCO_2eq/m^3$ bitumen	[30]
With cogeneration		365	$kgCO_2eq/m^3$ bitumen	[30]
Transportation by pipeline				
Transportation of dilbit- 500 km without diluent return	13.37–23.31	19.97	$kgCO_2eq/m^3$ bitumen	
Transportation of dilbit- 500 km with diluent return	16.1–26.13	22.78	$kgCO_2eq/m^3$ bitumen	
Transportation of dilbit - 1647 km without diluent return	43.61–77.21	65.79	$kgCO_2eq/m^3$ bitumen	
Transportation of SCO - 1147 km	15.36–28.73	16.73	$kgCO_2eq/m^3$ SCO	
Shipping by ocean tanker[l]				
SCO		23.05	$kgCO_2eq/m^3$ SCO	
Dilbit		46.06	$kgCO_2eq/m^3$ bitumen	
Combustion				
Conventional diesel		75.7	gm/MJ	[42]
Conventional gasoline		75.1	gm/MJ	[42]
Conventional jet fuel		73.2	gm/MJ	[42]
Refining[m]				
Coker SCO		39	$KgCO_2eq/bbl$	[30]
Hydroconversion SCO		45	$KgCO_2eq/bbl$	[30]
Dilbit		53.17	$KgCO_2eq/bbl$	[30]

[j]For the cogeneration case of surface mining and SAGD, a gas turbine is considered.

[k] Produced gas emissions from consumption and flaring are ignored in SAGD, since they form a very small portion of the total emissions [47].

[l]Shipping is considered from Vancouver to a port in China using an Aframax tanker with a capacity 729,000 bbl.

[m]A refinery with a capacity of 150,000 bpd of SCO and bitumen is considered and the diluent separation emissions are included.

Emissions from shipping SCO and dilbit include those from the boiler, the main engine (ME), and the auxiliary engine (AE). The energy consumed is in the form of HFO for the ME and the boiler, while for the auxiliary engine it is in the form of MDO. It was observed that ME emissions make up 79% and 57% of the total GHG emissions in shipping SCO and dilbit, respectively. However, the emissions from the boiler account for 35% and 9% of the total shipping emissions for dilbit and SCO, respectively. This study also calculated the GHG emissions from auxiliary engines to be 8% and 11% of the total shipping emissions for dilbit and SCO, respectively. Figures 29 and 30 show the GHG emissions from each system for both SCO and dilbit products.

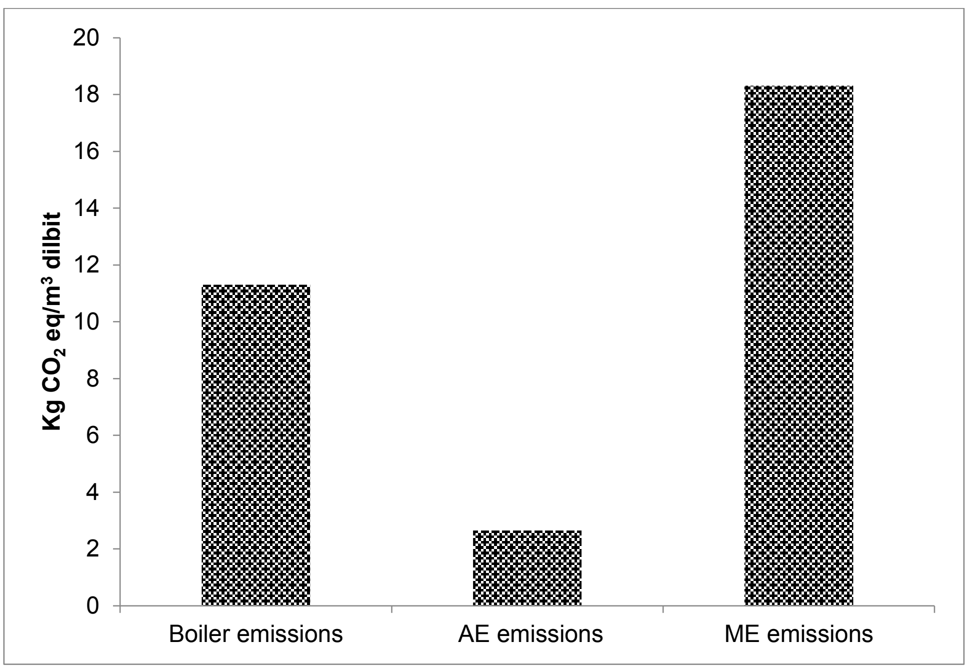

Figure 29: GHG emissions from shipping dilbit

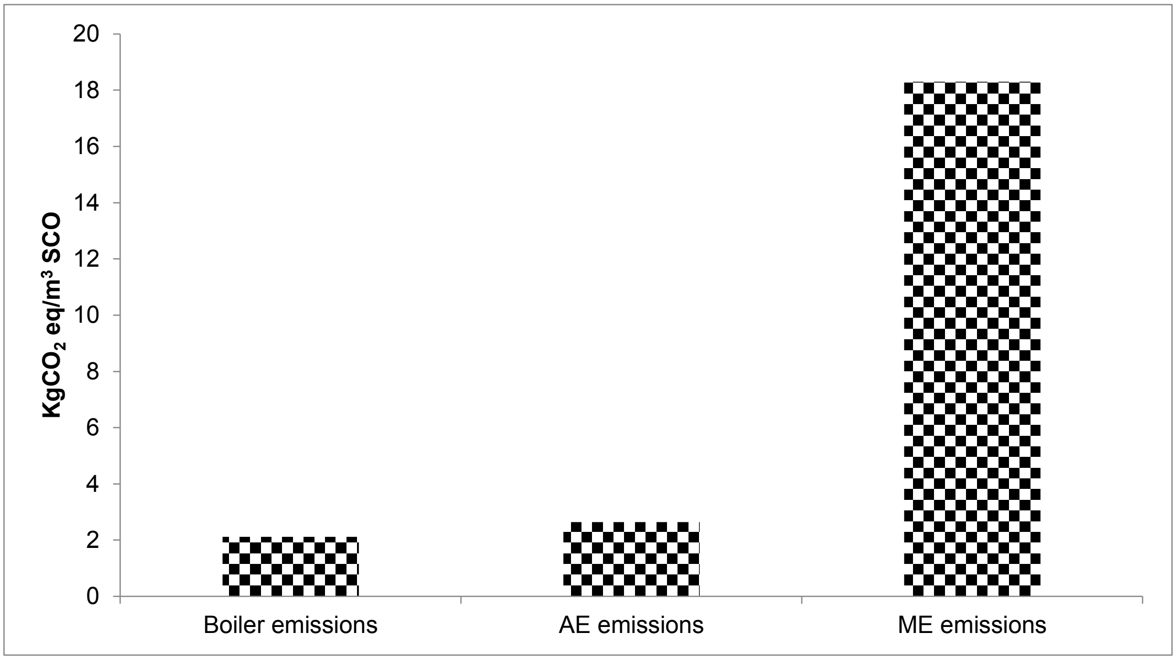

Figure 30: GHG emissions from shipping SCO

Refining GHG emissions form 9.47%–11.22% of the total WTW LC emissions in gasoline production. Combustion is the most GHG-intensive stage. Combustion GHG emission is 64.08%–70.19%, 67%–75% and 67%–76% for gasoline, diesel, and jet fuel, respectively. GHG emissions for each stage are shown in Table 18.

3.3.2 LC GHG emissions of the pathways

Figure 31 (A-C) shows the LC WTW GHG emissions of three transportation fuels used in China derived from Canadian oil sands products in eight pathways. These pathways were developed for the various extraction and upgrading technologies. It is clear from Figure 31 (A-C) that LC WTW GHG emissions from gasoline production are the highest, followed by diesel and jet fuel production. The LC emissions vary because of differences in extraction, upgrading, transportation, and refining emissions. Pathways 1-4 use SAGD for the extraction of bitumen from oil sands with variations in upgrading and transportation operations, while pathways 5-8 use surface mining.

The LC WTW GHG emissions for gasoline, diesel, and jet fuel are from 102.5–132.8, 96.08–128.5, and 91.9–124.6 g-CO_2eq/MJ, respectively. This wide range is because of the uncertainty in the each stage. Of all the pathways, pathway 5 has the lowest total LC GHG emissions. This pathway follows the extraction of oil sands by surface mining, then transportation of dilbit (500 km) with diluent return, upgrading by DCU followed by transportation of SCO (1147 km), shipping to China, refining, and combustion. Surface mining and the DCU upgrader consume less energy than SAGD and the HCU upgrader, respectively, thus emitting fewer GHGs. Pathway 4 has the highest WTW GHG emissions. In this pathway, bitumen is extracted through SAGD, transported as dilbit by pipeline 1647 km, shipped by oil tanker, upgraded by HCU, refined, and combusted in China. SAGD and the HCU upgrader are the GHG-intensive stages in this pathway. This is because a huge amount of natural gas is consumed to produce the steam required for SAGD and the hydrogen for the HCU.

Each LC stage contributes to total GHG emissions in different proportions depending on the pathway. Combustion has the highest portion of total GHG emissions, as mentioned earlier. Recovery and extraction, as well as upgrading and refining, have a significant impact on LC WTW GHG emissions. Emissions from shipping (0.64%–1.5%) and transportation (1.26%–2.14%) form a much lower percentage of WTW GHG emissions.

The LC WTW GHG emissions of different Canadian oil sands pathways were reported by Nimana et. al. [42] as 106.5–116 g-CO_2eq/MJ gasoline, 100.5–114.9 g-CO_2eq/MJ diesel, and 96.4–108.9 g-CO_2eq/MJ jet fuel. Those studies were conducted for the transportation fuels used in the U.S. However, the results from these studies are within the range of the values reported in this study for the transportation fuels used in China.

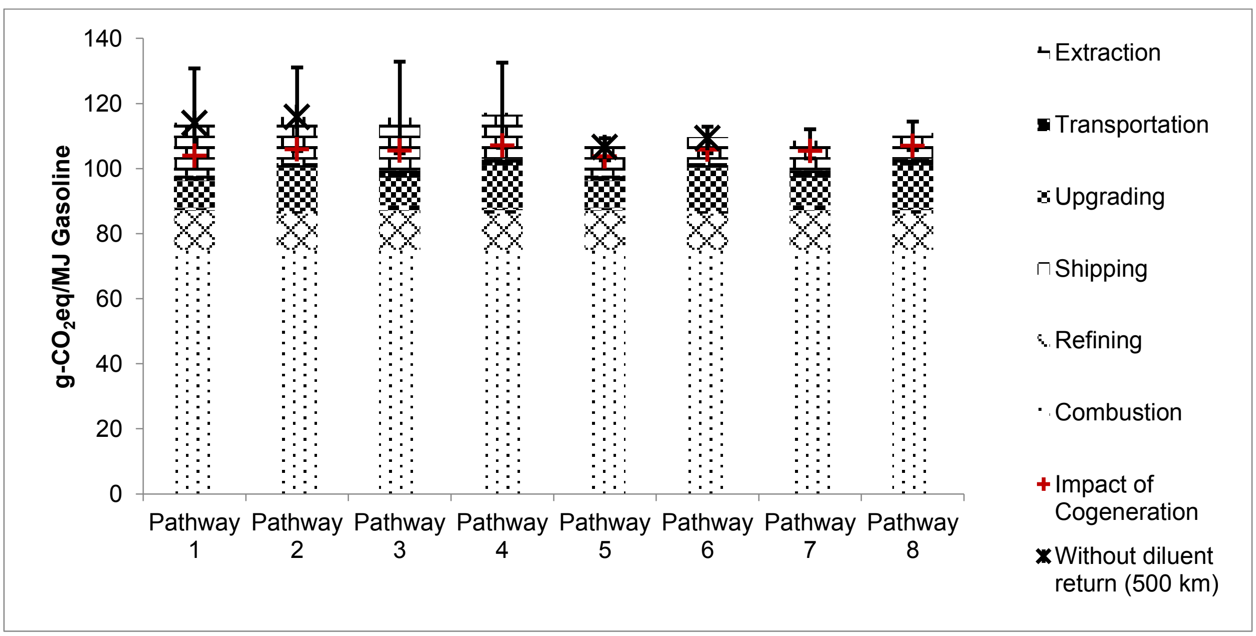

(A) LC WTW GHG emissions of different pathways for gasoline

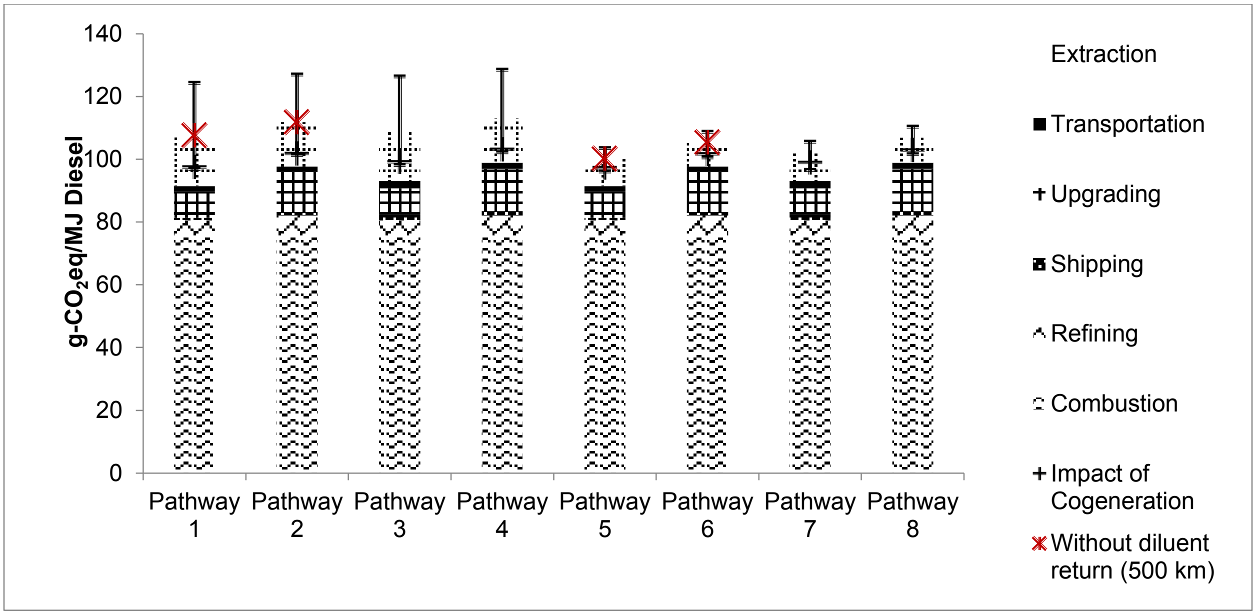

(B) LC WTW GHG emissions of different pathways for diesel

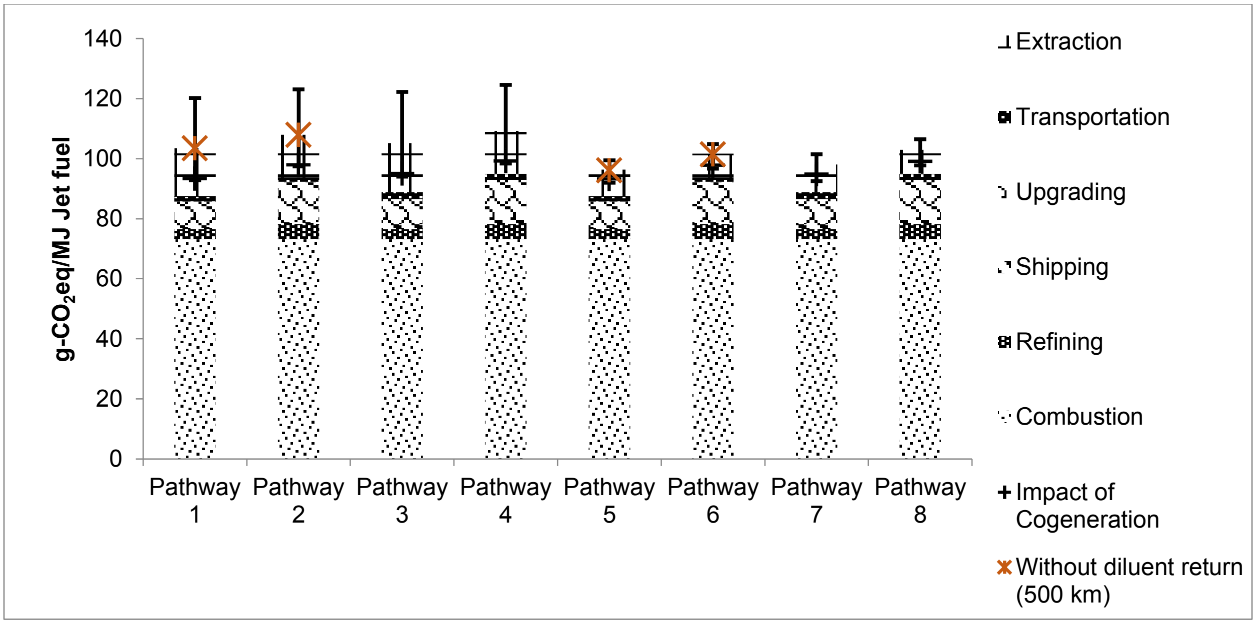

(C) LC WTW GHG emissions of different pathways for jet fuel

Figure 31: LC WTW GHG emissions for (A) gasoline, (B) diesel, and (C) jet fuel. The values for the WTW emissions of each transportation fuel were obtained by adding the lowest and highest values for recovery and extraction, transportation, shipping, and upgrading

3.3.3 Impact of cogeneration and diluent return condition

The impacts of cogeneration and diluent return condition on the pathways (wherever applied) are shown in Figure 31 (A-C). The diluent return condition is only applied for pipeline transportation of dilbit of 500 km. This data is included in the developed pathways by default. When the dilbit is transported 1647 km, it is assumed that the diluent is used in China. However, to observe the impact of "without diluent return condition" on WTW GHG emissions over 500 km, '×', indicating "without diluent return (500 km)," is shown in Figure 31. This condition has very little impact on overall LC GHG emissions.

Cogeneration is important for oil sand projects since excess produced electricity can be exported to the grid and given co-product GHG emission credits. The impact of cogeneration is shown in Figure 31 (A-C) for each pathway. The '+' (indicating the impact of cogeneration) shows the net GHG emissions of each pathway once the GHG emission credit for displacing high GHG-intensive grid electricity is applied. The cogeneration model is typically applied to recovery, extraction, and upgrading operations. Their combined effect on WTW GHG emissions is shown in Figure 31. The cogeneration model built in FUNNEL-GHG-OS developed by Nimana et al. [30, 31] to study the effects of cogeneration in recovery, extraction, and upgrading is used in this model to observe the impact of cogeneration on total WTW emissions in the eight pathways. For gasoline and diesel production, the cogeneration affects the WTW GHG emissions by 3%–9%. Pathways 1–4 are affected most by cogeneration. This is because these pathways include the SAGD operation, which is used for the extraction of bitumen from oil sands. This stage requires a huge amount of steam, which is produced by burning natural gas. Cogeneration highly impacts this stage. Surface mining and the DCU are less affected by cogeneration. Thus, pathways 5–8, which include these operations, are impacted less by cogeneration.

3.3.4 Comparison of LC GHG emissions with those from Middle Eastern countries

Very few studies address the LC WTW GHG emissions from Middle Eastern countries' fuels used in China. Most of the research studies energy use and GHG emissions from domestic crude. Yan and Crookes [44] reviewed life cycle studies of different fuels to identify the most reliable results as well as ranges of life cycle fossil fuel use, petroleum use, and GHG emissions intensity for various road transportation fuels in China. Ou et al. [131] developed a detailed model to estimate past trends of both direct and LC energy demand and GHG emissions in China's road transport sector and projected trends up to 2050. These studies do not include LC WTW GHG emissions from the crude from the Middle East.

Given the lack of data available in the public domain, this study developed the LC WTW GHG emissions from transportation fuel used in China derived from Saudi Arabian crude in order to compare the LC GHG emissions between Canadian oil sands products and Saudi Arabian crude. According to EIA 2014, China imports the largest amount of crude (16%) from Saudi Arabia [132]. The total LC WTW GHG emissions from transportation fuels derived from Saudi Arabian crude is 94.58 g-CO_2eq/MJ gasoline, 91.65 g-CO_2eq/MJ diesel, and 83.26 g-CO_2eq/M jet fuel. The LC WTW GHG emissions from Canadian oil sands products are higher than the LC GHG emissions from Saudi Arabian crude. This is because of the additional upgrading emissions Canadian oil sands products go through. In addition, the extraction emissions of Canadian oil sands products are much higher than Saudi Arabian crude's. The extraction emissions of Canadian oil sands products are 7.17%–14.23% of the total LC WTW GHG emissions, while Saudi Arabia's are only 2% of the total.

Combustion is the most GHG-intensive stage for Saudi Arabian crude. The range of emissions from the combustion stage is 79%–88%, depending on the fuel. Shipping and transportation emissions have very little impact on total GHG emissions. Refining emissions account for 18%, 14%, and 9% of the total emissions from gasoline, diesel, and jet fuel, respectively, for Saudi Arabian crude.

3.3.5 Sensitivity analysis

A sensitivity analysis was done for tanker capacity, crude density, the efficiencies of the boiler, the heat exchanger, and the pump, velocity, discharge rate, and maneuvering speed. The impact of these parameters on shipping was investigated for both SCO and dilbit. Figures 32 and 33 show that ocean tanker velocity and capacity have the largest impact on the shipping emissions of both products. Increasing the velocity increases the resistance. Thus, more power is required, resulting in more fuel consumption, which ultimately increases the GHG emissions. Parameters such as the efficiencies of the boiler, the heat exchanger, and the pump, maneuvering speed, crude density, and discharge rate have less impact on shipping emissions.

A Monte Carlo simulation was performed to evaluate the GHG emissions associated with shipping SCO and dilbit. All the uncertain input variables like capacity, density of crude, the efficiencies of the boiler, the heat exchanger, and the pump, velocity, discharge rate, and maneuvering speed were identified with their highest and lowest ranges. A random sampling was performed by using these uncertain input variables from the shipping model to generate GHG emissions figures for SCO and dilbit. Figures 34 and 35 show the GHG emissions ($kgCO_2eq/m^3$ of crude) for shipping SCO and dilbit to be 21.76–33.4 and 31.15–48.79, respectively, for 90% probability.

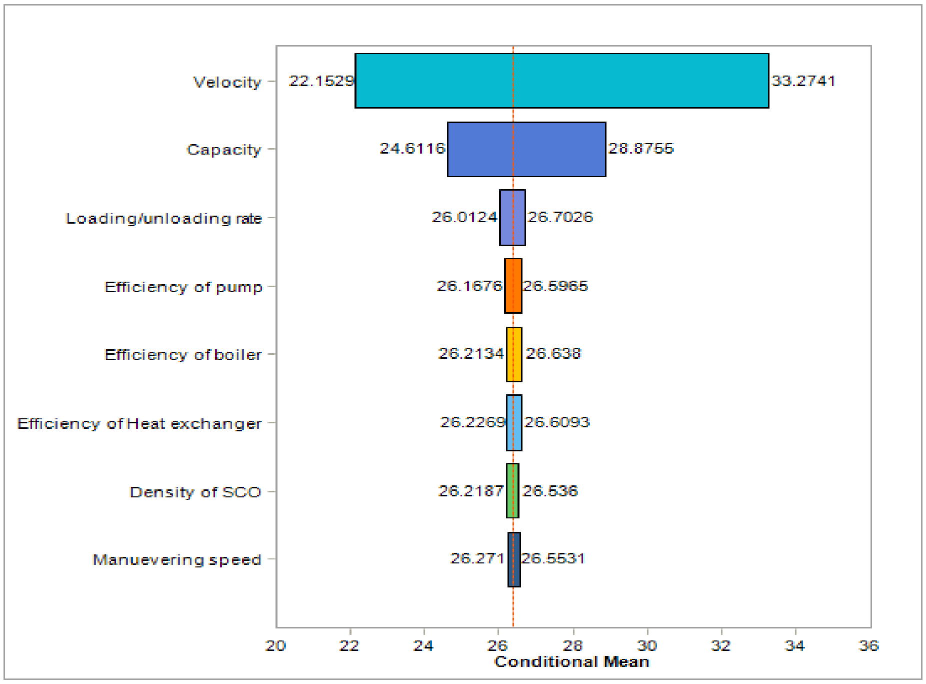

Figure 32: Sensitivity analysis of GHG emissions from shipping SCO

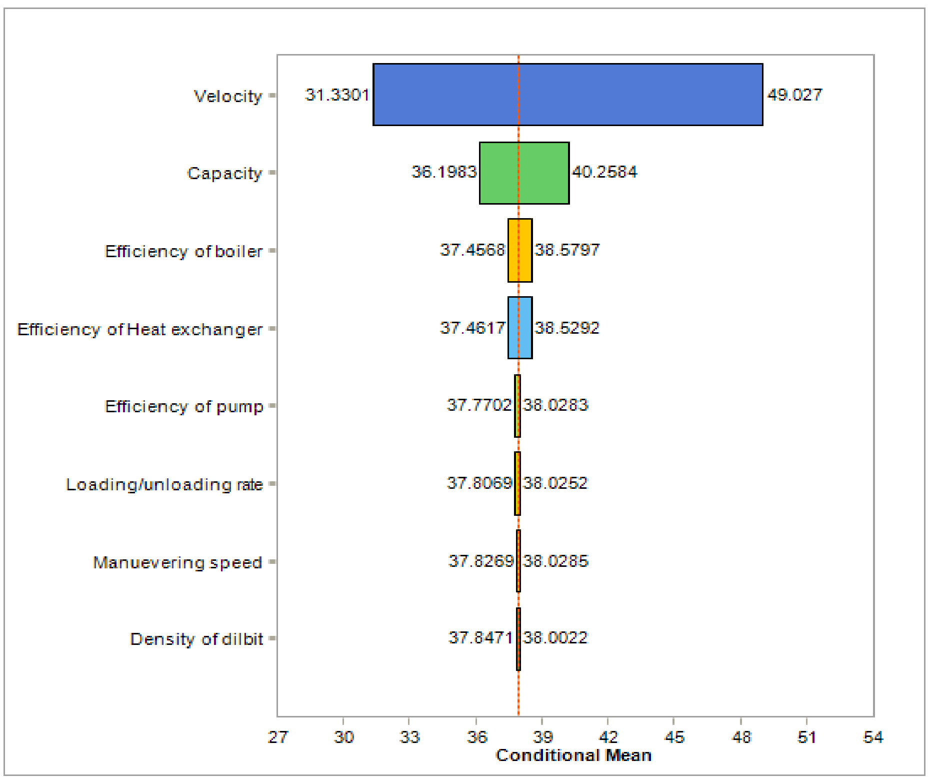

Figure 33: Sensitivity analysis of GHG emissions from shipping dilbit

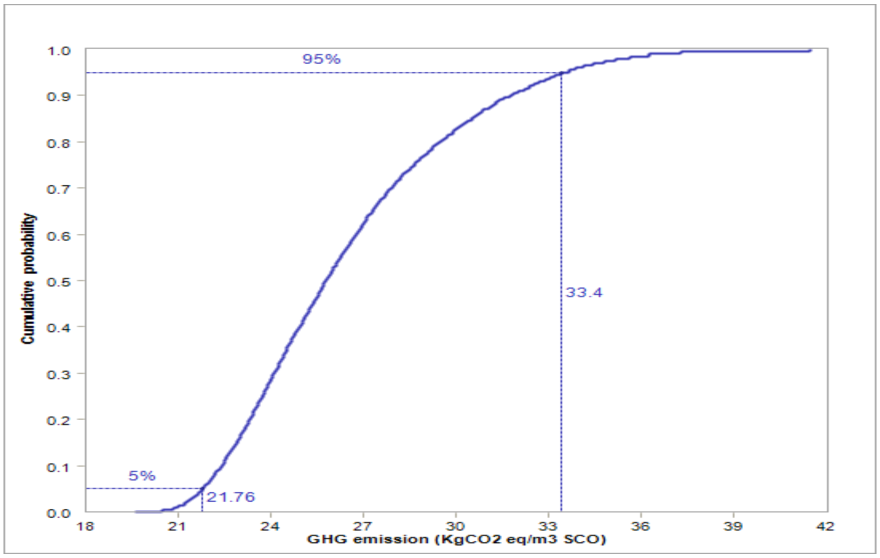

Figure 34: Ascending cumulative probability plot of GHG emissions for shipping SCO

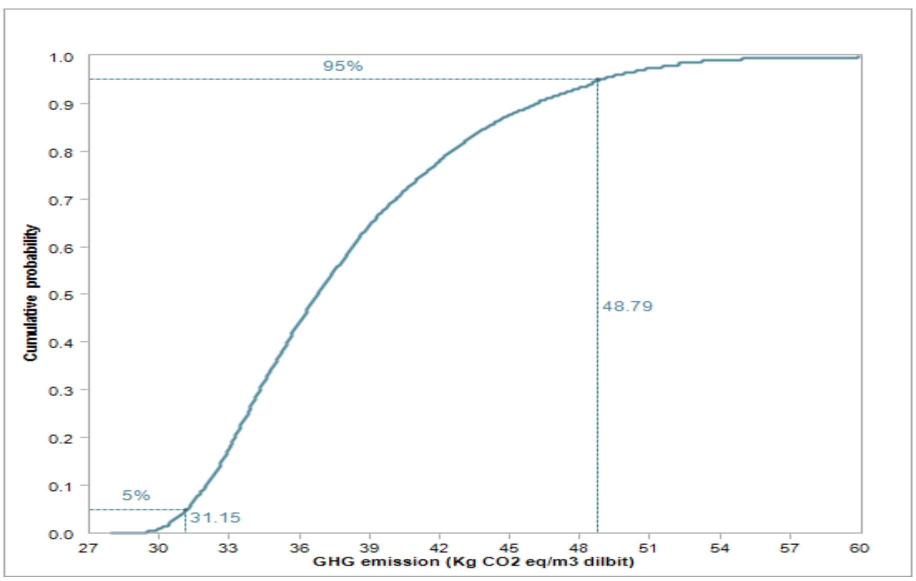

Figure 35: Ascending cumulative probability plot of GHG emissions for shipping dilbit

3.4 Conclusion

In this study, comprehensive WTW LC GHG emissions for the transportation fuels used in China derived from Canadian oil sands products was estimated. The GHG emissions include those from all the stages from recovery and extraction to the combustion of fuels in vehicle engines. Eight pathways were developed that represent future oil sands markets. Pathway 5 has the lowest LC WTW GHG emissions. This pathway includes surface mining and delayed coking as key stages; this pathway has lower WTW LC GHG emissions. In this pathway, bitumen is extracted in surface mining and the dilbit is transported by pipeline (500 km) to upgrade in delayed cokers; the produced SCO is transported by pipeline (1147 km) to the Westridge terminal where it is loaded into the tanker and shipped to China and finally refined in to produce gasoline and diesel. However, irrespective of the pathway, overall emissions can be reduced if the extraction technology can be improved such that the products require partial or no upgrading before being refined. New extraction technologies like N-solv and electromagnetic heating are still in the research phase and could be explored in future as an option to reduce overall emissions.

The results of our study show that gasoline production emits more GHGs than diesel and jet fuel production. This is because more energy is required for gasoline production. The findings also show that combustion contributes a significant portion of WTW LC emissions.

The LC WTW GHG emissions for gasoline, diesel, and jet fuel lie in the range of 102.5–132.8 g-CO_2eq/MJ gasoline, 96.08–128.5 g-CO_2eq/MJ diesel, and 91.9–124.6 g-CO_2eq/MJ jet fuel, respectively. This wide range shows the uncertainty in each stage of LC emissions. It is also observed that the LC WTW GHG emissions from Canadian oil sands products are higher than those from Saudi Arabian crude at 94.58, 91.65, and 83.26 g-CO_2eq/MJ for gasoline, diesel, and jet fuel, respectively. Canada's emissions are higher largely because of the upgrader unit used in the oil sands energy conversion chain, which increases overall LC emissions significantly.

From the sensitivity analysis conducted to assess the impact of various parameters on shipping, it was found that the velocity and capacity of the ocean tanker have the most impact on the shipping emissions of SCO and dilbit.

The results of this study will help government, industry, and policy makers in Canada and China come up with a policy framework that ensures the lowest GHG emissions pathway and strengthens the trade relationship in an environmentally friendly way. This work will also help focus on potential areas to improve in order to make the LC GHG emissions from Canadian oil sands products environmentally competitive with Middle Eastern countries.

Chapter 4[1]

Techno-economic and life cycle assessment of the natural gas supply chain from production sites in Canada to north and southwest Europe

4.1 Introduction

With energy security a high concern in the European Union's foreign policy agenda, Canada's abundant natural gas resources are of significant interest to the EU. While supply risks associated in the Canadian natural gas supply are recognized, as the U.S. is the sole customer of Canadian natural gas markets currently, the Canadian government is highly interested in exploring the potential market opportunity in Europe. However, the minimum supply chain costs and life cycle GHG emissions of the Canadian LNG supply chain in the delivery of LNG to Western Europe are unknown. Therefore, the supply chain costs and environmental risks associated with the delivery of Canadian LNG to Western Europe need to be evaluated through all possible routes. Some studies have been done from an economic perspective that address the cost of natural gas processing using different technologies [51, 52]. Other works, using data from the shale gas reserves in the U.S., have evaluated life cycle GHG emissions in the extraction and processing of shale gas [59-62]. None of these studies address supply chain costs or life cycle GHG emissions of the Canadian LNG supply chain in the delivery of LNG to Western Europe. This chapter discusses the development of techno-economic and life cycle assessment models used to compare the delivered costs and environmental risks of two supply chain routes to north and southwest Europe and to compare the supply chain costs and the LC GHG emissions of Canadian LNG with those of the main exporters (i.e., Norway, Russia, and Algeria) to Western Europe.

4.2 Scope and methodology

4.2.1 Scope

Figure 37 shows the scope this study used to evaluate the delivered costs and life cycle GHG emissions of the Canadian LNG supply chain to north and southwest Europe. The scope incorporates recovery, gas processing, transportation, liquefaction, shipping, and re-gasification. Canadian shale gas is first extracted from the reserve (Horn River and Montney are considered in this study), then transported by pipeline either to Canada's west or east coast, where the

[1] This version of chapter has been submitted to Natural Gas Science and Engineering by Elsevier: *Sapkota K., Oni O. A., Kumar A. Techno-economic and life cycle assessment of the natural gas supply chain from production sites in Canada to north and southwest Europe. Natural Gas Science and Engineering by Elsevier, 2017 (in review)*

natural gas is liquefied in a liquefaction facility and loaded into an LNG tanker, shipped to a destination port, and finally re-gasified for pipeline distribution as shown in Figure 36.

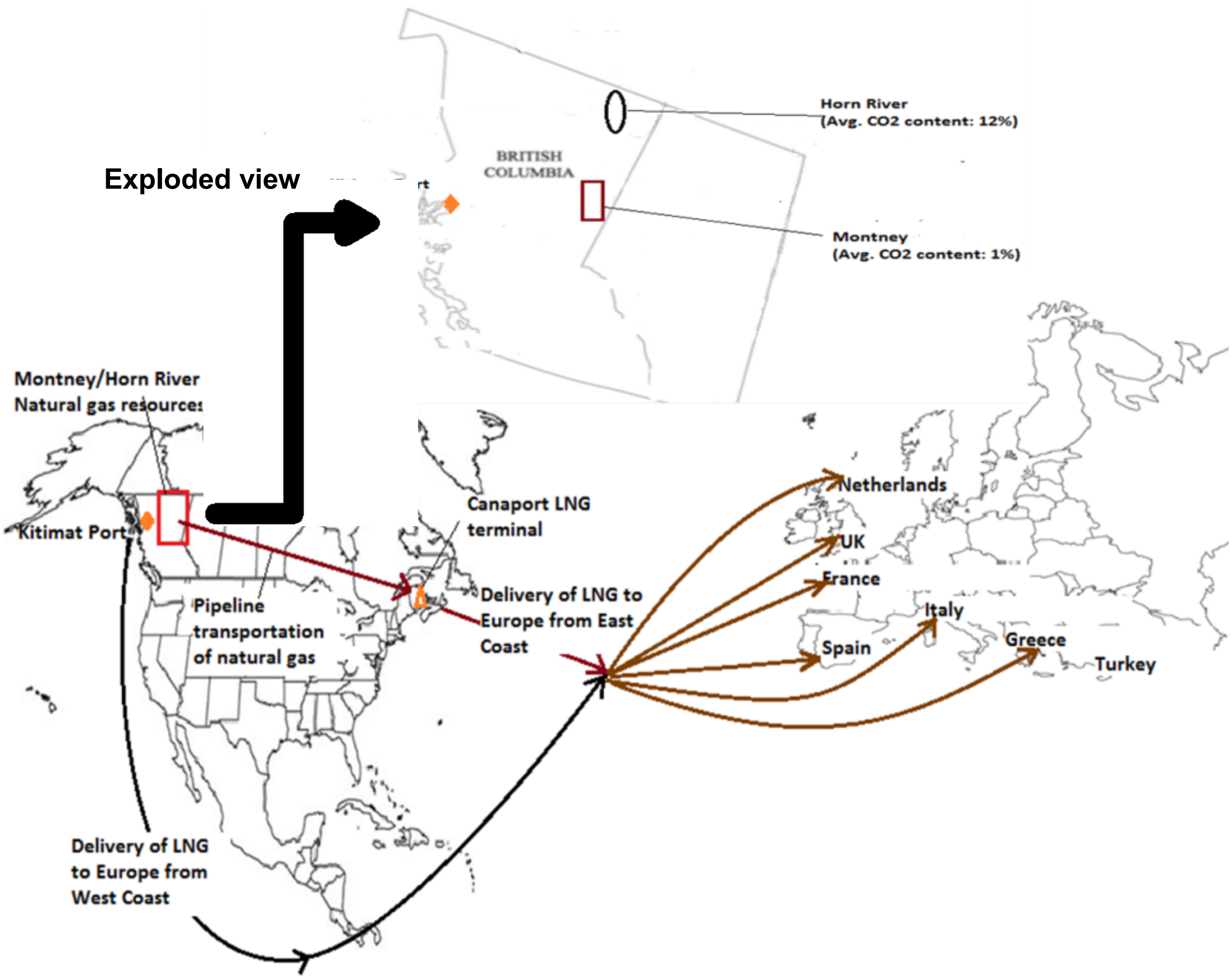

Figure 36: Map overview of the natural gas supply chain route from Canada to Europe

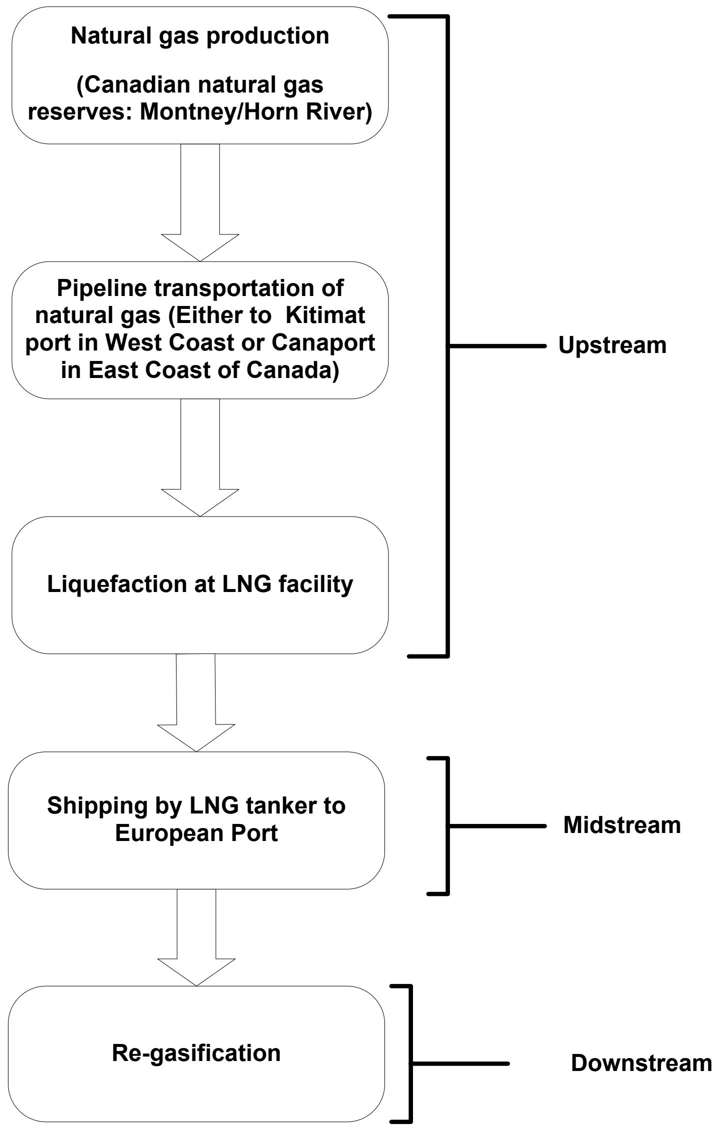

Figure 37: Scope of the natural gas supply chain to Europe

For the base case, Montney reserve is considered, since the shale gas reserve contains less CO_2 content in the gas. Supply chain costs are defined as the costs of delivering natural gas to the respective country and include production, pipeline transportation of natural gas, liquefaction, and shipping costs. Regasification is thus excluded from the supply chain costs but included in the life cycle GHG emissions estimation.

4.2.2 Methodology

4.2.2.1 Techno-economic assessment

A data-intensive techno-economic model was developed to evaluate the delivered costs of Canadian LNG to north and southwest Europe. In this work, all the major equipment and operating & maintenance costs considered to quantify liquefaction costs of the liquefaction facility, (a capacity of 10 million tonnes per annum [MTPA]), were taken from Raj et al. [58]. In addition to the liquefaction costs, production, pipeline transportation, and shipping costs were added to estimate the total delivered costs of Canadian LNG to Europe. The production costs of the two supply reserves considered in this study, Montney and Horn River, include well head price of gas and pipeline transportation costs. The well head costs of the Montney and Horn River resources are taken from an earlier study [133]. The pipeline transportation cost of natural gas from the natural gas reserves to the east coast was estimated based on a tariff system. Two supply chains routes were investigated, one from the west coast (Kitimat port) and other via the east coast (Canaport terminal), and compared to evaluate the more cost-effective pathway. The shipping costs of LNG (including total fuel cost, hiring cost, and port and passage fees) correspond to a 210,000 m^3 Q-Flex LNG carrier because this is the maximum size the Panama Canal can handle. For uniformity, shipping in a tanker of this size is considered for both supply chain routes. All the costs estimated in this study are for the year 2015.

4.2.2.2 Life cycle GHG emissions

4.2.2.2.1 LCA goal

The objective of this work is to develop a life cycle assessment (LCA) model in order to conduct the comprehensive well-to-port (WTP) and well-to-wire (WTW) life cycle analysis in the delivery of Canadian LNG to north and southwest Europe. The model was used to compare the GHG emissions from two supply chain routes, one via Canada's east coast and other via the west coast, and to identify the least GHG-intensive pathway. The GHG emissions presented in this study are based on the 100-year global warming potential factors taken from the Fifth Assessment Report of the Intergovernmental Panel on Climate Change 2013 [125]. The functional unit considered for the WTP and WTW life cycle is one g-CO_2eq per mega joule of natural gas and g-CO_2eq/kWh Canadian shale gas-fuelled electricity in Europe, respectively.

4.2.2.2.2 LCA system boundary

Figure 38 (A-B) shows the LCA system boundaries of the WTP stages of two supply chain routes in the delivery of Canadian LNG to north and southwest Europe. Recovery, gas processing, gas transmission by pipeline, liquefaction, shipping and re-gasification are the WTP stages considered in this study. For the base case, a pipeline transportation distance of 650 km is assumed in order to deliver the produced natural gas from the reserve to the Kitimat port while approximately 5150 km is assumed to transport natural gas to Canaport in the east coast of Canada. The primary objective of this work is to find out the least GHG-intensive route for the Canadian LNG supply chain. Fugitive, flaring and venting emissions from each stage of operations are included.

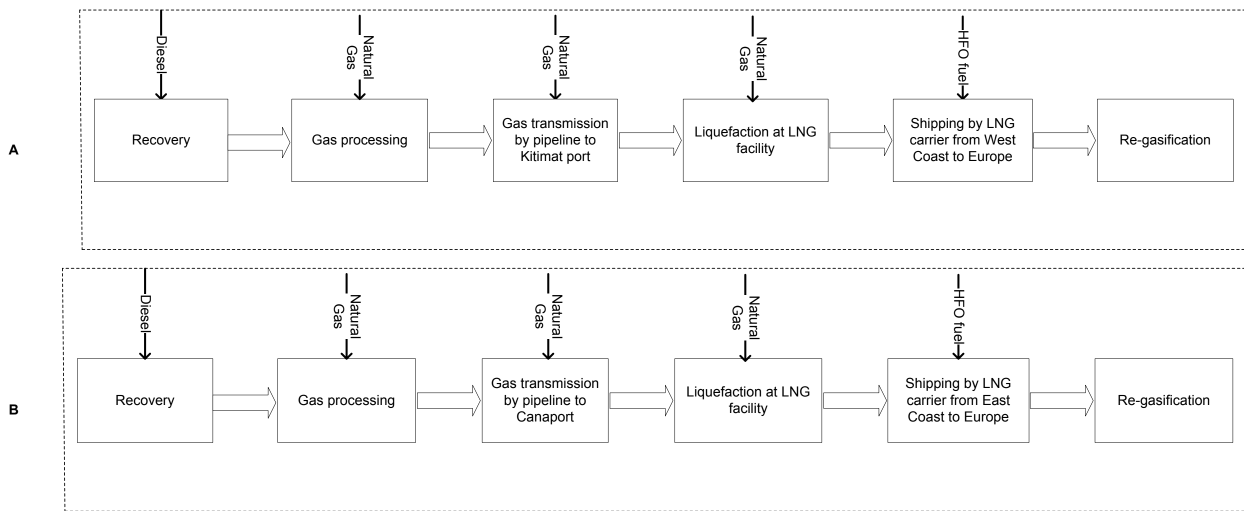

Figure 38: Canadian LNG routes (A): Pathway 1- Recovered natural gas from Montney/Horn River is processed in a surface processing facility, then transported by pipeline to a liquefaction facility in Kitimat Port (west coast) to be liquefied and shipped by LNG carrier to the destination port where it is re-gasified. (B): Pathway 2- Natural gas recovered from Montney/Horn River is processed in a surface processing facility, then transported by pipeline to a liquefaction facility in Canaport (east coast) to be liquefied and shipped by LNG carrier to the destination port where it is re-gasified.

4.3 Model description

The recovery of natural gas from the Montney Play/Horn River Basin is the first stage of the Canadian LNG supply chain to north and southwest Europe. The operations at this stage typically include drilling (horizontal and vertical), well pad construction, hydraulic fracturing, well completion, and production. The main energy input for this operation is in the form of diesel, which is mainly consumed for drilling operations and hydraulic fracturing by diesel powered equipment. The well head costs of the two supply reserves considered in this study (Montney and Horn River) are taken from an earlier study [133]. In this study, the costs of the Horn River Basin's well head are higher than Montney's due to the capital-intensive infrastructures reported by the former. Raj et al. [56] quantified the recovery emissions for a natural gas production value of 155 million tonnes; the calculation included flaring and fugitive emissions. The GHG emissions from diesel consumption, from the study by Raj et al. [56], are used to evaluate the total LC WTP GHG emissions. Further details are provided in previous work by Raj et al. [56].

The raw gas produced from the reservoir is sent to the gas processing unit operation; this is the second stage of the Canadian LNG supply chain. In this process, the gas impurities, mainly in the form of hydrogen sulfide, carbon dioxide, water, and other hydrocarbon fluids, are removed in a gas sweetening and a glycol dehydrator unit. The major costs in this operation include the costs associated with the equipment like the heat exchangers, absorber tower, stripper or regeneration column, pressure vessels, condensers and reboiler [51]. In the study by Raj et al. [58], four gas sweetening units with a flow rate of 359 million metric standard cubic feet per day (mmscfd) per unit were considered, while for the dehydration unit, five parallel units for each LNG train of 5 million tonnes per annum (MTPA) with four towers in each dehydration unit were considered. In this study, the cost was obtained for the gas processing unit from the work done by Raj et al. [58]. In this unit operation, natural gas is the main form of energy consumed in the reboiler heaters, pumps (in the dehydrator unit), the booster, reflux and circulation pumps, amine reboiler, and aerial cooler (in the gas sweetening unit). The GHG emissions from the natural gas consumption in the gas processing unit are taken from the study done by Raj et al. [56].

The third stage of the Canadian LNG supply chain is the pipeline transportation of natural gas to the liquefaction facility. In this study, two supply chain routes are considered, one to the Kitimat port (west coast) and one to the Canaport (east coast). The transportation cost of natural gas by pipeline is based on tariff systems. For the pipeline transportation of natural gas to the west coast, a pipeline of distance 650 km is considered for the default case, with an expected pipeline lifetime of 25 years and a capacity of 5 billion cubic feet per day (bcfd) [134]; and an approximate distance of 5,150 km is assumed for the transportation of natural gas to the east coast. Natural gas is the main fuel used in the compressor station for the pipeline transportation of natural gas. The methodology used by Raj et al. [56] was adapted to evaluate the GHGs emitted from the natural gas consumption in transporting natural gas by pipeline, and fugitive and venting emissions are calculated based on pipeline distance and compressor and meter station.

After the pipeline transportation of natural gas to the LNG facility, the liquefaction process starts. In this process unit, the natural gas is cooled to -155 °C in the cryogenic and propane heat exchanger and converted to LNG. The liquefaction cost and the GHG emissions are directly affected by the liquefaction technology. There are various technologies available for this operation, but this study considered the most-often used propane pre-cooled mixed refrigeration (APCI C3MR) process. The main cryogenic heat exchangers, compressors, and gas turbines are the major cost-intensive equipment in the liquefaction unit. Two LNG plant trains, each with a capacity of 5 million tonnes per annum, were considered by Raj et al. [58] to estimate the liquefaction cost of natural gas. In this study, those costs [58] were adapted to estimate the Canadian LNG supply chain costs to Europe. Most of the energy consumed in the liquefaction unit is by natural gas-driven turbines and acid gas incinerators. The GHG emissions of the gas turbines were estimated by Raj et al. based on the specific fuel consumption, emission factors, and the operation duration [56], and the GHG emissions from the acid incinerator and flaring and venting emissions in the liquefaction unit were adapted from Banholzer et al. [135].

After the natural gas is liquefied, it is loaded in an LNG tanker and shipped to the destination port. An LNG carrier (Q-Flex) of 210,000 m^3 capacity is considered in this study [136]. The GHG emissions and shipping costs vary with propulsion type and fuel. In this work, a pure HFO-burning propulsion system is considered, which uses heavy fuel oil (HFO) as the main fuel to power the marine engines; however, various combinations are possible. Two shipping distances are considered for two supply chain routes. The average nautical distance from Canada's east coast to Europe is approximately 3400 nautical miles (6296.8 kms), while from the west coast it is approximately 9300 nautical miles (17223.6 kms). These shipping distances are obtained by averaging the distances from the Canadian ports to all the major LNG import terminals in Europe (see Appendix C, Table S1), taken from the Portworld Distance Calculator [110].The shipping costs and emissions are evaluated based on the HFO fuel consumption in the marine engine.

Re-gasification is the last stage of the Canadian LNG supply chain considered in this study. In this operation, LNG is converted to natural gas by providing vaporizing heat. The GHG emissions from this operation are primarily from the combustion of fuel. The fugitive emissions from regasification operations are considerably lower [137]. The GHG emissions value for this operation is taken from a study by Skone et al. [138].

4.4 Results and discussion

4.4.1 Supply chain costs of shipping Canadian LNG to Europe

Figure 39 shows the supply chain costs in the delivery of Canadian LNG to major LNG import terminals in north and southwest Europe through two supply chain routes. For the default case, the delivery of Canadian LNG through pathway 1 (via the east coast) supply chain costs are US$ 10.94–12.93, while pathway 2 (via the west coast) costs are US$ 8.91–11.33, depending upon the destination country. Pathway 1 clearly has higher supply chain costs. This is mainly because of the pipeline transportation costs in the delivery of natural gas to the Canaport terminal in pathway 1 (east coast), which are 30–32% of the total supply chain costs, depending on the natural gas source. The wide range of values for the delivery of Canadian LNG is due to the differences in resources (Montney/Horn River), pipeline transportation, and shipping costs.

The supply chain costs were also compared in the delivery of Canadian LNG to Europe with the estimated border prices of natural gas from the main exporting countries (Norway, Russia, and Algeria).The estimated border prices of natural gas are for the first quarter of 2015 and taken from the report by the European Commission [139]. The prices show wide variation and are very susceptible to oil-indexed prices. The delivered costs of natural gas from these countries are lower than Canadian LNG. The main reason is the shorter distance for pipeline transportation and shipping of natural gas.

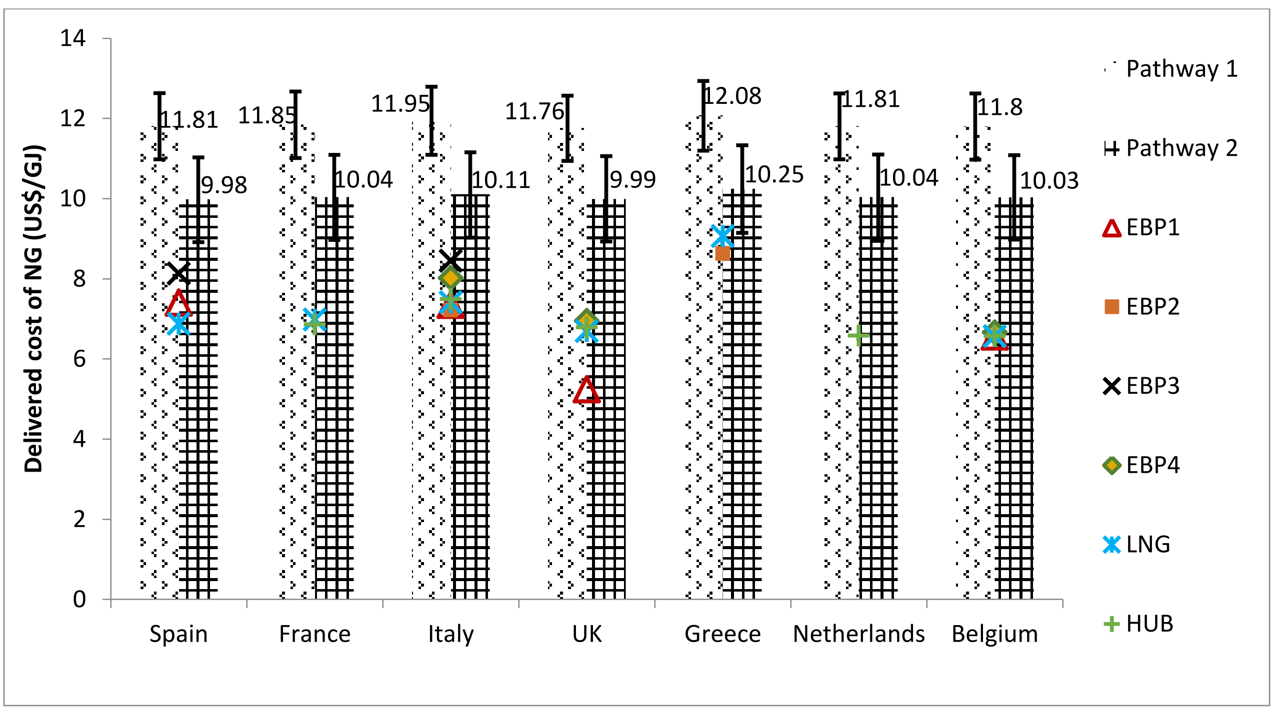

Figure 39: Comparison of the delivered costs of LNG. Pathway 1 is the delivered costs of Canadian LNG through the east coast route. Pathway 2 is the delivered costs of Canadian LNG through the west coast route. EBP1 is the estimated border price for gas supply from Norway, January - March 2015 [139]. EBP3 is the border price for gas from Algeria, January - March 2015 [139]. LNG prices from Belgium, Spain, France, and the UK are the landed prices for January - March 2015 [139]. LNG prices for Greece, Italy, and Lithuania are estimated based on customer data reported to ESTAT COMEXT for January - March 2015 [139]. EBP2 is the border price for gas from Russia, January - March 2015 [139]. EBP4 is the estimated border price of gas from the Netherlands, January - March 2015 [139]. EBP5 is the estimated border price of gas from Denmark, December 2014 - February 2015 [139].

4.4.2 Total WTP life cycle GHG emissions

Figures 40 and 41 show the total LC WTP GHG emissions in the delivery of Canadian LNG to different countries in Europe for two supply chain routes from the Montney and Horn River reserves, respectively. For the base case, the results show that the LC WTP GHG emissions for pathway 1 are 28.51–38.45 g-CO_2 eq/MJ and 22.94–30.15 g-CO_2eq/MJ for pathway 2. Pathway 1 is clearly more GHG intensive than pathway 2; this is because of the additional emissions in the transportation of natural gas to the east coast. The wide range of GHG emissions (including fugitive, flaring, and venting emissions) shows the uncertainty in each stage of operations. In pathway 1, natural gas recovered from Montney is processed in a surface gas processing facility and then transported by pipeline to a liquefaction facility in the east coast, liquefied, then loaded in an LNG tanker, shipped to a destination port, and finally re-gasified and distributed by pipeline; in pathway 2, recovered natural gas from Montney is transported to the Kitimat port in the west coast where it is liquefied and loaded into LNG tankers, shipped to a destination port, and finally re-gasified. For the default case, the emissions from the transportation of natural gas by pipeline make up 35–43% of the total WTP GHG emissions, depending on the shale gas reserves, for pathway 1, which is 29–36% more than the transportation emissions from pathway 2. The LC WTP emissions from Horn River are higher than Montney's because of the high CO_2 content (approximately 12%) in Horn River's gas.

The LC WTP GHG emissions in the delivery of Canadian LNG to Europe were compared with the gas imported to Europe either by pipeline in gaseous form or as LNG by LNG tanker (particularly from Russia to Germany and the United Kingdom, Qatar and Libya to Italy, and Algeria and Trinidad to Spain, as shown in Figure 40). Uncertainties exist in the GHG emissions values obtained in the delivery of natural gas or LNG from these countries due to differences in study system boundaries, methodologies, and technologies considered in the each stage of operation. However, the average GHG emissions of natural gas imported to Europe reported in the study by Taglia and Rossi [137] was 12.32 g-CO_2eq/MJ with emissions up to 18 g-CO_2eq/MJ (+45% variation) from Russia to Germany. The overall LC WTP GHG emissions from the Canadian LNG supply chain to Europe are comparatively higher because of the additional GHG emissions from both the long pipeline transportation of natural gas (for the east coast route) and the long shipping distance (for the west coast route).

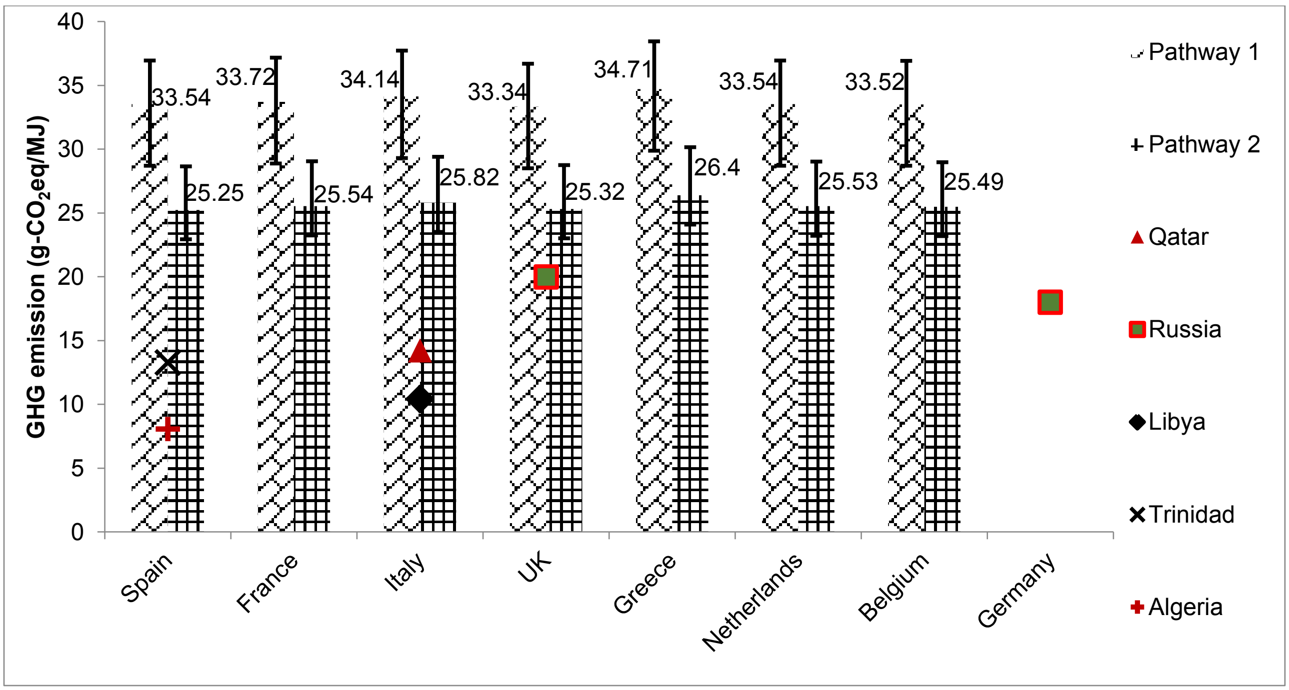

Figure 40: LC WTP GHG emissions of two supply chain pathways of Canadian LNG from the Montney reserve

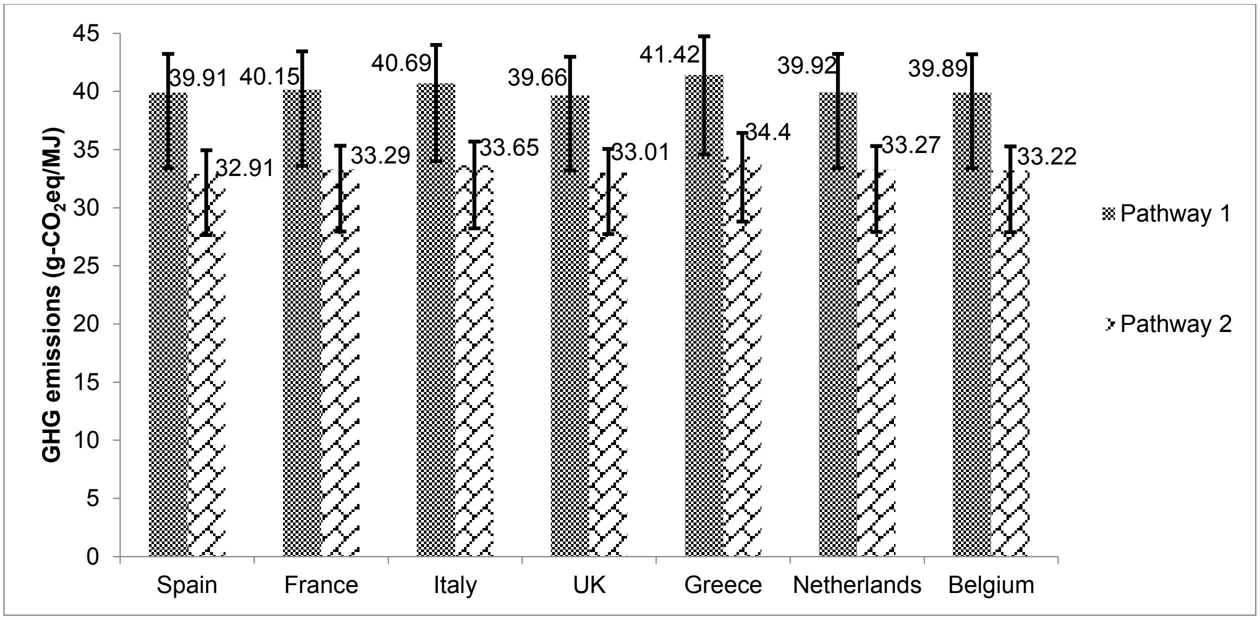

Figure 41: LC WTP GHG emissions of two supply chain pathways of Canadian LNG from the Horn River reserve

4.4.3 Well-to-wire life cycle GHG emissions

The well-to-wire life cycle GHG emissions include upstream (recovery, processing, pipeline transportation, and liquefaction), midstream (shipping), and downstream (re-gasification and power generation plant) emissions. Figure 43 shows the well-to-wire life cycle GHG emissions (g-CO_2eq/kWh) in the delivery of Canadian LNG to north and southwest Europe. The results show that a wide range of uncertainties exist due to the sparsely available data, particularly for Canada, for operations like drilling and completion emissions and gas composition as well as the quantity of gas vented during the processing phase and the lifetime productivity of the reserves, due to the infancy of Canadian shale gas extraction. For the base case, pathway 1 shows a range from 606–681 g-CO_2eq/kWh and pathway 2 shows a range from 563–619 g-CO_2eq/kWh for Montney reserve. The natural gas-fired power generation plant is the operation that emits the most emissions; it accounts for 60–67% of the total life cycle emissions of the entire LNG supply chain, depending upon the pathway followed, as shown in Figure 42. The other operations – recovery (5–6%), processing (2%), pipeline transportation (2–17%), liquefaction (10–11%), shipping (2–10%), and re-gasification (3%) – have considerably less impact on WTW life cycle emissions. The WTW GHG emissions from the Canadian LNG supply chain are comparatively higher than from the main exporter countries like Russia, Qatar, and

Algeria, as shown in Figure 43. An alternative natural gas resource in Eastern Canada might give a cheaper route for Canada.

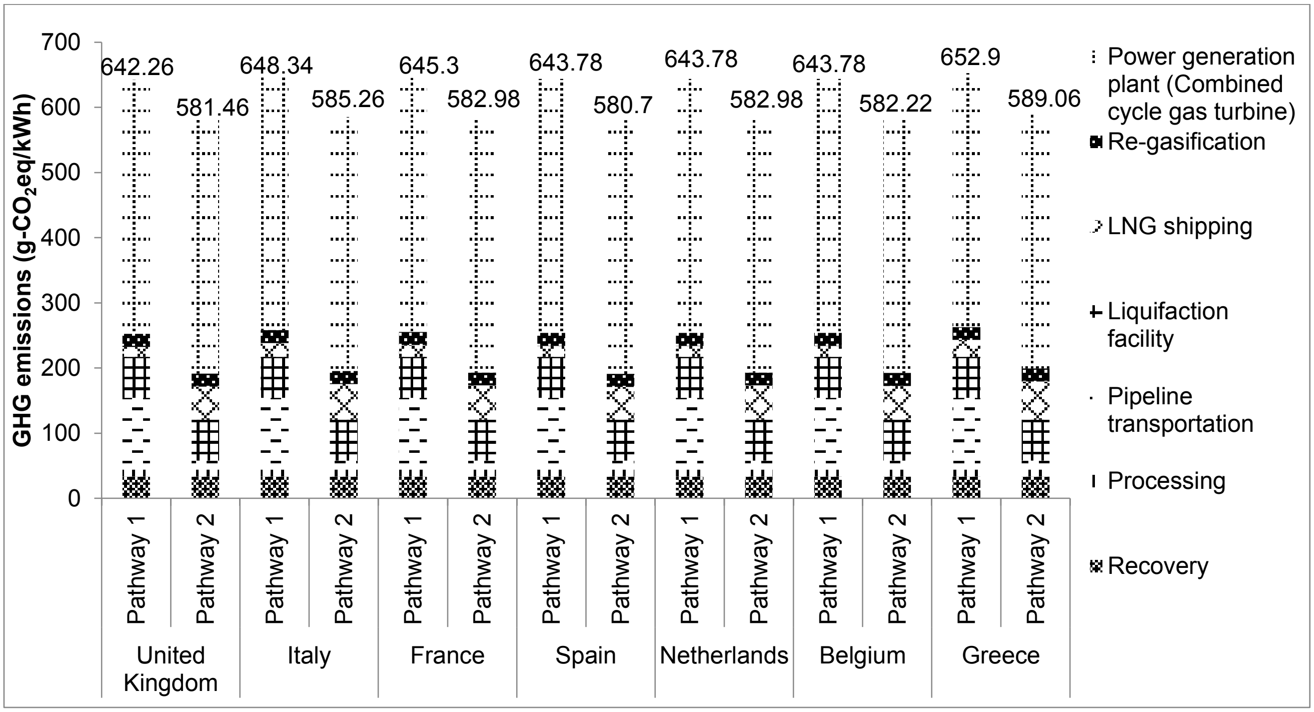

Figure 42: Breakdown of LC WTW GHG emissions of two supply chain pathways of Canadian LNG from the Montney reserve

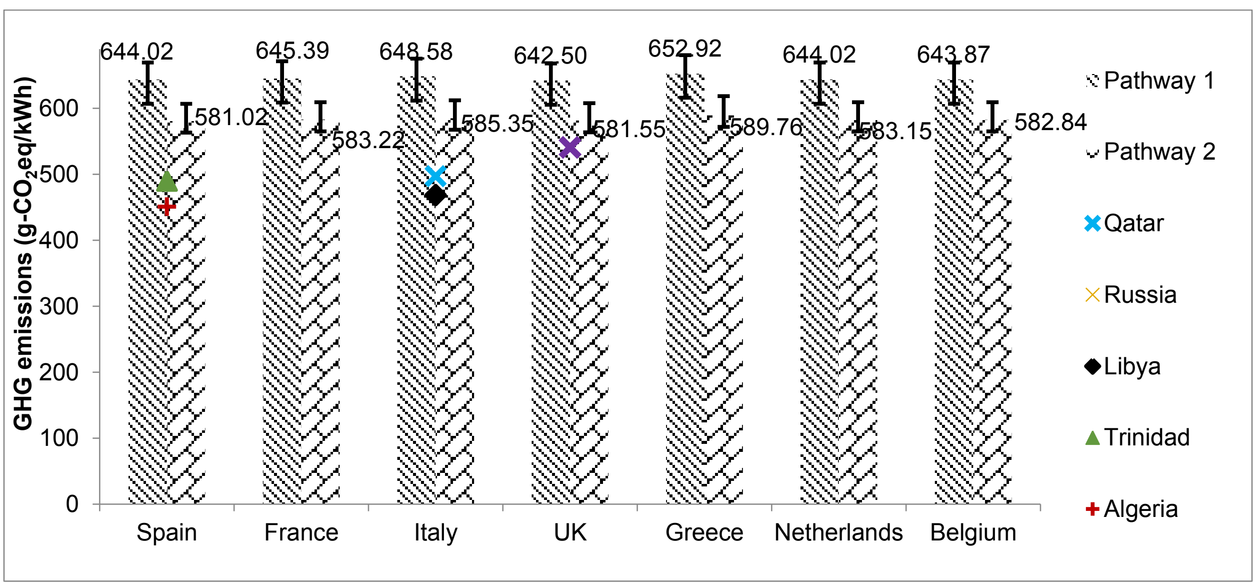

Figure 43: LC WTW GHG emissions of two supply chain pathways of Canadian LNG from the Montney reserve

4.5 Conclusion

Because Canadian shale gas development is still at an infancy stage, there is not much research from an economic or environment impact perspective in the delivery of Canadian LNG to Europe. To respond to this need and the importance of the abundant supply potential of Canadian shale gas being realized, this study evaluated and compared the delivered costs and environmental risks of two supply chain routes to north and southwest Europe. In this work, we developed data-intensive techno-economic and life cycle assessment models to evaluate the supply chain costs and total life cycle GHG emissions of Canadian LNG in the delivery to north and southwest Europe. It was estimated that the delivery of Canadian LNG through pathway 1 (via the east coast) was US$ 10.94 – 12.93, while pathway 2 (via the west coast) was US$ 8.91 – 11.33, depending upon the destination country, for the Montney Play as supply reserves. However, with improvements in recovery and liquefaction operations, supply chain costs can be reduced. The border prices of natural gas from the main exporters such as Norway, Russia, and Algeria to European countries show high variation and are very susceptible to oil-indexed prices. The reported border prices in the first quarter of 2015 from these countries are US$5.24 – 9.1/GJ; however, the Canadian shale gas costs to supply LNG are higher. Thus, other natural gas resources in Eastern Canada might provide a cheaper and more competitive alternative route for Canada.

The life cycle well-to-port (WTP) GHG emissions in the delivery of Canadian LNG to ports in north and southwest Europe are 28.51 – 38.45 g-CO_2 eq/MJ if pathway 1 route (via the east coast) is followed and 22.94 – 30.15 g-CO_2eq/MJ for pathway 2 (via the west coast). This wide range of uncertainties exists because of the sparsely available data, particularly for Canada, for emissions from operations like drilling and completion, gas composition, and flow back water treatment, as well as the amount of gas vented during the processing phase and the lifetime productivity of the reserves, due to the infancy of Canadian shale gas extraction. GHG emissions can be reduced if the vented and flared gas is captured with shale gas recovery and processing technology. The life cycle well-to-port (WTP) GHG emissions in the delivery of Canadian LNG to ports in north and southwest Europe are 28.51–38.45 g-CO_2 eq/MJ if pathway 1 route (via the east coast) is followed and 22.94–30.15 g-CO_2eq/MJ for pathway 2 (via the west coast) . This wide range of uncertainties exists because of the sparsely available data, particularly for Canada, for emissions from operations like drilling and completion, gas composition, and flow back water treatment, as well as the amount of gas vented during the processing phase and the lifetime productivity of the reserves, due to the infancy of Canadian shale gas extraction. GHG emissions can be reduced if the vented and flared gas is captured with shale gas recovery and processing technology.

Natural gas is imported to Europe in gaseous form by pipeline and LNG form by LNG tankers from exporting countries like Russia, Algeria, Norway, and Qatar. The GHG emissions reported in the literature are lower than the Canadian LNG supply chain. Therefore, finding alternative sources of natural gas in Eastern Canada could offer lower GHG-intensive substitutes to the Canadian LNG supply chain to Europe, reducing the large portion of supply chain transportation GHG emissions. However, currently there are insufficient data available to explore the market potential for Eastern Canada. The Government of Quebec have given priority to exploring the natural gas resource potential in that province, and in future, natural gas supply from this region is expected.

Chapter 5
Conclusions and recommendations for future work

This chapter describes the findings and conclusions of this work, points out limitations, and recommends a direction for future work.

5.1 Conclusions

In this study, the techno-economic and life cycle assessment of Canadian oil sands products and LNG from the production site to Asia-Pacific and Western Europe, respectively, was presented. The objective was to develop science-based credible comprehensive that will serve as a decision-making tool for policy makers, government, and industry.

Majority of the crude oil is imported to Asia-Pacific from the Middle East and Africa, while Europe imports significant portion of natural gas from Russia and Norway. Majority of these regions have potentially unstable political environment compared to Canada. The stable political system of Canada is more attractive, especially when there are geopolitical tensions. Furthermore, Canada's stable political system can help Asian and European countries build long-term contracts for a reliable supply of LNG and oil sands products. In order to explore potential of Canadian oil sands and LNG to their respective markets, this research was conducted. The first objective of this study was to develop a data-intensive techno-economic model to estimate production (SAGD), transportation (SAGD-upgrader-port in Vancouver), upgrading, and shipping costs of Canadian oil sands products to Asia-Pacific. This model was used to develop four pathways (two for SCO and two for dilbit) from production site to potential sea port destinations in the Asia-Pacific region. Supply chain costs (C$) per barrel of bitumen to China, Japan, and India range from 61–87, 60–86, and 62–90, respectively, depending on the pathway. These are the minimum delivered costs for Canadian oil sands projects to supply their products to China, Japan, and India. Supply chain costs include production, transportation, upgrading, and shipping costs. The results show that overall supply chain costs of Canadian oil sands products are influenced mostly by production and upgrading costs. Thus, a more economical extraction technology can reduce the overall supply chain cost. If the extraction technology can be improved such that its product requires partial or no upgrading before being refined, supply chain costs can be reduced significantly. The production and upgrading costs are mostly influenced by capital costs. The production and upgrading costs can be brought down if the capital costs are reduced through optimal process design or slight improvements in extraction and upgrading technologies.

Of the seven shipping scenarios (listed in Table 19), the most economical is scenario 5 (C$2.04/bbl SCO and C$2.20/bbl dilbit), where LNG and HFO are used as fuel in the main and auxiliary engines, respectively. The sensitivity analysis indicates that pipeline lifetime and capacity significantly impact transportation (pipeline) and shipping costs, respectively. The results of this study will provide useful information to policy makers, government, and industry, and help achieve in identifying the most economical and environmentally friendly pathway for diversifying markets in the Asia-Pacific region.

Table 19: Shipping Scenarios

Engine types	Fuels	Scenario	Shipping cost of SCO (C$/bbl)	Shipping cost of dilbit (C$/bbl)
Fuel use in Main and Auxiliary Engines				
Main engine: 1 x MAN S60MC8	MDO	1	2.92-3.71	3.56-4.46
Auxiliary engine: 1 x Aux. Diesel Gen 9L28/32H	MDO			
Main engine:1 x MAN B&W 7S50ME-C8.2-GI-TII	LNG	2	1.77-2.32	1.92-2.52
Auxiliary engine: 1 x Aux. Diesel Gen 9L28/32H	MDO			
Main engine: 1 x MAN S60MC8	HFO	3	2.07-2.82	2.39-3.27
Auxiliary engine: 1 x Aux. Diesel Gen 9L28/32H	HFO			
Main engine: 1 x MAN S60MC8	MDO	4	2.8-3.54	3.45-4.29
Auxiliary engine: 1 x Aux. Diesel Gen 9L28/32H	HFO			
Main engine: 1 x MAN B&W 7S50ME-C8.2-GI-TII	LNG	5	1.65-2.18	1.80-2.38
Auxiliary engine: 1 x Aux. Diesel Gen 9L28/32H	HFO			

Engine types	Fuels	Scenario	Shipping cost of SCO (C$/bbl)	Shipping cost of dilbit (C$/bbl)
Propulsion system				
Main engine: 1 x MAN S60MC8	HFO	6	2.31-3.16	2.65-3.64
Auxiliary engine: 1 x Aux. Diesel Gen 9L28/32H	MDO			
Main engine: 1 x Wartsila 12V50DF	HFO	7	2.45-3.25	2.77-3.69
Auxiliary engine: 1 x Aux. Diesel Gen 9L28/32H	MDO			

Another objective of this study was to present comprehensive well-to-wheel (WTW) life cycle (LC) GHG emission for the transportation fuels used in China derived from Canadian oil sands products. This analysis includes all the stages from recovery and extraction to combustion of fuels in vehicle engines. Eight pathways were developed that represent future oil sands markets. These include: (1) Pathway 1- Bitumen extracted from SAGD is transported by pipeline (500 km) and upgraded in delayed cokers; the produced SCO is transported by pipeline (1147 km), shipped to China, and there refined to produce gasoline and diesel, (2) Pathway 2- Bitumen obtained in SAGD is transported by pipeline (500 km) and upgraded in hydroconversion; the produced SCO is transported by pipeline (1147 km), shipped to China, and refined to gasoline and diesel, (3) Pathway 3- Bitumen recovered in SAGD is transported by pipeline (1647 km), shipped as dilbit to the destination port in China, and there upgraded in delayed cokers; finally, SCO is refined to diesel and gasoline, (4) Pathway 4- SAGD bitumen is transported by pipeline (1647 km), shipped as dilbit, and upgraded in hydroconversion, and the produced SCO refined to gasoline and diesel, (5) Pathway 5- Bitumen recovered in surface mining is transported by pipeline (500 km) and upgraded in delayed cokers, and the produced SCO is transported by pipeline (1147 km), shipped, and refined to produce gasoline and diesel, (6) Pathway 6- Surface-mined bitumen is transported by pipeline (500 km) and upgraded in hydroconversion, and the produced SCO is transported by pipeline (1147 km), shipped, and there refined to produce gasoline and diesel, (7) Pathway 7- Surface-mined bitumen is transported by pipeline (1647 km), shipped as dilbit to China, and upgraded in delayed cokers, and the produced SCO is refined to produce gasoline and diesel, (8) Pathway 8- Surface-mined bitumen is transported by pipeline (1647 km) and shipped as dilbit to be upgraded through hydroconversion in China; the produced SCO is refined to produce gasoline and diesel. Pathway 5 has the lowest LC WTW GHG emissions. This pathway includes surface mining and delayed coking as key stages; they reduce the WTW LC GHG emissions of this route. However, irrespective of the pathway, overall GHG emissions can be reduced if the extraction technology can be improved. New extraction technologies like N-solv and electromagnetic heating are still in the research phase and could be explored in future as GHG emissions-reduction options. It was determined that gasoline production emits the highest GHGs (among gasoline, diesel, and jet fuel production). This is because more energy is consumed for gasoline production. The findings also show that combustion contributes a significant portion of WTW LC emissions.

The LC WTW GHG emissions for gasoline, diesel, and jet fuel range from 102.5–132.8 g-CO_2eq/MJ, 96.08–128.5 g-CO_2eq/MJ, and 91.9–124.6 g-CO_2eq/MJ, respectively. These wide ranges show the uncertainty in each LC stage. It is also observed that the LC WTW GHG emissions from Canadian oil sands products are higher than from Saudi Arabian crude at 94.58, 91.65, and 83.26 g-CO_2eq/MJ for gasoline, diesel, and jet fuel, respectively. This is largely due to the upgrader unit in the oil sands energy conversion chain, which increases overall LC emissions significantly. From the sensitivity analysis conducted to assess the impact of various parameters on shipping, it was found that the velocity and capacity of the ocean tanker have the most impact on the shipping emissions of SCO and dilbit.

The results of this study will help government, industry, and policy makers in Canada and China in decision making that ensures a pathway with the lowest GHG emissions. The results will also help in identifying the most economical and environmentally friendly pathway for diversifying markets in the Asia-Pacific region.

The third objective of this study was to evaluate and compare the delivered costs and environmental risks of two supply chain routes of Canadian LNG, one from the west coast and the other via the east coast to north and southwest Europe. This study incorporates recovery, processing, transmission, liquefaction, shipping, and re-gasification with the consideration of two sources of Canadian natural gas reserves, Montney and Horn River. It was found that the delivered cost ($/GJ) of Canadian LNG (which includes recovery, processing, transmission, liquefaction and shipping costs) to Europe is 8.90–12.90 depending on the resource and pathway. The total well-to-port (WTP) GHG emissions (which include emissions from recovery, processing, transportation, liquefaction, shipping and re-gasification at the destination port) from the Canadian production site to Europe are 22.9–42.1 g-CO_2eq/MJ, depending on the resource and pathway. Natural gas is imported to Europe in various forms, either by pipeline or LNG from the major exporting countries like Russia, Algeria, Norway, and Qatar. The costs and GHG emissions values reported in the literature for the delivery of natural gas from these countries were lower than those for the Canadian LNG supply chain. Finding other sources of natural gas in Eastern Canada, which will reduce transportation distances, might provide a cheaper and less GHG-intensive alternative to the Canadian LNG supply chain.

5.2 Research limitations

The following are limitations of the current work:

1. The resistance model developed to calculate the total installed power of the engine for shipping dilbit and SCO to the destination port in the Asia-Pacific region has some limitations.
   - It is valid only for a Froude number below 0.24 [107].
   - It is valid only for certain prismatic coefficient ranges, i.e., $0.73 \leq C_p \leq 0.855$ [107].

   Any ocean tanker design beyond these ranges is out of the scope of this study.
2. For consistency, a maneuvering speed of the ocean tankers is assumed to be 5.8 knots, though in reality the speed varies from 3 to 8 knots depending on the ports [140]. A maneuvering distance of 25 km is assumed [140]. Variations in maneuvering speed are not accounted for in this research.
3. The life cycle assessment (LCA) model developed in this study to evaluate the overall emissions of the Canadian oil sands supply chain does not account for venting, flaring, and fugitive emissions.
4. In this work, the techno-economic model developed to evaluate the upgrading costs of SCO assumed the conventional methods of upgrading used in Canada, delayed coking and hydroconversion. However, partial upgrading needs to be evaluated in terms of energy consumption and the upgrading costs. This was not considered in this study.
5. The techno-economic model developed for the Canadian LNG supply chain in this thesis is based on a discount cash flow analysis (DCF) and the empirical relation used to estimate the process parameters. Improvements in recovery and liquefaction operations are possible through the optimization of the process, but that is beyond the scope of this study.

5.3 Recommendations for future work

While this thesis presents the techno-economic and life cycle assessment of the Canadian oil sands products supply chain from Alberta to the Asia-Pacific region, the scope of this study can be extended. The following are recommendations for future work:

1. The enhancement of new oil sands extraction technologies: Oil sands technologies are still in the research phase. SAGD technology is used to extract bitumen, as the majority of oil sands reserves can be extracted this way. However, new technologies like solvent-based extraction and electromagnetic heating are still in the research and development phase and should be studied in future as an option to reduce the total supply chain costs and overall GHG emissions.
2. Improvements in the current life cycle assessment (LCA) model: The life cycle assessment developed in this study does not account for flaring, fugitives, land use, equipment, and infrastructure construction emissions. Research should be conducted to include the aforementioned associated emissions in order to identify their effects on the overall supply chain. GHG emissions from shipping dilbit and SCO are considered in particular for the two-stroke mechanical engine; however, other engines like electrical, bio-fuel, LNG-based engines are also possible. The lack of emissions data in the public domain for these engines makes it difficult to model their GHG emissions. In order to understand the impact of these engines on overall shipping emissions, it is important to incorporate all the engines in the current shipping model.
3. The impact of integrated operations: The model costs for the extraction and upgrader integration were not considered in this study. Stand-alone operations for SAGD and upgraders were studied to estimate production and upgrading costs. However, operations can be integrated and could have an impact on energy consumption, capital cost, and GHG emissions. Insights from an integrated model are required to understand the impact of integrating operations.
4. The impact of multi-phase operations: The capital cost of operations significantly depends on whether it is a grass-root operation or the expansion of an existing system. In the current study, we have studied only the first phase of SAGD and upgrading operations. It is imperative to understand the impact of plant expansion in the costs. Hence, further study is required to evaluate the impact of multi-phase operations.
5. Upgrading configurations: In the current research, two types of upgraders, delayed coking and hydroconversion, were studied. Others, like Syncrude's fluid coking [141] and Opti-Nexen's gasification [142] are already-existing upgrading technology. Their product yields are different. The energy consumption, GHG emissions, and capital costs also vary. Therefore, techno-economic and GHG emission studies of these upgrading configurations should incorporate an evaluation of their GHG emission and capital costs as a part of further study.

6. Traffic delay issues: The pipeline transportation and shipping models developed in this study do not directly account for the traffic delay issues. The traffic delay can occurs due to overcrowding of the export routes, reduction in speed of vessel, or when there are incidents like collision, spillage, damage, fire, etc. In long term contract projects, the reliable supply of products is always a high concern. Delivery of the products reliably and one schedule is sometimes challenging due to these traffic delay issues. This affects the supply chain costs with the addition of transportation cost incurred in the delivery of the products. There is a wide range of uncertainty that exists in traffic delay issues. In order to evaluate their impacts in the delivery costs of the products, further detailed study is needed.
7. Natural gas resources in Eastern Canada: In this thesis, most of the natural gas resources in Western Canada were investigated. However, other natural gas resources in Eastern Canada might provide a cheaper and more competitive alternative route for Canada to supply its product to Western Europe. Currently there is insufficient data available to explore the market potential for Eastern Canada. Recent estimates show that the recoverable natural gas from shale gas reserves in Quebec could be around 40 trillion cubic feet (tcf) [143]. The governments of Quebec and research partners are exploring the natural gas resource potential in the province. In future, a supply of natural gas from this region is expected. Thus, further techno-economic and life cycle GHG emissions studies are required in order to understand the effect of natural gas resources in Eastern Canada on Canadian LNG markets.

References

[1] Alberta Government. Alberta Energy: Facts and Statistics; 2016. <http://www.energy.alberta.ca/oilsands/791.asp> (accessed January 14, 2016).

[2] Halari AA. Effective project management of oil & gas projects: A model for oil sands' SAGD plants (desertation). Calgary, AB, University of Calgary; 2010. 350 p.

[3] Woo YP. Chinese lessons: state-owned enterprises and the regulation of foreign investment in Canada. China Economic Journal. 2014;7:21-38.

[4] Hackett D, Noda L, Grissom S, Moore M, Winter J. Pacific Basin Heavy Oil Refining Capacity. SPP Research Paper. 2013.

[5] Canadian Association of Petroleum Products. Crude oil forecast, Markets and Transportation; 2016. 550 p. < http://www.capp.ca/publications-and-statistics/publications/284950> (accessed October 27, 2016).

[6] Anthony HC, Steven C. Chinese Strategy and Military Modernization in 2015: A Comparative Analysis; 2015. 569 p. (accessed July 12, 2016).

[7] U.S Energy Information Administration. China International energy data and analysis; 2015 <https://www.eia.gov/beta/international/analysis.cfm?iso=CHN> (accessed January 21, 2016).

[8] Hart Energy and MathPro Inc. Technical and Economic Analysis of the Transition to Ultra-Low Sulphur Fuels in Brazil, China, India and Mexico; 2012. < http://www.theicct.org/sites/default/files/publications/ICCT_ULSF_refining_Oct2012.pdf> (accessed October 27, 2016).

[9] Morgan JP. China oil and gas; 2013 <http://pg.jrj.com.cn/acc/Res/CN_RES/INDUS/2013/2/5/8408e6d7-0648-4e58-9c35-c802f39d96c1.pdf> (accessed January 21, 2016). 2013.

[10] U.S Energy Information Administration. Country Analysis Brief: Japan; 2017. <https://www.eia.gov/beta/international/analysis.cfm?iso=JPN> (accessed September 7, 2017).

[11] Stratas Advisors. Asia: Refinery Capacity and Configuration; 2016. <https://stratasadvisors.com/api/GeneratePdf?url=http%3A%2F%2Fstratasadvisors.com%2Fen%2FInsights%2F072516-Asia-Refinery-Capacity&title=Asia%3A%20Refinery%20Capacity%20and%20Configuration&secure=False.> (accessed September 7, 2017).

[12] Kahrl F, Hu J, Kwok G, Williams JH. Strategies for expanding natural gas-fired electricity generation in China: Economics and policy. Energy Strategy Reviews. 2013;2:182-9.

[13] Wang C, Cai W, Lu X, Chen J. CO 2 mitigation scenarios in China’s road transport sector. Energy Conversion and Management. 2007;48:2110-8.

[14] Wang W, Zhang M, Zhou M. Using LMDI method to analyze transport sector CO 2 emissions in China. Energy. 2011;36:5909-15.

[15] Chen GQ, Zhang B. Greenhouse gas emissions in China 2007: inventory and input–output analysis. Energy Policy. 2010;38:6180-93.

[16] Foss M. Alberta's Energy Markets:Opportunities and Challenges; 2012 <http://www.realestateforums.com/ref/old/edmontonref/docs/2012/matthew_foss.pdf> (accessed January 21, 2016).

[17] Platts. New Crude, New Markets; 2013 <https://www.platts.com/IM.Platts.Content/InsightAnalysis/IndustrySolutionPapers/NewCrudesNewMarkets.pdf> (accessed January 21, 2016).

[18] Tarnoczi T. Life cycle energy and greenhouse gas emissions from transportation of Canadian oil sands to future markets. Energy Policy. 2013;62:107-17.

[19] Kocak KA, Micco PD. The quest for natural gas pipelines; 2016 <http://www.europarl.europa.eu/RegData/etudes/STUD/2016/586626/EPRS_STU(2016)586626_EN.pdf> (accessed February 24, 2017).

[20] King & Spalding. LNG in Europe 2016/2017: An Overview of LNG Import Terminals in Europe; 2016 <http://www.energylawexchange.com/kslaw/wp-content/uploads/2017/01/1-LNG-In-Europe_dec-2016-redu.pdf> (accessed February 13, 2017).
[21] Italian Institute for International Political Studies. LNG in Asia and Europe: converging prices, diverging basins; 2015 <http://www.ispionline.it/en/energy-watch/lng-asia-and-europe-converging-prices-diverging-basins-13770> (accessed February 7, 2017).
[22] Energo Journal. Ukrainian Energy Politics; 2016 <https://enerpojournal.com/2016/11/14/ukrainian-energy-politics/> (accessed February 7, 2017).
[23] Kumar S, Kwon H-T, Choi K-H, Cho JH, Lim W, Moon I. Current status and future projections of LNG demand and supplies: A global prospective. Energy Policy. 2011;39:4097-104.
[24] Söderbergh B, Jakobsson K, Aleklett K. European energy security: The future of Norwegian natural gas production. Energy Policy. 2009;37:5037-55.
[25] Chi-Chyong K, Kazmin R. The economics of global LNG trade: the case of Atlantic and Pacific inter-basin arbitrage in 2010-2014. 2016.
[26] Jones D, Dufour M, Gaventa J. Europe's declining gas demand trends and facts on European gas consumption; 2015 <https://www.e3g.org/docs/E3G_Trends_EU_Gas_Demand_June2015_Final_110615.pdf> (accessed February 24, 2017).
[27] Council of European Energy Regulators. CEER Analysis on the role of LNG to improve security of supply; 2016 <www.ceer.eu/.../2016/C15-LNG-25-03_LNG-SoS%20Analysis_3-Feb-2016.pdf> (accessed February 13, 2017).
[28] National Energy Board. Canada's energy future 2016: Energy supply and demand projections to 2040; 2016 <https://www.neb-one.gc.ca/nrg/ntgrtd/ftr/2016/index-eng.html#s6> (accessed February 13, 2017).
[29] Medlock KB. Modeling the implications of expanded US shale gas production. Energy Strategy Reviews. 2012;1:33-41.
[30] Nimana B, Canter C, Kumar A. Energy consumption and greenhouse gas emissions in upgrading and refining of Canada's oil sands products. Energy. 2015;83:65-79.
[31] Nimana B, Canter C, Kumar A. Energy consumption and greenhouse gas emissions in the recovery and extraction of crude bitumen from Canada's oil sands. Applied Energy. 2015;143:189-99.
[32] Méjean A, Hope C. Modelling the costs of non-conventional oil: A case study of Canadian bitumen. Energy Policy. 2008;36:4205-16.
[33] Olateju B, Kumar A. Techno-economic assessment of hydrogen production from underground coal gasification (UCG) in Western Canada with carbon capture and sequestration (CCS) for upgrading bitumen from oil sands. Applied Energy. 2013;111:428-40.
[34] Betancourt-Torcat A, Elkamel A, Ricardez-Sandoval L. A modeling study of the effect of carbon dioxide mitigation strategies, natural gas prices and steam consumption on the Canadian Oil Sands operations. Energy. 2012;45:1018-33.
[35] Ordorica-Garcia G, Elkamel A, Douglas P, Croiset E, Gupta M. Energy optimization model with CO 2-emission constraints for the Canadian oil sands industry. Energy & Fuels. 2008;22:2660-70.
[36] Giacchetta G, Leporini M, Marchetti B. Economic and environmental analysis of a Steam Assisted Gravity Drainage (SAGD) facility for oil recovery from Canadian oil sands. Applied Energy. 2015;142:1-9.
[37] Hulskotte J, van der Gon HD. Fuel consumption and associated emissions from seagoing ships at berth derived from an on-board survey. Atmospheric Environment. 2010;44:1229-36.
[38] Wang C, Corbett JJ, Firestone J. Modeling energy use and emissions from North American shipping: Application of the ship traffic, energy, and environment model. Environmental science & technology. 2007;41:3226-32.

[39] National Energy Board. Canada's Oil Sands opportunities and challenges to 2015: An update; 2006 <https://www.neb-one.gc.ca/nrg/sttstc/crdlndptrlmprdct/rprt/archive/pprtntsndchllngs20152006/pprtntsndchllngs20152006-eng.pdf> (accessed April 26, 2016).
[40] GHGenius model 4.03. Prepared for Natural Resources Canada. (S&T)2 Consultants Inc.; 2013.
[41] GREET WM. Model 4.02 a. Argonne National Laboratory, US Department of Energy. 2012.
[42] Nimana B, Canter C, Kumar A. Life cycle assessment of greenhouse gas emissions from Canada's oil sands-derived transportation fuels. Energy. 2015;88:544-54.
[43] Keesom W, Unnasch S, Moretta J. Life cycle assessment of North American and imported crudes prepared for Alberta Energy Research Institute. Chicago, Illinois. 2009.
[44] Yan X, Crookes RJ. Life cycle analysis of energy use and greenhouse gas emissions for road transportation fuels in China. Renewable and Sustainable Energy Reviews. 2009;13:2505-14.
[45] Verma A, Nimana B, Olateju B, Rahman MM, Radpour S, Canter C, et al. A techno-economic assessment of bitumen and synthetic crude oil transport (SCO) in the Canadian oil sands industry: Oil via rail or pipeline? Energy. 2017;124:665-83.
[46] Nimana B, Verma A, Di Lullo G, Rahman MM, Canter CE, Olateju B, et al. Life cycle analysis of bitumen transportation to refineries by rail and pipeline. Environmental science & technology. 2016;51:680-91.
[47] Charpentier AD, Kofoworola O, Bergerson JA, MacLean HL. Life cycle greenhouse gas emissions of current oil sands technologies: GHOST model development and illustrative application. Environmental science & technology. 2011;45:9393-404.
[48] Bergerson JA, Kofoworola O, Charpentier AD, Sleep S, MacLean HL. Life cycle greenhouse gas emissions of current oil sands technologies: surface mining and in situ applications. Environmental science & technology. 2012;46:7865-74.
[49] Charpentier AD, Bergerson JA, MacLean HL. Understanding the Canadian oil sands industry's greenhouse gas emissions. Environmental research letters. 2009;4:014005.
[50] Abella JP, Bergerson JA. Model to investigate energy and greenhouse gas emissions implications of refining petroleum: impacts of crude quality and refinery configuration. Environmental science & technology. 2012;46:13037-47.
[51] Peters L, Hussain A, Follmann M, Melin T, Hägg M-B. CO 2 removal from natural gas by employing amine absorption and membrane technology—a technical and economical analysis. Chemical Engineering Journal. 2011;172:952-60.
[52] Netusil M, Ditl P. Comparison of three methods for natural gas dehydration. Journal of natural gas chemistry. 2011;20:471-6.
[53] Hureau G, Jordan L. Waiting for the Next Train? An Assessment of the Emerging Canadian LNG Industry. 2015.
[54] Baron R, Bernstein P, Montgomery WD, Tuladhar S. Macroeconomic impacts of LNG exports from the United States. Economics of Energy & Environmental Policy. 2015;4:37-58.
[55] Javanmardi J, Nasrifar K, Najibi S, Moshfeghian M. Feasibility of transporting LNG from South-Pars gas field to potential markets. Applied thermal engineering. 2006;26:1812-9.
[56] Raj R, Ghandehariun S, Kumar A, Linwei M. A well-to-wire life cycle assessment of Canadian shale gas for electricity generation in China. Energy. 2016;111:642-52.
[57] Raj R, Ghandehariun S, Kumar A, Geng J, Linwei M. A techno-economic study of shipping LNG to the Asia-Pacific from Western Canada by LNG carrier. Journal of Natural Gas Science and Engineering. 2016;34:979-92.
[58] Raj R, Suman R, Ghandehariun S, Kumar A, Tiwari MK. A techno-economic assessment of the liquefied natural gas (LNG) production facilities in Western Canada. Sustainable Energy Technologies and Assessments. 2016;18:140-52.

[59] Jiang M, Griffin WM, Hendrickson C, Jaramillo P, VanBriesen J, Venkatesh A. Life cycle greenhouse gas emissions of Marcellus shale gas. Environmental Research Letters. 2011;6:034014.
[60] Howarth RW, Santoro R, Ingraffea A. Methane and the greenhouse-gas footprint of natural gas from shale formations. Climatic Change. 2011;106:679.
[61] Stephenson T, Valle JE, Riera-Palou X. Modeling the relative GHG emissions of conventional and shale gas production. Environmental science & technology. 2011;45:10757-64.
[62] Hultman N, Rebois D, Scholten M, Ramig C. The greenhouse impact of unconventional gas for electricity generation. Environmental Research Letters. 2011;6:044008.
[63] Gray MR. Tutorial on Upgrading of oil sands bitumen. <https://www.ualberta.ca/~gray/Links%20&%20Docs/Web%20Upgrading%20Tutorial.pdf> (accessed October 14, 2015). Department of Chemical and Material Engineering, University of Alberta.
[64] Ordorica-Garcia G, Croiset E, Douglas P, Elkamel A, Gupta M. Modeling the energy demands and greenhouse gas emissions of the Canadian oil sands industry. Energy & Fuels. 2007;21:2098-111.
[65] Kinder Morgan. Trans Mountain Pipeline System; 2015. < http://www.kindermorgan.com/pages/business/canada/transmountain.aspx > (accessed January 20, 2016).
[66] Clarksons. Clarksons Research; 2015. <http://wfr.clarksons.net/wfr/register/default.aspx?ref=hl> (accessed December 31, 2015).
[67] Holtrop J, Mennen G. An approximate power prediction method. 1982.
[68] Holtrop J, Mennen G. A statistical power prediction method. International Shipbuilding Progress. 1978;25.
[69] ITTC – Recommended Procedures and Guidelines: Testing and Extrapolation Methods, Propulsion, Performance, Predicting Powering Margins. 24th International Towing Tank Conference Proceedings. Edinurgh, UK, 2005. p. 1-5. 24th International Towing Tank Conference Proceedings. p. 1-5.
[70] United States Environmental Protection Agency. Draft Regulatory Impact Analysis: Control of Emissions of Air Pollution from Category 3 Marine Diesel Engines; 2009 <https://nepis.epa.gov/Exe/ZyPDF.cgi/P10024CN.PDF?Dockey=P10024CN.PDF> (accessed October 27, 2016).
[71] Gray MR. Course notes - ChE 522. Fundamentals of oil sands Upgarading. Edmonton, Alberta: University of Alberta; 2013.
[72] Energy Institute. HM 40 guidelines for the crude oil washing of ships' tanks and the heating of crude oil being transported by sea; London, 2004 < http://www.nasmaritime.com/DOCUMENTS/GUIDE%20for%20COW.pdf> (accessed October 27, 2016). London.
[73] Statoil. Facts Steam Assited Gravity Drainage; 2014 <http://www.statoil.com/no/About/Worldwide/NorthAmerica/canada/OilSands/Downloads/sagd.pdf> (accessed January 14, 2016).
[74] Alberta Government. Alberta Oil Sands Industry Quarterly Update; 2015 <http://www.albertacanada.com/files/albertacanada/AOSID_QuarterlyUpdate_Fall2014.pdf> (accessed January 23, 2016).
[75] National Energy Board. Market Snapshot: In-Situ Oil Sands Producers More Efficient, Using Less Steam per Barrel in 2014; 2015 <https://www.neb-one.gc.ca/nrg/ntgrtd/mrkt/snpsht/2015/05-01nstlsnd-eng.html> (accessed January 21, 2016). 2015.
[76] Xiaodong L, Ernesto F. Electrical Submersible Pumps System; 2013. IEEE Industry Applications Magazine.

[77] Heins W. Is a paradigm shift in produced water treatment technology occurring at SAGD facilities? Journal of Canadian Petroleum Technology. 2010;49:10-5.
[78] Rudyk S, Spirov P. Upgrading and extraction of bitumen from Nigerian tar sand by supercritical carbon dioxide. Applied Energy. 2014;113:1397-404.
[79] Alberta Energy Regulator. In Situ Performance Presentations; 2016 <http://www.aer.ca/data-and-publications/activity-and-data/in-situ-performance-presentations> (accessed January 25, 2016).
[80] Das S. Improving the performance of SAGD. SPE International Thermal Operations and Heavy Oil Symposium: Society of Petroleum Engineers; 2005.
[81] Kapadia PR, Wang JJ, Kallos MS, Gates ID. Practical process design for in situ gasification of bitumen. Applied Energy. 2013;107:281-96.
[82] Triangle Three Engineering Limited. Technical Audit Report Gas Over Bitumen Technical Solutions; 2010 <http://www.energy.alberta.ca/Oil/pdfs/IETPGoBAudit.pdf> (accessed January 25, 2016).
[83] Lightbown V, et al. High Temperature De-Oiling of SAGD Produced Water. World Heay Oil Congress. 2015;15-180.
[84] W.F. Heins. Operational data from world's first SAGD facilities using evaporators to treat produced water for boiler feed water. Canadian Petroleum Technology. 2009;47.
[85] Nyboer J, Groves S. A review of Existing Cogeneration Facilities In Canada; 2012 <http://www2.cieedac.sfu.ca/media/publications/Cogeneration_Report_2012_Final.pdf> (accessed October 27, 2016).
[86] Humphreys KK. Basic cost engineering: CRC Press; 1995.
[87] Olateju B, Kumar A. Hydrogen production from wind energy in Western Canada for upgrading bitumen from oil sands. Energy. 2011;36:6326-39.
[88] David M, Mellisa M, Dinara M, Charu K, Gurinder G, Peter H. Green Bitumen: The Role of Nuclear, Gasification, and CCS in Alberta's Oil Sands. Canadian Energy Research Institute; 2008.
[89] Idaho National Laboratory. Nuclear-Integrated Oil Sands Recovery via Steam Assisted Gravity Drainage; 2010 <https://art.inl.gov/NGNP/NEAC%202010/INL_NGNP%20References/TEV-704%20Nuclear%20Assisted%20Oil%20Sands%20Rec%20via.pdf> (accessed October 27, 2016).
[90] Pettinau A, Ferrara F, Amorino C. Techno-economic comparison between different technologies for a CCS power generation plant integrated with a sub-bituminous coal mine in Italy. Applied Energy. 2012;99:32-9.
[91] Bersak AF, Kadak AC. Integration of Nuclear Energy with Oil Sands Projects For Reduced Greenhouse Gas Emissions and Natural Gas Consumption. Massachusetts Institute of Technology. 2007;23:1-83.
[92] Keesom W, Unnasch S, Moretta J. Life cycle assessment of North American and imported crudes prepared for Alberta energy research Institute; 2009 <http://www.eipa.alberta.ca/media/39640/life%20cycle%20analysis%20jacobs%20final%20report.pdf> (accessed January 25, 2016).
[93] B. Alberto. An integrated energy optimization model for the Canadian Oil Sands industry (dessertation). Waterloo, Ontario,: University of Waterloo; 2011. 106 p.
[94] S. Bengt. Canada's oil sands resources and its future impact on global oil supply: Uppsala University. < http://www.peakoil.net/uhdsg/OilSandCanada.pdf> (accessed October 27, 2016). Uppsala University.
[95] Netzer D. Alberta bitumen processing integration study. Report by Netzer, D. and Associates for the province of Alberta economic development department investment and industrial branch. Department of Energy and Industry Sponsor; 2006.

[96] Choquette-Levy N. Should Alberta upgrade oil sands bitumen? An integrated life cycle framework to evaluate energy systems investment traddeoffs: University of Calgary; 2011.
[97] Dunbar RB. Canada's oil sands-A world scale hyrocarbon resource; 2009 <http://www.strategywest.com/downloads/StratWest_OilSands.pdf> (accessed January 25, 2016). Calgary: Strategy West Inc.
[98] Romain HL, John PE. Technologies, markets and challenges for the development of Canadian Oil Sands Industry; 2007.
[99] Gemayel EG. Integration and simulation of a bitumen upgrading facility and an IGCC process with carbon capture (dessertation): Ottawa, University of Ottawa; 2012. 102 p.
[100] Dinara M, Carlos AM, Rob M. Canada. Canadian oil sands supply costs and development projects (2014-2048); 2014.
[101] Lee B, Charles M, Frank G. Development of the write process for pipeline-ready heavy oil; 2009 < http://www.osti.gov/scitech/servlets/purl/958564/ <accessed October 28, 2016).
[102] Cairns M. Crude oil by rail: Part I and II Potential for the movement of Alberta Oil Sands crude oil and related products by Canadian railways. 2013.
[103] Subramanian RS. Pipe Flow Calculations; 2016. <http://web2.clarkson.edu/projects/subramanian/ch330/notes/Pipe%20Flow%20Calculations.pdf > (accessed February 20, 2016).
[104] McAllister E. Pipeline Rules of Thumb Handbook-Quick and Accurate Solutions to Your Everyday Pipeline Engineering Problems. Elsevier. 2009.
[105] MAN Diesel & Turbo, Propulsion trends in tankers;2016. <http://marine.man.eu/docs/librariesprovider6/technical-papers/propulsion-trends-in-tankers.pdf?sfvrsn=20> (accessed January, 2016).
[106] MAN Diesel & Turbo, Basic principles of ship propulsion; 2016 <https://marine.man.eu/docs/librariesprovider6/propeller-aftship/basic-principles-of-propulsion.pdf?sfvrsn=0> (accessed May 17, 2016).
[107] Hasan S. Impact of EEDI on Ship Design and Hydrodynamics A Study of the Energy Efficiency Design Index and Other Related Emission Control Indexes. 2011.
[108] MAN B&W Diesel A/S, Engine Selection Guide Two-stroke MC/MC-C Engines; 2000. <https://www.fsb.unizg.hr/ship-design/esg.pdf> (accessed December 12, 2015).
[109] MAN Diesel & Turbo, L28/32H Project Guide - Marine Four-stroke GenSet compliant with IMO Tier II; 2015. <http://marine.man.eu/applications/projectguides/4stroke/manualcontent/PG_M-II_L2832H.pdf> (accessed December 20, 2015).
[110] Portworld Distance Calculator; 2016. <http://www.portworld.com/map> (accessed February 12, 2016).
[111] Platou RS. The Platou Report 2015; 2015 <http://shipbroker.no/wordpress/wp-content/uploads/2015-04-Platou-Monthly.pdf> (accessed February 20, 2016).
[112] Crude Quality Inc. Bringing the crude oil industry together with data; 2016 <http://www.crudemonitor.ca/home.php> (accessed May 25, 2016).
[113] Environment Canada. Federal Government Technical Report: Properties, Composition and Marine Spill Behaviour, Fate and Transport of Two Diluted Bitumen Products from the Canadian Oil Sands; 2013 <http://www.ec.gc.ca/scitech/6A2D63E5-4137-440B-8BB3-E38ECED9B02F/1633_Dilbit%20Technical%20Report_e_v2%20FINAL-s.pdf> (accessed May 17, 2016)

[114] National Institute of Statistics and Economic Studies. International prices of imported raw materials - Heavy fuel oil (Rotterdam) - Prices in US dollars per tonne - FOB - 1% of sulfur; 2016 <http://www.insee.fr/en/bases-de-donnees/bsweb/serie.asp?idbank=001642883> (accessed March 2, 2016). 2016.

[115] Bunker Index MDO; 2014 <http://www.bunkerindex.com/prices/bixfree_1405.php?priceindex_id=4>(accessed March 2, 2016).
[116] Heins W. Operational data from the world's first SAGD facilities using evaporators to treat produced water for boiler feedwater. Journal of Canadian Petroleum Technology. 2008;47.
[117] Li W, Fu F, Ma L, Liu P, Li Z, Dai Y. A process-based model for estimating the well-to-tank cost of gasoline and diesel in China. Applied Energy. 2013;102:718-25.
[118] MAN B&W S50ME-C8.2-GI IMO Tier II Project Guide; 2014 <http://marine.man.eu/applications/projectguides/2stroke/content/epub/S50ME-C8_2-GI.pdf> (accessed January 5, 2016).
[119] Wartsila 50DF Product Guide;2014 <http://www.wartsila.com/docs/default-source/product-files/engines/df-engine/wartsila-o-e-w-50df-pg.pdf?sfvrsn=3> (accessed January 20, 2016).
[120] Wang B. Technical and Economical Comparison of Propusion Alternatives for Modern LNG Carriers. 2015.
[121] National Institute of Statistics and Economic Studies. Statistics: raw materials price indices and international prices; 2017. <https://www.insee.fr/en/statistiques/serie/001642883?idbank=001642883>(accessed September 9, 2017).
[122] Savage B. Notice of change for emission factor for increased grid electricity usage. Climate change secretariat-environment and water, Government of Alberta, Edmonton, Alberta. 2011.
[123] U.S. Energy information administration. PADD regions enable regional analysis of petroleum product supply and movement. 2012. <http://www.eia.gov/todayinenergy/detail.cfm?id¼4890 > (accessed August 18, 2016).
[124] ISO (International Standardization Organization), 2006. Environmental management – life cycle assessment - principles and framework. ISO 14040. Genève, Switzerland.
[125] Intergovernmental Panel on Climate Change (IPCC) 2013. Climate Change 2013: The Physical Science Basis. Working Group I Contribution to the Fifth Assessment Report of the Intergovernmental Panel on Climate Change. Chapter 8: Anthropogenic and Natural Radiative Forcing. < http://www.ipcc.ch/pdf/assessment-report/ar5/wg1/WG1AR5_Chapter08_FINAL.pdf> (accessed August 16, 2016).
[126] Cai H, Brandt AR, Yeh S, Englander JG, Han J, Elgowainy A, et al. Well-to-wheels greenhouse gas emissions of Canadian oil sands products: Implications for US petroleum fuels. Environmental science & technology. 2015;49:8219-27.
[127] Exhaust Gas Emission Control Today and Tomorrow: Application on MAN B&W Two-stroke Marine Diesel Engines. < http://marine.man.eu/docs/librariesprovider6/technical-papers/exhaust-gas-emission-control-today-and-tomorrow.pdf?sfvrsn=22 > (accessed August 20, 2016).
[128] MAN Diesel & Turbo. How to Influence CO2. < http://marine.man.eu/docs/librariesprovider6/technical-papers/how-to-influence-co2.pdf?sfvrsn=18 > (accessed August 20, 2016)

[129] Aspentech. 'Refinery-wide mode.hscl'- a sample case for refinery model in Aspen HYSYS v7.3. 2014.
[130] International Energy Agency (IEA). Energy Technology System Analysis Programme: Oil refineries; 2014. <https://iea-etsap.org/E-TechDS/PDF/P04_Oil%20Ref_KV_Apr2014_GSOK.pdf> (accessed September 9, 2017).
[131] Ou X, Zhang X, Chang S. Scenario analysis on alternative fuel/vehicle for China's future road transport: Life-cycle energy demand and GHG emissions. Energy policy. 2010;38:3943-56.

[132] U.S. Energy Information Administration (EIA): China International Analysis; 2015. < http://energy.gov/sites/prod/files/2016/04/f30/China_International_Analysis_US.pdf> (accessed September 9, 2016).
[133] Macquarie Private Wealth: Canadian LNG: the race to the coast; 2012 <http://www.investorvillage.com/uploads/8056/files/Cdn_LNG_100912.pdf> (accessed February 21, 2017).
[134] Coastal GasLink Pipeline Project: Greenhouse Gas Emissions Technical Data Report; 2014 <http://a100.gov.bc.ca/appsdata/epic/documents/p392/d37367/1394553608449_d56d24ee466441db246e16e23e42e730633649487df1686d6220780282b5a309.pdf> (accessed February 23, 2017).
[135] LNG Canada export terminal. Greenhouse gas management technical data report; 2014 <http://a100.gov.bc.ca/appsdata/epic/documents/p398/d38157/1415050258003_KGyFJXmP1x2sG8wCmyvdfS27j60hvHtwhPJZxGRMqpgdrdszwXMw!-1038573416!1415046831474.pdf> (accessed February 23, 2017).
[136] Sinha R, Nik WMNW. Investigation of propulsion system for large LNG ships. IOP Conference Series: Materials Science and Engineering: IOP Publishing; 2012. p. 012004.
[137] Taglia A, Rossi N. European Gas Imports: GHG emissions from the supply chain; 2009 <http://www.aaee.at/2009-IAEE/uploads/fullpaper_iaee09/P_238_Taglia_Antonio_31-Aug-2009,%2017:24.pdf> (accessed February 22, 2017).
[138] T.J. Skone, G. Cooney, M. Jamieson, J. Littlefield, J. Marriott. Life cycle greenhouse gas perspective on exporting liquefied natural gas from the United States, National Energy Technology Laboratory; 2014 <https://energy.gov/sites/prod/files/2014/05/f16/Life%20Cycle%20GHG%20Perspective%20Report.pdf> (accessed February 28,2017).
[139] European Commission. Quarterly Report on European Gas Markets: Market Observatory for Energy; 2015 <https://ec.europa.eu/energy/sites/ener/files/documents/quarterly_report_on_european_gas_markets_q1_2015.pdf> (accessed February 21, 2017).
[140] United States Environmental Protection Agency. Proposal to Designate an Emission Control Area for Nitrogen Oxides, Sulfur Oxides and Particulate Mattert; 2009. <http://www.eia.gov/todayinenergy/detail.cfm?id¼4890 > (accessedSeptember 9, 2017).
[141] House PK, Saberian M, Briens CL, Berruti F, Chan E. Injection of a Liquid Spray into a Fluidized Bed: Particle− Liquid Mixing and Impact on Fluid Coker Yields. Industrial & engineering chemistry research. 2004;43:5663-9.
[142] Rettger P, Arnold J, Brandenburg B, Felch C. The Long Lake integrated upgrading project: status report and discussion of soot processing. 2006 Gasification Technologies Council Conference, Washington, DC2006. p. 1-4.
[143] Government of Quebec. The St. Lawrence , Source of Wealth: Strategic environmental assessment program on offshore oil and gas exploration and development; 2014 <ftp://ftp.mrn.gouv.qc.ca/Public/Bibliointer/Mono/2014/01/1001821.pdf> (accessed February 28, 2017).

Appendix A

Supporting Information:

Nomenclature

SCO- Synthetic crude oil

VLCC- Very large crude carrier

HFO- Heavy fuel oil

MDO- Marine diesel oil

bbl- Barrel

SAGD- Steam Assisted Gravity Drainage

1. Resistance Model

We used the calm water resistance developed with Holtrop and Mennen's approximate power prediction approach [67] and statistical power prediction method [68] to evaluate the total installed power of the engine. The resistance calculated at different ocean tanker speeds is shown in Figure S1.

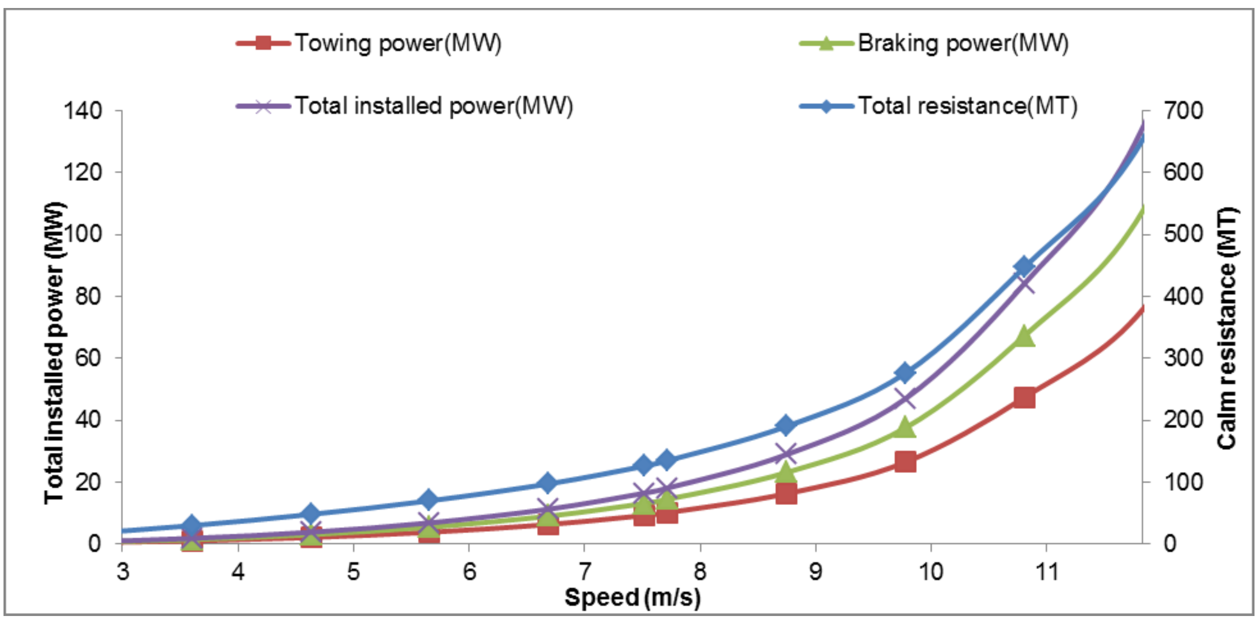

Figure S1: Total installed power and resistance of the vessel at different speeds

2. Comparison of shipping cost for different size tankers

Figure S2 shows shipping costs per barrel SCO and dilbit from the Westridge terminal in Vancouver to the port of China for different vessel sizes. A VLCC and Suezmax are used to evaluate the impact of size on shipping cost. It is clear from Figure S2 that the shipping costs of SCO and dilbit decrease gradually with increases in vessel size. This occurs due to economies of scale. A VLCC has lower shipping costs per barrel SCO and dilbit (C$1.7 and C$2.1, respectively) than Aframax and Suezmax. The shipping costs of SCO and dilbit using Suezmax are by 9% and 8% below Aframax's. However, VLCC consumes the most fuel, particularly due to increases in the fuel consumption in the main engine, discharging, cargo heating in the storage tank, and while discharging (see Figure S3).

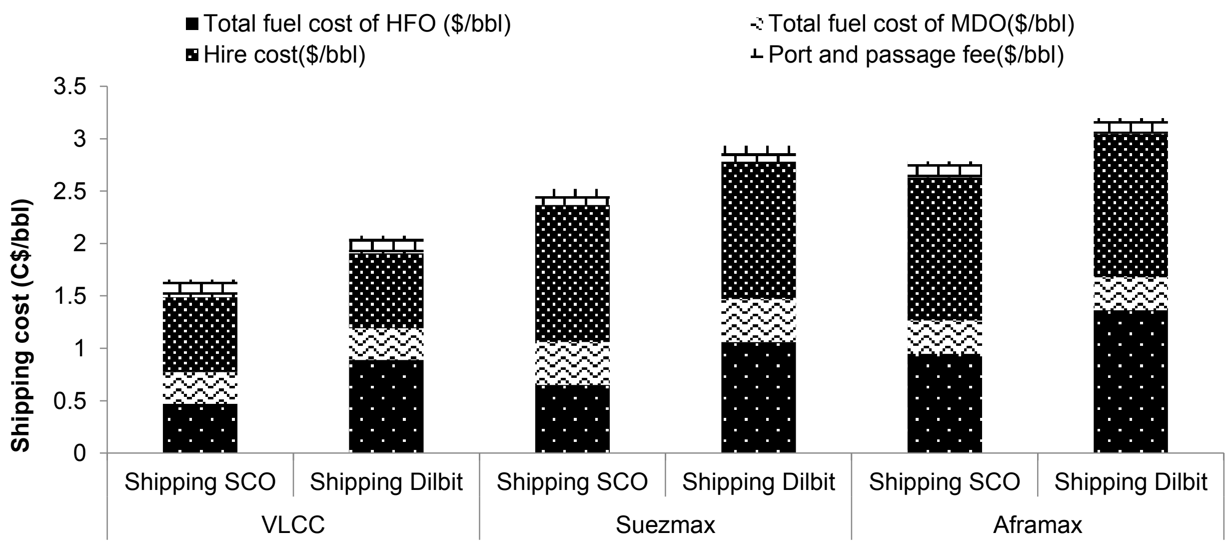

Figure S2: SCO and dilbit shipping costs by tanker size

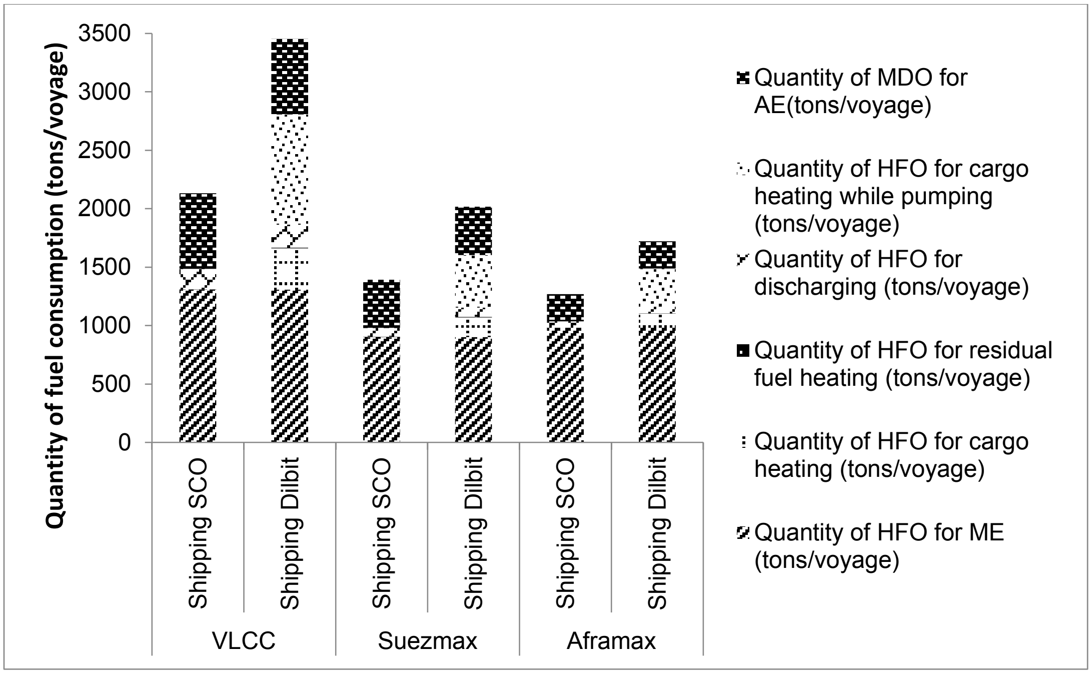

Figure S3: Fuel consumption by tanker size

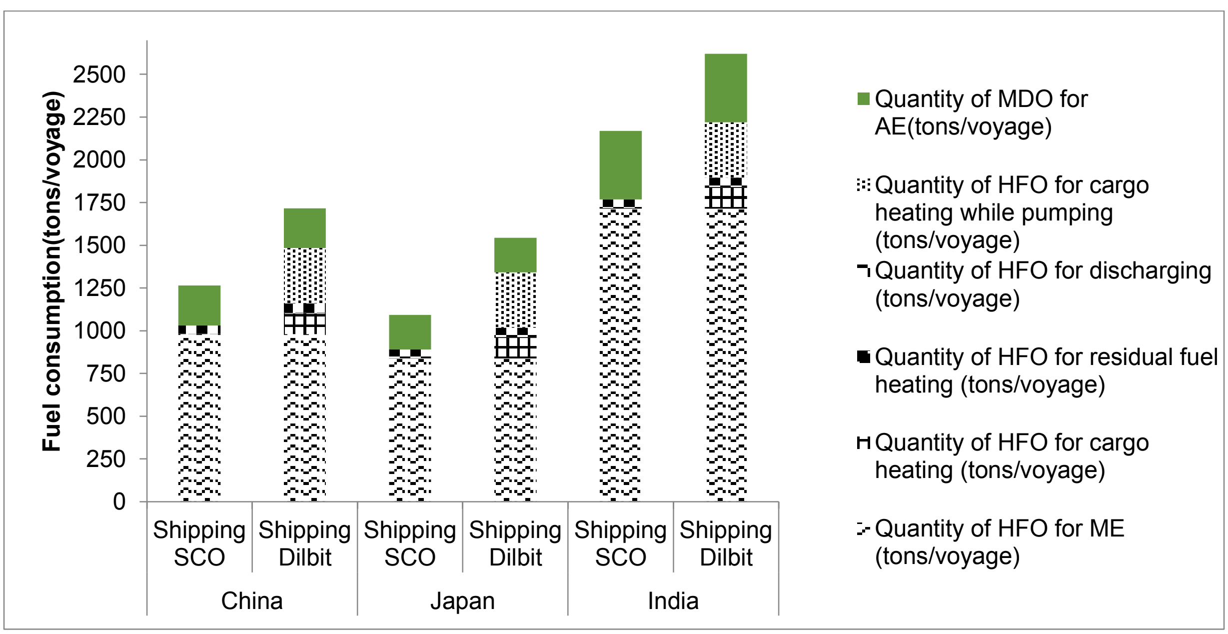

Figure S4: Fuel consumption for shipping to China, Japan, and India

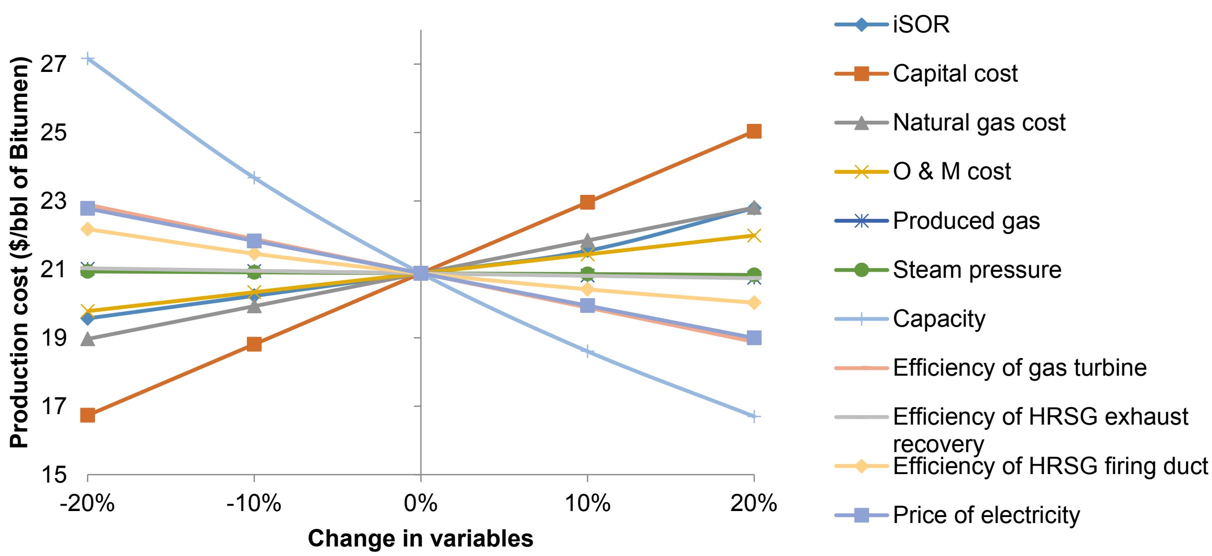

Figure S5: Sensitivity of key parameters on a SAGD plant with cogeneration

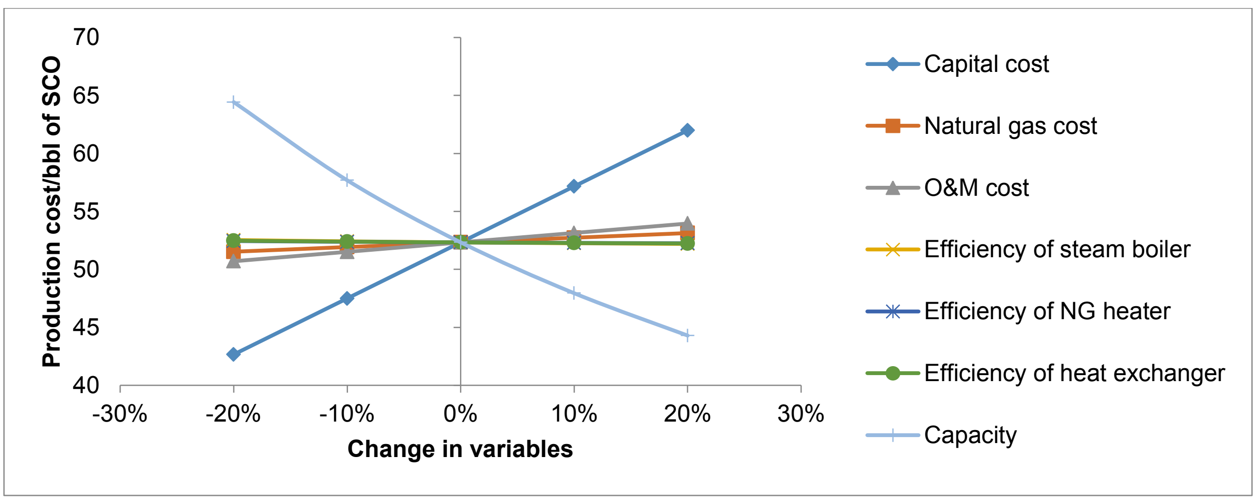

Figure S6: Sensitivity of key parameters on an HCU without cogeneration

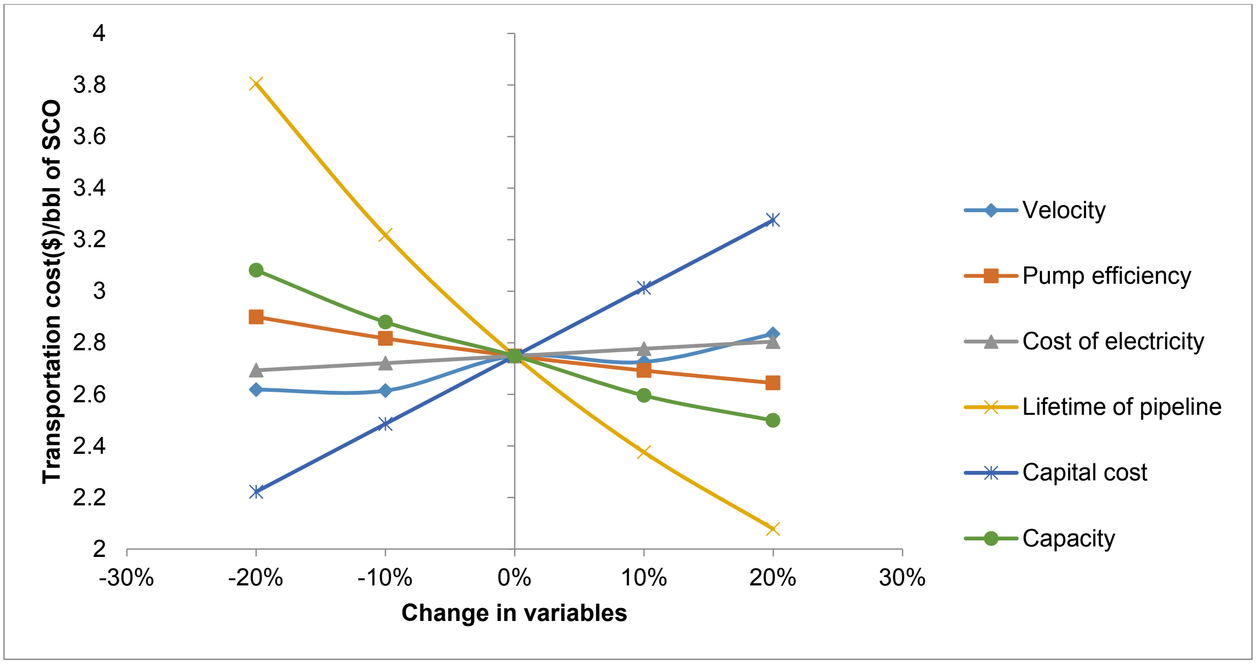

Figure S7: Sensitivity of key parameters on SCO transportation (1147km)

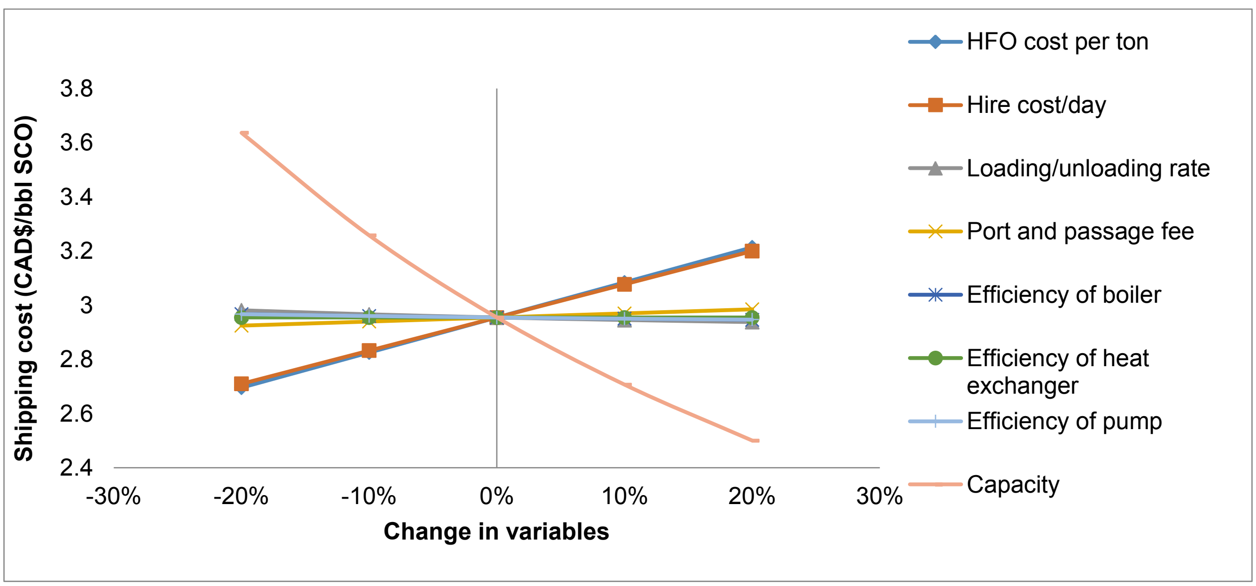

Figure S8: Sensitivity analysis of key parameters on the shipping cost of SCO

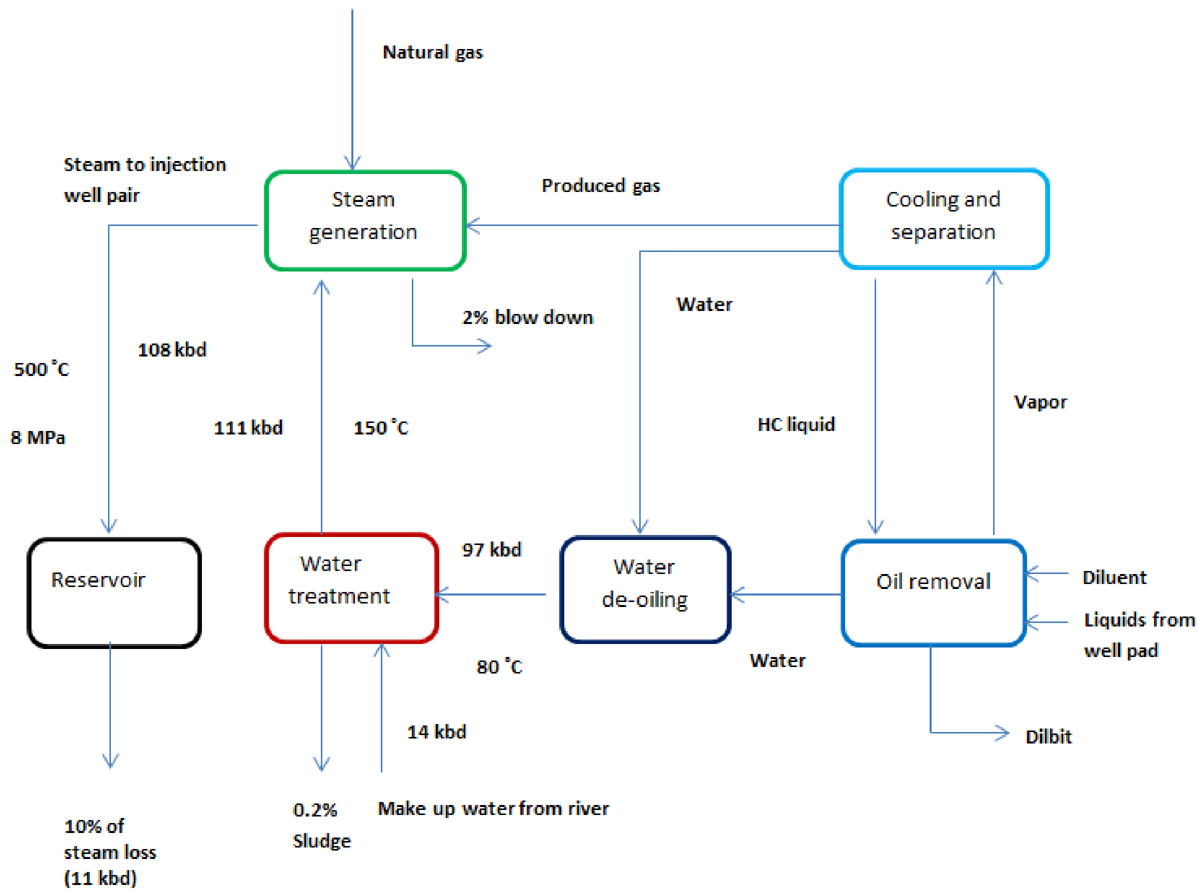

Figure S9: SAGD flow model without cogeneration

Table S1: Refineries in China [8]

Company	Location/refinery name	Capacity (b/d)
Sinopec	Beijing Yanshan	220,000
Sinopec	Guangzhou	250,000
Sinopec	Jinling	270,000
Sinopec	Jiujiang	130,000
Sinopec	Maoming	270,000
Sinopec	Qilu	210,000
Sinopec	Shanghai Gaoqiao	250,000
Sinopec	Wuhan	170,000
Sinopec	Zhenhai Refining & Chemical	460,000
Sinopec	Anqing	110,000
Sinopec	Changling	160,000
Sinopec	Luoyang	160,000
Sinopec.	Qingdao Petchem Co	100,000
Sinopec	Cangzhou	70,000
Sinopec	Jingmen	120,000
Sinopec	Shijiazhuang Ref & Chem	100,000
Sinopec	Shanghai Petchem	280,000
Sinopec	Tianjin	250,000
Sinopec	Yangzi Petchem	180,000
Sinopec	Tahe	100,000
Sinopec	Baling	80,000
Sinopec.	Fujian Refining & Petchem	240,000
Sinopec	Hainan Petchem	160,000

Company	Location/refinery name	Capacity (b/d)
Sinopec	Jinan	100,000
Sinopec	Qingdao Refining	200,000
Sinopec	Zhanjiang Dongxing Petchem	100,000
CNPC	Fushun Petchem	200,000
CNPC	Jinxi	140,000
CNPC	Daqing Refining & Petchem	160,000
CNPC	Lanzhou Petchem	200,000
CNPC	Jilin	200,000
CNPC	Jinzhou Petchem	140,000
CNPC	Dushanzi Petchem	200,000
CNPC	Dagang Petchem	100,000
CNPC	Liaoyang	200,000
CNPC	Karamay Petchem	70,000
CNPC	Urumqi	110,000
CNPC	Dalian Petchem	400,000
CNPC	Dalian WEPEC	200,000
CNPC	Ningxia	100,000
CNPC	Changqing Petchem	100,000
CNPC	Qinzhou	200,000
CNPC	Qianguo	50,000
CNPC	Huabei	100,000
CNPC	Qingyang	60,000
CNPC	Liaohe Petchem	100,000
CNPC	Liaoning, Zhenhua Oil	200,000

Company	Location/refinery name	Capacity (b/d)
CNPC	Renqiu	100,000
CNPC	Harbin	100,000

Table S2: Chinese investment in Canada's oil and gas sector [3]

Investor	Date	Size (C$)	Sector	Target	Location
CNOOC	February 2013	$ 15.1 B	Oil and gas	Nexen	Alberta (AB)
Petro China	February 2012	$ 1 B	Oil and gas	Royal Dutch Shell PLC	British Columbia (BC)
Petro China	January 2012	$ 680 M	Oil and gas	Athabasca Oil Sands Corp	Alberta (AB)
Sinopec	October 2011	$ 2.2 B	Oil and gas	Daylight Energy	Alberta (AB)
CNOOC	July 2011	$ 2.1 B	Oil and gas	Opti Canada	Alberta (AB)
Sinopec	January 2011	$ 100 M	Oil and gas	Enbridge Inc.	Alberta (AB)
China Investment Corp	May 2010	$ 1.23 B	Oil and gas	Penn West Corporation	Alberta (AB)
Sinopec	April 2010	$ 4.56 B	Oil and gas	Syncrude	Alberta (AB)
Sinopec	June 2009	$ 8.3 B	Oil and gas	Addax Petroleum Corp	Alberta (AB)
Petro China	2009	$ 1.9 B	Oil and gas	Athabasca Oil Sands Corp	Alberta (AB)

Table S3: Non-Chinese investment in Canada's oil and gas sector [3]

Investor	Origin	Date	Size (C$)	Target
Statoil	Norway	April 2007	$ 2.2 B	North American Oil Sands Corporation

Investor	Origin	Date	Size (C$)	Target
PTTEP	Thailand	November 2010	$ 2.4 B	KKD Oil Sands Partnership
Korea National Oil Corporation (KNOC)	South Korea	December 2010	$ 525 M	Hunt Oil Company of Canada

3. Mathematical formulas used in the evaluation of total supply chain costs of the different pathways

List of Equations

Equation 1: Continuity equation: $A_1v_1 = A_2v_2$

Equation 2: Head loss (m/m): $h_f/L = fv^2/2gD$

Equation 3: Power of each pump (Pa), $P = \Delta P*Q/\eta$

Equation 4: Distance between booster stations (m), $d = \Delta P/ (h_f/L)*\rho*g)$

Equation 5: Number of booster stations, $N=L/d$

Equation 6: Natural gas required (m^3/m^3 bitumen) $= iSOR*(H_s - H_w)/q*\eta_b*LHV$

Equation 7: Pump system efficiency $= HP_{pump} / KW_{system\ input}$

Equation 8: $C_1/C_2 = (Q_1/Q_2)^n$

Equation 9: Power consumed in evaporators (KW) $= C * M * \Delta t$

Equation 10: $HP_{pump} = Q'* \Delta P*1.7*10^{-5}$

Equation 11: $C_t=C_t+C_{OM}$

Equation 12: $OI=R_t-C_t$

Equation 13: $NI=OI-C_c$

Equation 14: $DCF_k=NI_k/ (1+i)^k$

Equation 15: $P_E = P_B \times \eta_H \times \eta_o \times \eta_R \times \eta_s$

Equation 16: $C_b = \Delta / (L_{wl} \times B \times D_{design})$

Equation 17: $C_m = A_m / (B \times D_{design})$

Equation 18: $C_w = A_{wl} / (L_{wl} \times B)$

Equation 19: $F_u = L_f \times SFO \times P \times S_{hr} / 10^6$

where,

A = Area of cross section for the pipe (m^2)

ΔP = Pump pressure differential (Pa)

Q = Volume flow rate of each pump (m^3/s)

η = Efficiency of the pump

h_f/L = Head loss due to friction per unit length (m/m)

f = Friction factor

v = Velocity of flow (m/s)

g= Gravitational acceleration (m^2/s)

D= Inside diameter of pipe (m)

L= Total length of pipe (m)

ρ = Density of commodity (kg/m^3)

M= Vapor mass flow rate (ton/hr)

Δt = Temperature in ˚C

C= 2.5 – 3.0 depends on size of evaporator

HP_{pump} = Hydraulic horse power that is imparted to fluid by pump

$KW_{system\ input}$ =Total amount of electrical power in kilowatt supplied to the system

Q'= Volumetric flow rate through each stage in B/D

ΔP= Pressure increase across the pump in psi

iSOR = Instantaneous steam-oil ratio (dry)

H_s = Enthalpy of steam (100% quality) at 8 MPa and 500 ˚ C

H_w = Enthalpy of boiler feed water at 150 ˚ C

q= Quality of steam

η_b = Steam boiler efficiency

LHV= Lower enthalpy value of natural gas

C_1= Cost of plant 1

Q_1= Capacity of plant 1

C_2= Cost of plant 2

Q_2= Capacity of plant 2

n=Scale factor

C_t= Total annual cost ($/year)

C_{tf}= Total fuel cost ($/year)

C_{OM}= Total O&M cost ($/year)

OI= Operating income of the unit ($/year)

R_t= Total revenue ($/year)

NI= Net income of the unit

C_c= Capital cost of unit

DCF= Discounted cash flow

i= Discount rate

K= Considered year

P_E= Towing power

P_B= Brake power

η_H= Hull efficiency

η_o= Open water propeller efficiency

η_R= Relative rotative efficiency

η_s= Shaft efficiency

C_b= Block coefficient

C_m= Midship section coefficient

C_w= Water plane coefficient

C_p= Prismatic coefficient based on length on waterline

SFO= Engine specific fuel consumption, g/KWhr

P = Power of engine (KW)

L_f = Load factor

S_{hr} = Sailing hours

Appendix B

S1. Mathematical formulas used in the evaluation of total LC WTW GHG emissions of the different pathways

Equation S1: $Upstream\ emissions\ allocated\ to\ finished\ fuel\ (i)(g-CO2eq/day) =$

$$Upstream\ emissions\ (g-CO2eq/day) \times \frac{E_i}{\sum_{i=j,k,l} E_i}$$

where E_i is the total energy content of the product (i) (MJ/day), and j, k, and l stand for gasoline, diesel, and jet fuel, respectively. As the functional unit of this study is MJ-fuel, it is necessary to convert the emissions in g-CO_2eq/day to g-CO_2eq/MJ-fuel; this is done with Equation S2.

Equation S2: $Upstream\ emissions\ allocated\ to\ finished\ fuel\ (i)(g-CO2eq/MJ) =$

$$\frac{Upstream\ emissions\ allocated\ to\ finished\ fuel\ (i)(g-CO2eq/day)}{Total\ energy\ content\ of\ product\ (i), E_i\ (MJ/day)}$$

Appendix C:

Table S1: Major LNG import terminals in Europe [20]

Import Terminals	Capacity (m^3)
Zeebrugge Terminal	266,000
Fos Cavaou Terminal	267,000
Fos Tonkin Terminal	75,000
Montoir de Bretagne	267,000
Dunkerque	267,000
Revithoussa Terminal	130,000
La Spezia	70,000

Import Terminals	Capacity (m^3)
Isola di Porto Levante	152,000
FSRU OLT Offshore LNG Toscana	155,000
Klaipeda	160,000
Gate Terminal	266,000
Sines Terminal	216,000
Barcelona LNG Terminal	266,000
Cartagena LNG Terminal	266,000
Huelva LNG Terminal	173,400
Bilbao Bahia de Bizkaia Terminal	270,000
Sagunto Terminal	267,000
El Musel Terminal	266,000
Mugardos (El Ferrol) Terminal	266000
Marmara Ereglisi Terminal	266000
Aliaga LNG Terminal	265,000
Grain LNG Terminal	265,000
Dragon LNG	217,000
South Hook LNG	250,000

1. Mathematical formulas used in the evaluation of delivered costs and GHG emissions of the Canadian LNG supply chain

Equation 1: Emissions from extraction (g-CO_2eq eq/MJ) = $E_1 \times E_{f1}$

Equation 2: Emissions from hydraulic fracturing (g- CO_2eq) = $E_2 \times C_1 \times T_1$

Equation 3: Emissions from pipeline transportation of natural gas (t/y) = $E_r \times E_c \times U_c$

Equation 4: Emissions from liquefaction facility (t/y) = $E_r \times O \times E_{f2} \times U_c$

Equation 5: Emissions from shipping LNG (tonnes/year) = $P_r \times E_{f3} \times N \times U_c$

Equation 6: $C_1/C_2 = (Q_1/Q_2)^n$

Equation 7: Delivered costs (US$/GJ) = $P_c + Pt_c + L_c + S_c$

where,

E_1 = Energy consumed per unit energy extracted (MJ/MJ)

E_{f1} = Emission factors for extraction (g-CO_2eq /MJ)

E_2 = Emission factors for the pump (g CO_2eq/hp-hr)

E_r = Exhaust flow rate (kg/s)

E_c = Exhaust CO2 concentration (wt fraction)

U_c= Unit conversion

F_r = Fuel (m3/h)

O = Operation duration (h/y)

E_{f2} = Emissions factor for pipeline transportation of natural gas (g/m3)

P_r = Power rating (kW)

E_{f3} = Emission factor from combustion of HFO in the marine engine (g/kW)

N = Number of LNG ship visits per year

C_1= Cost of plant 1

Q_1= Capacity of plant 1

C_2= Cost of plant 2

Q_2= Capacity of plant 2

n=Scale factor

P_c = Production cost of natural gas (US$/GJ)

P_{tc} = Pipeline transportation cost of natural gas (US$/GJ)

L_c = Liquefaction cost of natural gas (US$/GJ)

S_c = Shipping cost of LNG by LNG carrier (US$/GJ)